Optimization of the Glass Fiber Forming Process for Single-Tip and Small-Number-Tip Positions

By

Christa R Ansbergs

Submitted to the Department of Mechanical Engineering in partial fulfillment of the requirements for the degree of

Master of Science in Mechanical Engineering

and the degree of

Bachelor of Science in Mechanical Engineering

at the

MASSACHUSETTS INSTITUTE OF TECHNOLOGY

June 1999

Author.....
Department of Mechanical Engineering
May 17, 1999

Certified by.....
John H. Lienhard V
Associate Professor of Mechanical Engineering
Thesis Supervisor

Accepted by.....
Ain Sonin
Chairman of Graduate Studies
Department of Mechanical Engineering

Optimization of the Glass Fiber Forming Process for Single-Tip and Small-Number-Tip Positions

by

Christa R Ansbergs

Submitted to the Department of Mechanical Engineering on May 17, 1999 in partial fulfillment of the requirements for the degree of Master of Science in Mechanical Engineering and the degree of Bachelor of Science in Mechanical Engineering

Abstract

The design of fiberglass manufacturing setups has evolved largely by trial and error. Efforts are now in place to achieve a better understanding of the fiber forming process. To facilitate this research, a smaller and simpler version of the full-scale fiber forming process is being used. This system has vastly different geometry and produces a small number of fibers. Work in this project has concerned optimization of the small-scale process to more closely match the behavior to production line fiberglass forming positions, such that results of experiments on the smaller system are applicable to the full scale system. Efforts were also put into simplification of the system, such that process variables can more easily be isolated for further study.

The primary effort of this project was put into controlling glass head pressure. On the full-scale system constant glass depth is maintained and the glass weight controls the flow rate of glass through the fiber forming tips. On the small system flow rate is controlled by a combination of changing glass weight and added air pressure. The pressure control system developed in this project uses glass resistance to measure glass depth and outputs a signal to a solenoid valve to add the appropriate amount of air pressure above the glass. The glass resistance measuring system had to be calibrated for a range of temperatures. Resistance data was collected while mass flow of glass was monitored. From the mass flow glass depth was calculated to an accuracy of 3%. When set to simulate the full-scale fiberglass forming operation the pressure control valve can control pressure to within 4.5% of 5.5 kPa required pressure.

A new fiber winding system was designed and implemented. This system assures even distribution of fibers along the axis of a winder drum, speed control to within 1%, and limited vibration transmission to the fibers while they are in the forming and cooling regions.

The pressure control and winder control systems were incorporated into the same LabView interface to assure ease of use. From the interface an operator can set winder speed and total head pressure and monitor the control of both to assure that the system is behaving appropriately.

Thesis supervisor: John H. Lienhard V
Title: Associate Professor of Mechanical Engineering

Acknowledgements

I would like to acknowledge and thank PPG Industries, Fiber Glass Research Center for sponsoring the research presented in this report. Specifically I'd like to thank Jerry Bergman for making me one of "Jerry's Kids" – for initiating the idea of getting PPG involved in the EIP program and thus laying the foundation for this thesis back in 1996.

A big round of thanks goes to Reed Grundy , Dana Coyne and Hal Stedrack for initially developing the glass level sensing probe that became the bulk of my thesis work and for giving me assistance in understanding and adapting it. Thanks also to Gene Palamera, Cheryl Richards and Terry Love for miscellaneous other assistance and for making my stay at the FGRC a little brighter.

I want to thank Brett McKeone for putting up with me while we shared lab space and doing a lot of the work of setting up the nine-tip fiber forming position at MIT, and also Prof. Lienhard for providing that lab space and for being my advisor.

And most importantly I want to thank Dr. Allen Roach for being an amazingly cool boss, mentor, and friend. He gave me advice and assistance countless times, was generous with his time and managed to make work fun. He also managed to shelter me from a lot of potentially disruptive forces at the FGRC.

Contents

List of Figures

List of Tables

Chapter 1

1 Introduction

PPG's full-scale fiberglass forming process consists of a large brick melting tank, a long brick fore-hearth down which molten glass flows and a series of platinum bushings under the glass pool through which glass is extruded. The holes in the platinum bushing are large compared to the final fiber diameter and it is stretched to its final diameter by a high-speed winder. After the glass leaves the bushing, cooling air is blown on it, water is sprayed on it, and a sizing compound is applied to bind the fibers together and to create whatever chemical conditions PPG's customers desire for their applications.

A fiberglass melting tank is on the order of 5 m (16 feet) wide by 5 m (16 ft) long and has a glass depth on the order of 1 m (3 ft). Typically two fore-hearths leave the tank in opposite directions and each accommodates 50-100 forming positions, spaced approximately every 1 m (3 ft). The fore-hearths are about 0.5 m (1.5 ft) wide and the glass depth is 25-30 cm (10-12 inches). Glass is fed into the melting tank in powdered form, using screw feeders. The flow rate of powdered glass into the tank is matched to the flow rate of total glass leaving the bushings and in this manner the glass depth in the fore-hearth is precisely controlled. Glass in the tank and in the fore-hearth is melted and kept hot with natural gas burners.

Each forming position contains a single platinum bushing, which has between 800 and 4000 fiber-forming tips, arranged in parallel rows and spaced about 0.5 cm (0.25 inches) apart. The bushing is electrically heated to around 1500 K (2250° F). The bushing temperature is controlled based on readings from two thermocouples welded into the platinum of the front and back of the bushing. Power is

introduced to the bushing on the sides and some power is drained off to one side or other based on differences in reading between the two thermocouples. Cooling water with attached heat-sink cooling fins runs through pipes set near channels through the center of the bushing. Even with cooling water compensation and power compensation there are still large variations in actual tip temperature, due to edge and corner effects and proximity to the power terminals and cooling pipes.

Glass cools rapidly after leaving the bushing tips and has solidified by the time it is about 0.5 cm (0.25 inches) from the tip. The solidification region is called the forming cone, as the glass necks down in approximately a cone-shape before reaching its final diameter. The solidification temperature is 1390 K (1860° F). The glass then has about 1 m (3 ft.) to cool to 365 K (200° F) such that the surfactant (binder) can be applied without denaturing. The fibers are then gathered together into bundles by passing them over graphite shoes with slits in them and continue to travel downward to the winder. The winder speed depends on the size of the fiber being produced and is typically between 15 m/s (50 ft/sec) and 90 m/s (300 ft/sec). Typical fiber sizes are 5 μm to 30 μm. A diagram of a full-scale fiber forming position can be seen in Figure 1.1.

The design of such fiberglass manufacturing setups has evolved largely by trial and error. Efforts are now in place to achieve a better understanding of many aspects of the fiber forming process. Specifically, research is being done on the effect of introducing water spray on the fibers, the formation of the thermal and fluid boundary layers around the fiber, and how these affect fiber cooling. Cooling methods and cooling rates are especially important as they affect the space that the process takes up, the rate at which fibers can be produced, and the control of fiber size uniformity, all of which are very important to commercial fiber production.

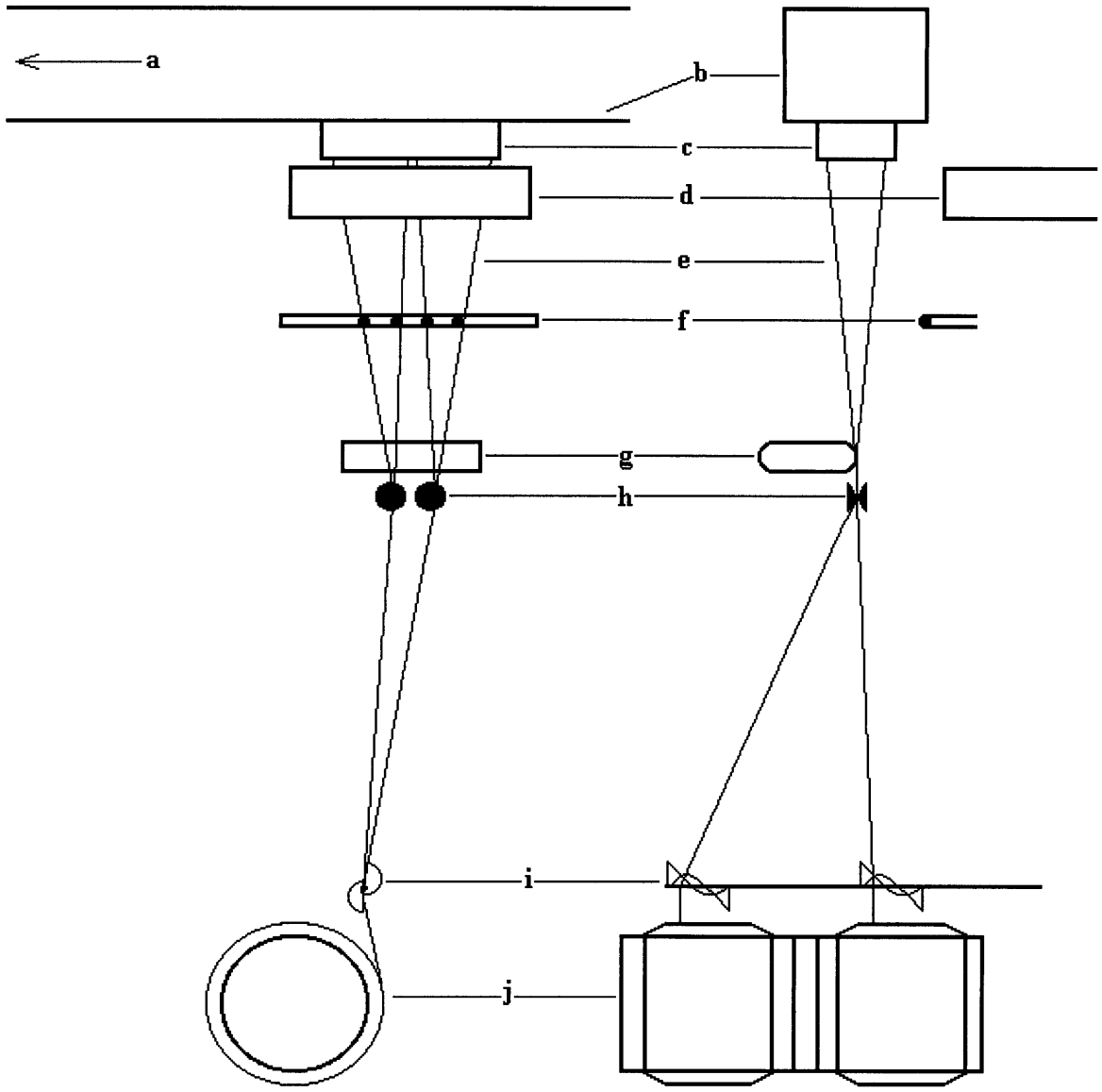

Figure 1.1: Diagram of a Typical Production Line Fiber Forming Position

a. to melting tank
b. brick fore-hearth
c. platinum bushing well suspended below fore-hearth
e. 800-2000 fibers
f. water spray nozzles
g. surfactant applicator
h. graphite shoes (cylinders with central V-shape) to bundle fibers together
i. spiral to cause even package build and make fibers easier to unwind
j. high speed winder drum, 30 cm (12 inch) diameter, speed on order of 1500 RPM with speed degenerating as package builds to maintain constant pull speed

To facilitate this research, a smaller and simpler version of the full-scale fiber forming process is being used. The advantages of the small-scale system are that it can be set up in locations remote from PPG's plants and that it

can be run with less interference from environmental effects and from process variables which are not being studied at the time. It is possible to run this system with no cross-air flow, no water sprays and no surfactant applied. It can more easily be placed in a controlled environment with ambient air temperature controlled and ambient air turbulence limited. Also, the number of fiber forming tips is smaller (the two systems this project is concerned with have one and nine tips), which makes it easier to precisely control forming temperature and limits the thermal and fluid interaction between fibers, simplifying measurement and analysis of the system.

The system is referred to as a small marble-melt fiber-forming position because it melts marbles instead of powdered glass. The chemical composition of the powder and the marbles is identical, so that once the glass is molten its original form no longer affects operation of the system. It is referenced here as "small" because it has, at most, nine fiber forming tips. PPG also has larger fiber forming positions which also melt marbles but are considerably larger, having on the order of 100 fiber forming tips and having significantly different geometry from the systems with which this project is concerned. The well of the small marble-melt position is formed entirely of platinum, continuous with the platinum of the bushing. It is electrically heated through the lower portion and is small enough that no additional heating is required further up. The bushing control thermocouple is welded a small distance up from the actual bushing, such that temperature control is more precise than on a production forming position.

There are two such systems with which this project is concerned; a single-fiber system and a nine-fiber system. The two have nearly identical glass well geometry. The single fiber small marble-melt fiber forming position was not originally designed for the type of research being done with it now and its origins explain the discrepancies between it and the full-scale process and some of its limitations. The original purpose of the system was to form fibers for tensile tests on glasses with various compositions. The sample needed for such a test was only on the order of 30cm. The system would have to be run for a period of time to assure that temperature and airflow conditions had reached steady state before the sample was taken. Several samples would be taken on a given day. Still, this did not account for a very large mass of glass being necessary. Because of this the system was designed with a shallow glass well and not enough glass depth to make up the necessary pressure to run the system. Additional pressure was added on by air pressure top of the glass. Precise control of the head pressure was not

necessary as the sample fiber length was short and precise diameter control was unnecessary. Precise winder speed control was also unnecessary, for similar reasons.

Optimization of the small marble melt fiber forming process is necessary to more closely match the behavior of the marble melt to the production line forming positions. Also, it is necessary to simplify the behavior of the marble melt position such that process variables can be isolated for further study. Variables that this project is interested in controlling include; glass head pressure, winder speed and stability, fiber vibration and ease of use of the entire system. Other system variables, such as glass temperature, glass composition, water spray and cross-air flow, are either to be considered already adequately controlled or are the topic of study in other current projects. The end result of single-tip and small-number-tip marble melt optimizations will be a process with fewer unknowns and variations. The process will be controlled such that relations between bushing temperature, cross-air flow and temperature, water spray variables, forming cone properties, fiber break rates, and fiber diameter can be explored in detail without too much interference.

Chapter 2

2 Head Pressure Control

2.1 Problem Definition and Requirements

The variation of glass head pressure has a huge effect on process variables of interest, in particular fiber diameter and fiber break rate. On the production line, forming positions run off a huge tank and the depth of glass in the fore-hearth controls the head pressure. This in turn is controlled by matching the rate of addition of fresh powdered glass to the known production rate. Since the tank has a huge reservoir and a fairly constant pull rate, averaged over many positions, this method leads to negligible fluctuations in glass depth. Control of the single tip marble-melt position is much less precise. Glass is added to the reservoir only once, at the beginning of the day or trial. Since the depth of the bushing well is much lower than on the production fore-hearth, air pressure is applied to the space above the glass. The small marble melt is the only process PPG utilizes that cannot run purely on glass weight. Since the system is pressurized and since there is only a small heated area for glass to melt in there is no good way to add glass during the course of a trial.

The current system for air pressure adjustment is very imprecise and there is no system in use for accurately measuring or calculating changes in the underlying glass depth over time. Over the course of a day, the underlying glass depth declines as glass flows through the bushing and the air pressure above remains constant. During a trial meant to simulate the production line this accounts for on the roughly a 25% change; from an equivalent of 35 cm (14 inches) of glass depth to an equivalent of 25 cm (10 inches) of glass depth with the well empty. The Figures 2.1, 2.2 and 2.3 show a geometric comparison between the production line, the single tip and the nine-tip bushings

and bushing wells. A 25% change in head pressure accounts for a change in mass flow of 25% as well. Fiber diameter can range from, for example, 15 μm with a full glass well to 12 μm when the well nears empty.

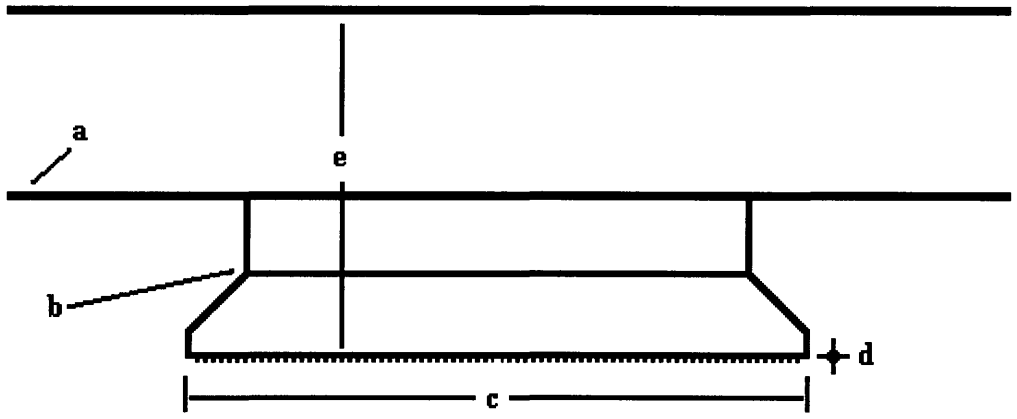

Figure 2.1: Geometry of Typical Forming Line Bushing Well

a. brick fore-hearth – continuous glass flow left to right
b. platinum bushing well extending below fore-hearth. 800-2000 cylindrical tips extend below. Set in insulating cement.
c. width on order of 45 cm (18 inches)
d. depth on order of 12 cm (5 inches)
e. total glass height 25 cm (10 inches)

Any improved system has to work within the confines of the existing bushing well geometry. Total glass level cannot be increased without altering current glass melter geometry. The current glass melter also does not have the capability of maintaining constant glass level by adding new glass during a run. So air pressure will continue to be used and will have to be variable. There needs to be some method of determining the depth of glass and thus determining the required air pressure. There is no known requirement for accuracy – it was simply designed as accurately as possible with the available equipment. The other requirement is simplicity of use. The method that requires the least user intervention was selected.

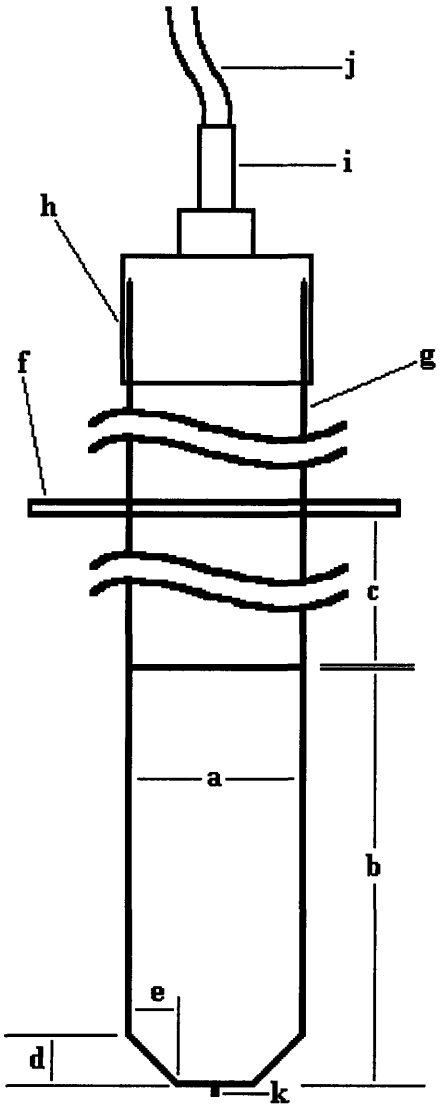

Figure 2.2: Single Tip Marble Melt Well Geometry

a. 2.86cm (1.152 inches)
b. 7.6cm (3 inch) high square section of well, 1.5mm (0.06 inch) thick platinum walls
c. 10cm (4 inch) high circular section of well, thin platinum walls
d. 0.95cm (0.375 inches) – angle on left and right sides – front and back at right angles to bushing.
e. 0.95cm (0.375 inches)
f. flange attaching platinum section to brass section – screwed together and sealed with high temperature gasket material
g. circular brass section
h. screw-on brass cap
i. quick-release fitting
j. air hose
k. single platinum fiber-forming tip, extending 3.2 mm (0.127 inches) below bushing plate, 2 mm (0.08 inches) outer diameter, 1 mm (0.04 inches) inner diameter.

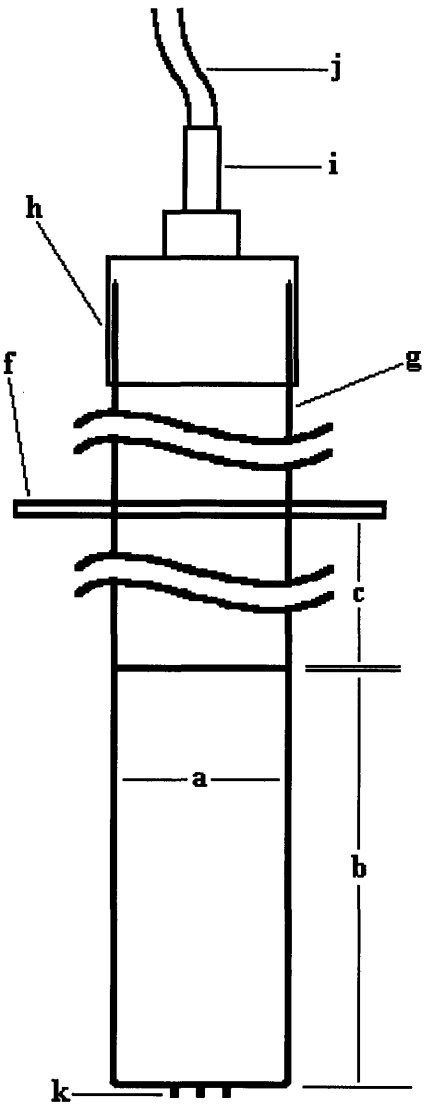

Figure 2.3: Nine Tip Marble Melt Well Geometry

a. 2.86cm (1.152 inches)
b. 7.6cm (3 inches) high square section of well with 1.5 mm (0.06 inch) thick platinum walls
c. 10cm (4 inch) high circular section of well with thin platinum walls
f. flange attaching platinum section to brass section – two sections are screwed together and sealed with high temperature gasket material
g. circular brass section
h. screw-on brass cap
i. quick-release fitting
j. air hose
k. nine platinum fiber-forming tips, 3.7 mm (0.145 inches) apart, extending 3.2 mm (0.127 inches) below bushing plate, 2 mm (0.08 inches) outer diameter, 1 mm (0.04 inches) inner diameter.

2.2 Pressure Regulation Methods Considered

Both feedback control and off-line control based on calculations were considered. Either method requires replacing the air pressure adjustment control with something which is more precise and which can be controlled automatically. This problem needed to be solved first, before the actual control can be implemented. Research was done into different pressure control devices and the most appropriate was be selected. Selection criteria were: precision of the device; operating range of the device; and cost.

Off-line control could be approached in a couple of different ways. There currently exists a forming cone model that predicts, among other things, the mass flow rate of the glass based on several process variables. This model was created with multiple-tip production-line positions in mind, so some work would need to be done to correlate the model with the behavior of the single tip. This could be accomplished by pulling packages under various conditions, weighing them to determine mass flow, and comparing the results to the forming-cone model prediction. Package is the term PPG uses for a length of continuously wound fiberglass, pulled from winder startup to winder stop or fiber breakage. Conditions to be varied include; head pressure, bushing temperature, and winder speed. In this case, head pressure would be approximated based on an initial known glass depth minus half of the measured mass of the package pulled, to find an average glass depth. Glass depth would be calculated based on known bushing well dimensions and measured mass of marbles inserted into bushing well at the beginning of the run with mass of glass drained measured and subtracted from this. Once this data was collected, it would be used to either adjust the code of the forming cone model or develop calibration curves to adjust the results of it to the single tip. Head pressure would be adjusted incrementally throughout the day with the rate of change based on calculated mass flow for the type of package being pulled.

A simpler, though less accurate, method would be to calculate an averaged mass flow throughout a full day of operation and adjust pressure at a constant rate. The appropriate mass flow rate can be determined by timing how long it takes a known mass to empty out of the bushing well. To determine whether this method has acceptable error margins it would be necessary to determine a range of products the single tip position will be used to produce and to pull several of them throughout the course of a day, weigh them, and determine the variation in mass flow rate.

For both of the above methods, variations in inside dimensions of the bushing well could have a sizable effect on glass depth and thus head pressure. Measurements should be done of the volume of cold glass left on the sides of the bushing well after the bushing well is drained. If the magnitude is large enough to make a difference, calculations of glass depth should take it into account.

The control method with the best potential accuracy is feedback control. A sensor could be placed in the bushing well measuring either pressure at the base of the pool of glass or measuring glass level. Level sensors would have to be able to withstand high temperatures (up to 1650 K or 2500° F) and measure a range of 7.6-10 cm (3-4 inches) (the approximate depth of the glass in a single-tip bushing well) within an acceptable error margin. Current production line control conditions and precision of available air pressure control devices would determine acceptable error. Pressure sensors would have to be able to withstand similar temperatures and be able to measure pressures on the order of 5.5 kPa (the pressure induced by 25 cm or 10 inches of glass) and have reasonable precision.

Of the above methods it was determined that measuring glass level and adding necessary air pressure on top of this with an automatically controlled pressure regulator was the best solution. It was decided that calculation methods would involve too much user input – entering parameters into a model or weighing packages. A feedback method could be programmed to adjust for some system parameters automatically. A calculation method would also be less able to deal with conditions that vary over the course of a run. Pressure sensors would be problematical to employ due to the high temperatures involved and the corrosive chemical environment of the molten glass. An appropriate glass level measurement system was identified that determines glass level based on resistance of the glass. This system required calibration, which took up the bulk of effort involved in this portion of the project.

2.3 Equipment

2.3.1 Glass Level Sensor

The level sensor selected for this project was developed at PPG in 1997. It was intended for use on the large marble-melt positions where it would be hooked up to a controller that would add glass from a pre-melter to keep the glass head level constant. The system works by measuring the resistance of the glass between a probe and the

side-wall of the bushing well using a Wheatstone bridge and a rectifier to convert the AC signal to DC. The signal passed through the glass must be AC, because a DC signal has a tendency to cause platinum to erode. A diagram of the level sensor circuitry is shown is Figure 2.4.

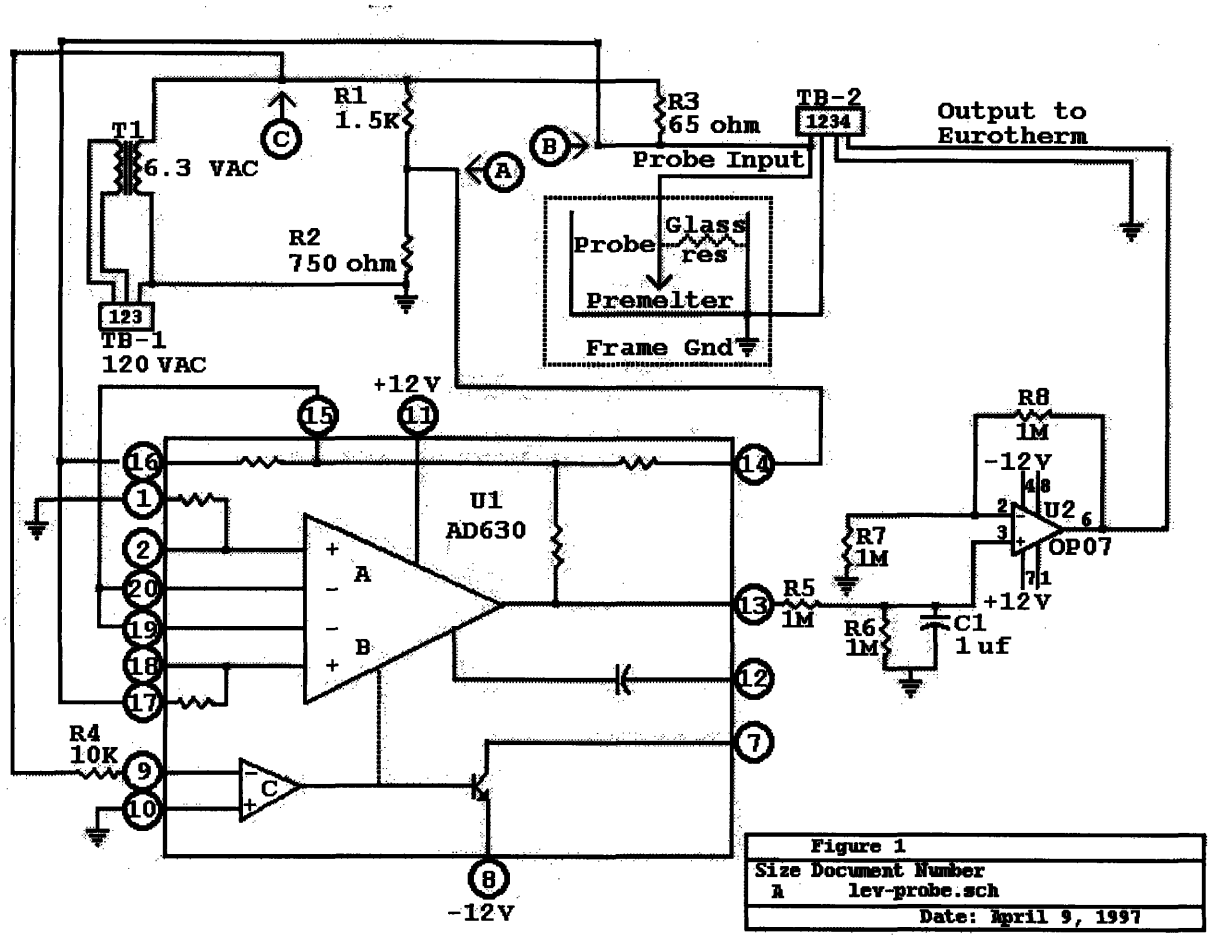

Figure 2.4: Diagram for Original Probe Electronics Setup

The above diagram was obtained from Hal Stedrack at PPG's Fiberglass Research Center. It indicates how the probe would be set up for use on the large marble-melt position. The Eurotherm Controller, indicated in the diagram, is a unit similar to the temperature controls on the bushings. It takes in a set point and attempts to maintain it as constant as possible. In this case it would be maintaining a constant glass depth by addition of fresh melted glass to be melted in the pre-melter.

As there are only minor differences between the setup indicated in for the large marble melt fiber-forming position and the setup on the small marble melt fiber-forming position, the same diagram is used for

representation. On the small marble melt the probe is inserted into the glass melter instead of the pre-melter (the small marble melt has no pre-melter – glass is melted in the same well that acts as a reservoir). The output, instead of going to a Eurotherm Controller, in sent to the data acquisition card for use in a data acquisition and signal generation program what will be described later in greater detail.

Basic knowledge of resistance was used to assess the suitability of the level-sensing system to the geometry of the single-tip bushing well. Resistance is inversely proportional to glass depth, if cross-sectional area, glass composition and glass temperature are held constant. Resistance is also a function of temperature, as indicated in Figure 2.5. The data in Figure 2.5 are courtesy of Cheryl Roach, at PPG's FiberGlass Research Center. Temperatures at which data was taken for this project are indicated with larger points on the graph. Resistance data was only available at every 55.6 K (100° F), so the points in between 1475 K (2200° F) and 1535 K (2300° F) have been extrapolated. Resistance is given as:

Equation 2.1 $$R = e\frac{l}{A}$$

where e is the resistivity, l is the length of the resistor and A is the cross-sectional area.

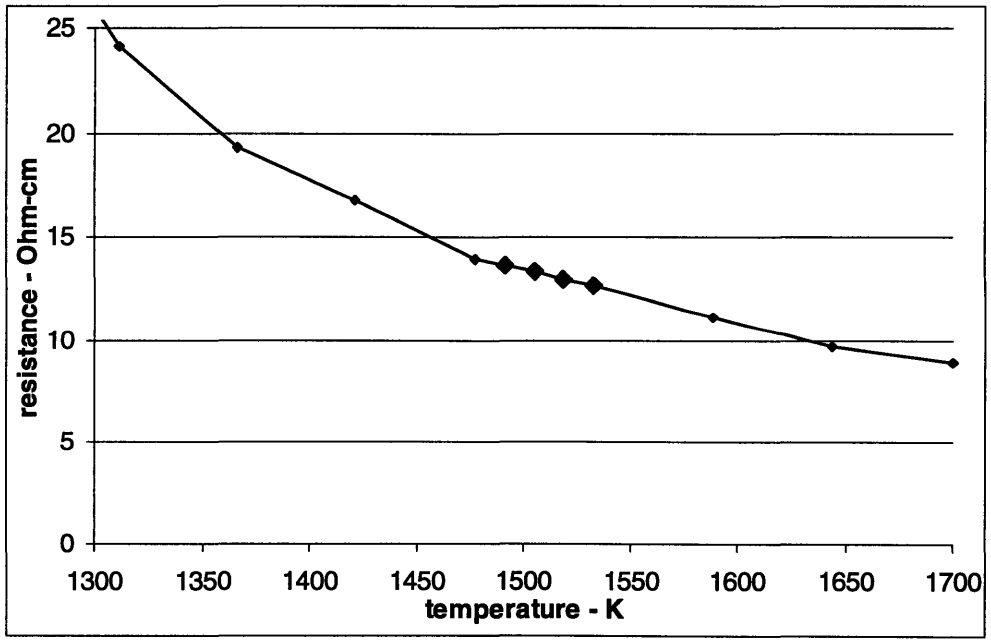

Figure 2.5: Glass Resistivity in Relation to Temperature

The original system was tested with two different probes; a platinum probe of 2.3 mm (0.09 inches) in diameter, and a platinum-covered long-life thermocouple of 1.5 mm (0.06 in) in diameter. A thermocouple was used because of the sensitivity of glass resistance to temperature and because of the large size of the pre-melter on the position the level-sensor was originally tested on. The bushing well was large enough that the temperature read by the bushing thermocouples did not necessarily match the temperature at the location of the probe. The resistivity of e-glass varies 12.7-13.7 Ohm-cm (5-5.4 Ohm-inches) between 1490 K (2225° F) and 1535 K (2300° F). This would cause the resistance to vary by 7.3% in this temperature range, a difference significant enough to necessitate taking glass temperature into account in interpreting probe output voltage. The magnitude of resistance change due to the differing geometry of the single-tip well (vs. the marble-melt well) was not known. It was assumed that the resistor values in the Wheatstone Bridge would have to be altered due to the difference in geometry of the large and small marble melt bushing wells, but it turned out that the resistance range was comparable for the probe placement selected.

It was decided to build the pure-platinum probe, because the probe will be placed only 9.53 mm (0.375 inches) from the bushing-control thermocouples and it was assumed that the few degrees of difference that may be present is a small enough temperature error that it can be ignored. There were also problems with using a thermocouple; the thermocouple probe used in the original system was not platinum-coated over a long enough section to work with the geometry of the single-tip bushing well. The section of the probe that was not platinum coated would be dissolved by volatile compounds in the air space above the glass. The other option was to have a thermocouple built and housed in a platinum tube, but the diameter would have been much larger and it was thought that it might lead to the resistance being too low. The probe is a 2.3 mm (0.09 inches) diameter platinum wire and is sheathed in alumina (a ceramic) above the glass level to give it support against deformation and to electrically isolate the wire from the bushing well. The probe has been mounted in the screw cap for the bushing well. This cap also contains the nozzle where the air-pressure has been introduced. The air nozzle was moved to the side of the cap to allow the platinum probe to be mounted through the top. Figure 2.6 shows the probe inserted into a single-tip bushing well. The configuration in the nine-tip well is similar.

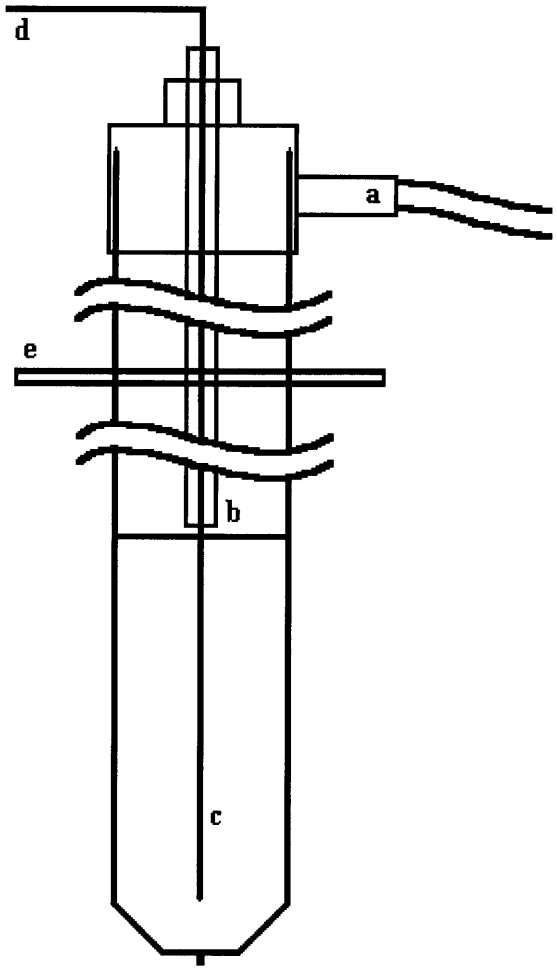

Figure 2.6: Platinum Probe Geometry in Single-Tip Bushing Well

a. Air pressure hose with quick-connect fitting moved to side of cap to accommodate probe
b. Alumina sheath stiffens probe against bending and acts as electrical insulation between platinum wire and brass fitting that screws into bushing well. 10 cm (4 inches) of platinum wire left exposed below sheath, 26.5 cm (10.5 inches) total sheath length, 6.3 mm (0.25 inches) outer diameter, 3.2 mm (0.125 inches) inner diameter
c. Platinum wire, 2.29 mm (0.09 inches) diameter
d. Platinum wire attached to positive input of probe electronics from this point
e. Bushing well attached to ground of probe electronics from this point

The glass level measurement system consists of the 2.3 mm (0.09 inches) diameter platinum probe housed in an alumina sheath, the electronics from the previous probe, a DAQ card (an AT-MIO-16E-10 from National Instruments), and a visual basic program for data acquisition. The visual basic program was originally written by Chris Bruckhoff and was modified for this project by Christa Ansbergs. It was first tested refined in the single-tip marble melt bushing well. The data acquisition program is designed to take data as fast as possible and display the average of each 100 points on the screen. This ends up being

about one such average every 2 seconds, if the computer processor is not multitasking. The program then saves to disk the average of all points taken each minute.

In work on the nine-tip system, Lab-View is being used to control input data and output set-points. A VI (Virtual Instrument) is configured to read an input of 1-10 V from the probe and record this voltage into a file. The number of points taken per second can be adjusted within the program with default of 25 and the number of seconds to average and save can also be adjusted. After many points are taken and averaged the value if sent to another VI to compute the required output. This voltage is then sent to an output on the card. The platinum probe and I/O card used are the same.

A new set of electronics were built for use on the nine tip system following the schematic in Figure 2.4, as the old set could not be sent from PPG. The completed system was tested with a 25-Ohm potentiometer in series with various fixed resistors to get a calibration curve. The curve matched closely with curves from the previous electronics, confirming that it had been built correctly and that all components were functioning within specifications. Calibration curves for both sets of electronics are shown below, in Figure 2.7.

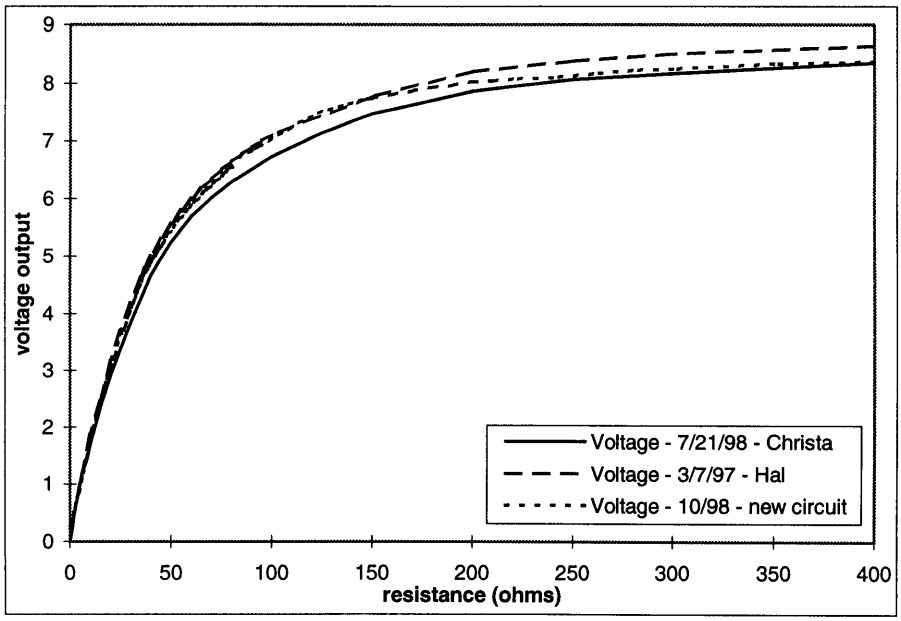

Figure 2.7: Calibration Curves for Old and New Probe Electronics

Differences in the curves for the original circuit as measured by Hal and Christa are expected to be due to burn-in of the parts over time and some measurement error. Differences between the old and new circuit are expected to be due to slight variations in the parts used.

2.3.2 Pressure Control

The pressure adjustment device selected is the Asco Joucomatic Sentronic Pneumatic Proportional Valve, series 601. This is a solenoid valve that contains a pressure sensor at the outlet and adjusts force going to the solenoid coils until output pressure reaches the set point. A higher pressure is supplied to the inlet. An input voltage or current controls the set point. The smallest range the valve can be calibrated to cover is 0-1psi. To simulate the production line, the range this valve will need to control is from approximately 3.5-5.5 kPa (0.5-0.8 psi). Since the system will not always be run to simulate the production line a valve with a somewhat larger range has been selected, 0-7.5 psi. Error is in the range of 0.5% of total span. This corresponds to the pressure changing in increments of 0.25 kPa (0.035 psi), or about 12.5% of the total change. In a simulation of the full scale fiberglass forming process this represents an error of 4.5%.

The valve requires a 24 V power supply and draws a maximum of 500 mA current. The pressure source of the valve is attached with 6.35 mm (0.25 inch) tubes through a hand-adjust pressure-regulator to a ~120 psi shop air source. The valve is designed to work with a supply pressure of no more than 30 psi, so the regulator is used to limit the supply pressure to within specs. This value does not have to be exact so a hand-adjust valve is adequate. The hand pressure adjust has also been used as an interim solution to adjust air pressure until calibration curves could be developed for the level sensing probe and hooked up to the pressure adjust valve. The valve also requires the input air to be filtered to 50 μm, so an air filter from purchased McMaster-Carr that filters to 5 μm was attached to the supply line upstream of the hand-adjust pressure regulator. Additional filtration will not be harmful and it was the least expensive model of the appropriate size.

2.4 Probe Calibration Methods

Calibration curves were made by running the system from the well being full to completely empty, collecting voltage data from the probe electronics with the I/O card continuously. A rough calculation based on an average marble size indicated that the single tip well could hold approximately 14 marbles and the nine tip well could hold 15. The single tip well was generally run with only 9 or 10 marbles, as the smaller number of tips meant a lower glass flow rate and even this amount of glass took about six hours to drain from the bushing during standard operating conditions. The nine-tip system was generally run with 14 or 15 marbles.

Marbles are inserted into the well cold and bushing temperature is slowly brought up to 1590 K (2400° F) over a time of 30 minutes to one hour. On the nine-tip setup it is possible to perform multiple runs in the course of a day and sometimes the well was refilled while still at elevated temperature. To do this the bushing controller would be set to maintain constant power instead of trying to maintain constant temperature. The bushing temperature would fall rapidly at first and eventually begin to heat back up. Once it began to heat up the bushing controller was again set to control temperature and temperature was slowly brought back up to 1590 K (2400° F). The temperature is held at 1590 K (2400° F) for an hour to assure that all marbles have melted, that impurities in the glass are burned away, and that air bubbles percolate to the surface of the glass. Such bubbles, if still trapped in the glass, could cause a false glass height reading by the probe. This is known as curing the glass. During curing on the single-tip system an air hose was directed at the tip to cool the glass at the exit and limit the mass of glass which dripped during this time. On the nine-tip system this was not done. The platinum level sensing probe is inserted into the well at the same time as the marbles, but due to the narrow diameter of the well it cannot fit past the marbles. It is left resting on top of the cold marbles and allowed to slide down into the glass as the marbles melt.

After the hour of melting time is up the temperature is brought back down to operating temperature. This takes on the order of 10 minutes. The platinum probe is set to its operating height of 0.95 cm (0.375 inches) above the bushing. The probe is pushed down until it makes contact with the bushing (though

gravity has usually performed this operation already during the melting phase) and this height is marked on the alumina sheath. It is then drawn up until 0.95 cm (0.375 inches) more of the sheath is exposed and the brass fitting is tightened in place. Air pressure is then brought up to the desired level for the run and maintained constant for the duration of the run. The data acquisition system is started up some time between initial glass warm-up and final head pressure setting, though the data is only used starting at the time the first package is wound in. It was found that monitoring voltage during startup was often useful as voltage outputs gave insight into the behavior of the probe and electronics and aberrant behavior could indicate failures in some part of the level sensing system.

The height 0.95 cm (0.375 inches) was chosen as a compromise between having the probe far enough from the bushing for glass height change to significantly alter total resistance and close enough to have the level sensing system be accurate over a useful range. On the single-tip system, 0.95 cm (0.375 inches) also happens to be the height at which the slanted sides of the bushing well begin and the bushing well cross-section begins to change. As a result the calculation of glass depth based on mass becomes slightly more complicated; for a curve-fit of glass depth vs. time a separate curve would have to be made for this lower section and thus data reduction effort is increased. It seemed worthwhile to avoid this. Although the nine tip bushing well has no slanted lower section, it was determined that the 0.95 cm (0.375 inches) probe height was appropriate and that uniformity in this would lead to better comparisons of data between the two wells.

The probe was tested for a range of different operating conditions. On the single tip system a standard set of conditions was developed and used for several test runs for the purpose of assessing repeatability. These settings are; 1505 K (2250° F) bushing set temperature, 9.14 m/s (1800 ft/min) winder speed, 5.5 kPa (22 in-H_20) air pressure above the glass, and ambient air conditions (no forced air flow). In other runs these setting were altered to determine system sensitivity to them. A low speed run was taken with the winder at 4.57 m/s (900 ft/min) (other conditions the same) and the high pressure run was taken with head pressure at 8 kPa (33 in-H_20) (other conditions the same). It was determined that winder speed and head pressure variables do not affect probe readings, other than by changing the glass flow rate. Since glass height is already being separately calculated for all runs it was seen as unnecessary to track winder

speed and head pressure on future calibration runs. Bushing, temperature, however, alters glass resistance and thus does affect probe readings. Separate calibration curves were thus made for bushing temperatures of 1490 K (2225° F), 1505 K (2250° F), 1520 K (2275° F), and 1535 K (2300° F), which covers the useful range at which the system can be run without excessive fiber breakage. Extrapolation can be used to predict probe response somewhat outside of this range and interpolation to determine behavior for other temperatures within this range. The number of temperature calibration points was limited based on time constraints.

Glass depth at different times during the day was calculated based on; the initial mass of glass, glass density, known bushing-well dimensions, and mass of glass having exited the bushing well. Mass of marbles inserted into the well was measured, as was the mass that dripped out during melting and curing of the glass. Packages were measured at regular intervals (between 15 and 30 minutes) and their start and stop time recorded. The length of time at which packages were taken varied somewhat due to fiber breakage, but attempts were made to keep the package times uniform. Glass that dripped between packages was also collected and kept so that accuracy of measurements could be checked. The mass of all packages ($m_{package}$) and drippings (m_{drip}) should add up to the initial mass measurement of marbles inserted into the well, and in all cases it did to within ±3%, calculated as

Equation 2.2 $$error = \frac{m_{initial} - \sum m_{package} + m_{drip}}{m_{initial}}.$$

On the single tip setup the mass of glass drippings between each two packages was small enough not to be easily measurable and thus only the sum of all drippings was measure. In the nine-tip setup the mass flow rate was significantly larger and thus drippings between packages were recorded separately.

For work on the single tip setup packages were first cooked at 379 K (223° F) for 20 minutes to get rid of excess moisture then weighed on a balance. It was determined that the amount of moisture being absorbed was insignificant in relation to other measurement error and so this practice was dispensed with in work on the nine-tip system. Packages were initially weighed to the nearest 0.001 g since a balance with that accuracy was available. However, when it became necessary to purchase a new balance for work on the single tip, calculations indicated that 0.1 g of accuracy was all that was necessary, based on the

accuracy of output which the pressure adjust valve will be able to provide. A mass of 0.1 g of glass accounts for a depth change of 0.05 mm. A full run would consist of at most 20 separate mass measurements, accounting for a total accumulated error of 2 g mass or 1 mm depth by the end of the day. The pressure adjust valve which will be used is capable of adjusting to an accuracy of 1 cm worth of glass depth.

Depth at any given time was calculated as:

Equation 2.3 $$depth(T) = \frac{m_{initial} - \sum (m_{packages} + m_{drip})}{\rho_{glass} \times A_{melter}}$$

Where the summation is for measured mass of all packages and all drips up to time T. A_{melter} is the cross sectional area of the glass melting well. The value of glass density used was 2.5 g/cm^3. For times between packages when mass was not directly measured mass was calculated as:

Equation 2.4 $$m_{drip} = \frac{m_{previous-package}}{t_{previous-package}} \times t_{drip}$$

Where t_{drip} is the time the melter was left dripping between the end of the previous package and the start of the following package, $m_{previous\text{-}package}$ is the mass of the previous package and $t_{previous\text{-}package}$ is the time the previous package ran for. In this manner a series of points giving glass level vs. time would be obtained. Since the error in tracking mass of glass in the bushing was determined to be less than 3% at the end of all runs, 3% is the estimated error for depth calculations mid-run as well. Third order polynomial curve fits were produced with Stat-Graphics and Microsoft Excel. In some cases conditions were not uniform over the full course of a run. Several times the system head pressure was turned down and left for an hour or so while the operator was not available to collect packages. In these cases separate curves were obtained for the different conditions; one curve for before the pressure was changed, a linear fit while the pressure was turned off (because only two points are available), and another curve-fit of up to 6th order for the time after.

For all calculations it was assumed that the bushing well was uniformly square, though there were probably some slight variations. It was also assumed that no glass remained in the well after the head pressure air began exiting through the tips, though some small amount probably remained stuck to the

walls, due to the relatively high viscosity of molten glass. When the output voltage of the probe reaches a final value (approximately 8.7 V) and remains constant it is assumed that the glass level has reached the end of the probe and is 0.95 cm (0.375 inches) above the bushing. There may be some variation in output voltage due to molten glass sticking to the probe and forming a contact even as the glass level falls below the level of the probe, but it assumed that this effect does not last long and can be ignored. There does not seem to be any simple way of observing this to assure that it is the case.

Data is initially recorded as probe electronics output voltage vs. time. This is combined with level vs. time data obtained in the above manner. In this fashion voltage vs. depth curves have been obtained and up to 6^{th} order polynomial curve-fits (depending on what lowest order best fit the data) were produced with Stat-Graphics and Microsoft Excel. Polynomials of increasing order were created until the R^2 index of accuracy (see section 2.6) no longer improved. These are, in turn, combined with the specifications of the pressure adjust valve, consisting of required input voltage vs. desired pressure output, which is calibrated to be linear by the manufacturer. The final equations entered into the marble melt control program relate measured probe electronics voltage directly to desired output voltage to the pressure control valve. The final system will also determine when the 0.95 cm (0.375 inch) glass level has been reached and will continue to calculate glass level based on extrapolation from previous data as well indicate to the user that the glass is about to run out and needs to be refilled.

Validation of the pressure adjust system was performed by running the small marble melt position with the pressure adjust valve installed and collecting packages in the same manner as the original calibration process. As data from this validation run is just as valid as data from initial calibration runs, voltages were taken during the calibration run and used to improve the accuracy of the calibration, in the event that the original calibration curve was found to be inaccurate. This step was never performed in the single-tip model as the pressure adjust valve did not arrive in time. Work on the single tip was largely to work out the details of the level measurement system and to work out initial problems with it. The nine-tip system will be run with the level sensing and pressure adjust equipment permanently installed.

2.5 Problems Encountered and Solutions

When the probe and electronics were initially hooked up to the single-tip system output was not in the voltage range expected. Figure 2.7 illustrates the probe voltage output ranging between 0 V and 8.7 V, but as Figure 2.8 illustrates, the voltage range recorded on from the first attempts at calibration curves varied to negative voltage values. The curves shown in that graph are sorted by date, as they otherwise had no defining characteristics. All were taken at the standard conditions defined in section 2.4; 1505 K (2250° F) bushing set temperature, 9.14 m/s (1800 ft/min) winder speed, 5.5 kPa (22 in-H_20) air pressure above the glass, and ambient air conditions (no forced air flow). There is some scatter in curve placement because depths were not explicitly calculated for each curve. An average depth curve-fit was established for all of the above graphs combined and their various times were matched to it at a single calculated height of 2.8 cm (1.1 inches). Since all curves were taken at the same nominal conditions the amount of variation shown in the graph cannot be accounted for by this simplified mass flow calculation.

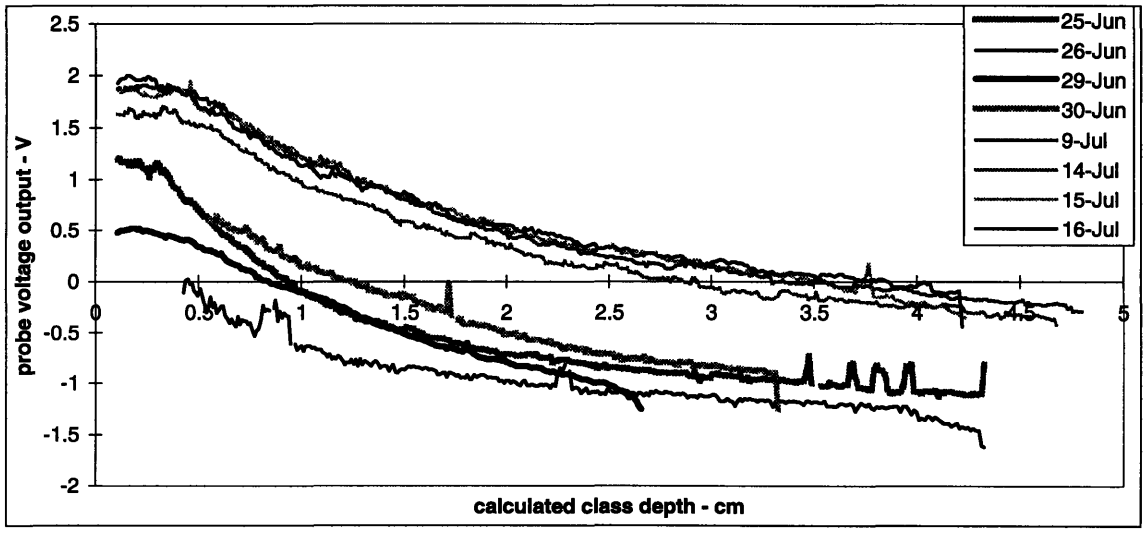

Figure 2.8: Voltage vs. Glass Depth Initial Calibration Curves

Between June 30th and July 9th a repair was made to the bushing controller which resulted in varied power output levels. This was taken as evidence that variation of curves and voltage offset of curves was

due to the system responding to bushing power. The following experiments were undertaken to confirm this.

During cool down of the bushing after a trial bushing power was reduced in large increments of 10% of total bushing power at a time. This caused temperature to drop off from an initial value of 1590 K (2400° F) rapidly at first and then more slowly until it reached 700 K (800° F), the temperature at which the power could safely be turned to zero. If the system had been responding only to temperature it was expected that the system response would drop or rise rapidly at first and then more slowly. If the system was responding to bushing power it was expected that output would drop or rise rapidly at once and then hold steady. The second phenomenon was observed. At high bushing power (30-80%) voltage output fell by a small increment with each drop in bushing power. At low bushing power (0-20%) voltage rose by large increments with each drop is bushing power. The results are shown in Figure 2.9. After time 16:48 there is a large spike up to 3 V at 10% power and then to 8.7 V with 0% power. This is not shown simply for purposes of increased resolution in the range in which the remainder of the data fell. Figure 2.10 illustrates the power settings used to create the plot in Figure 2.9.

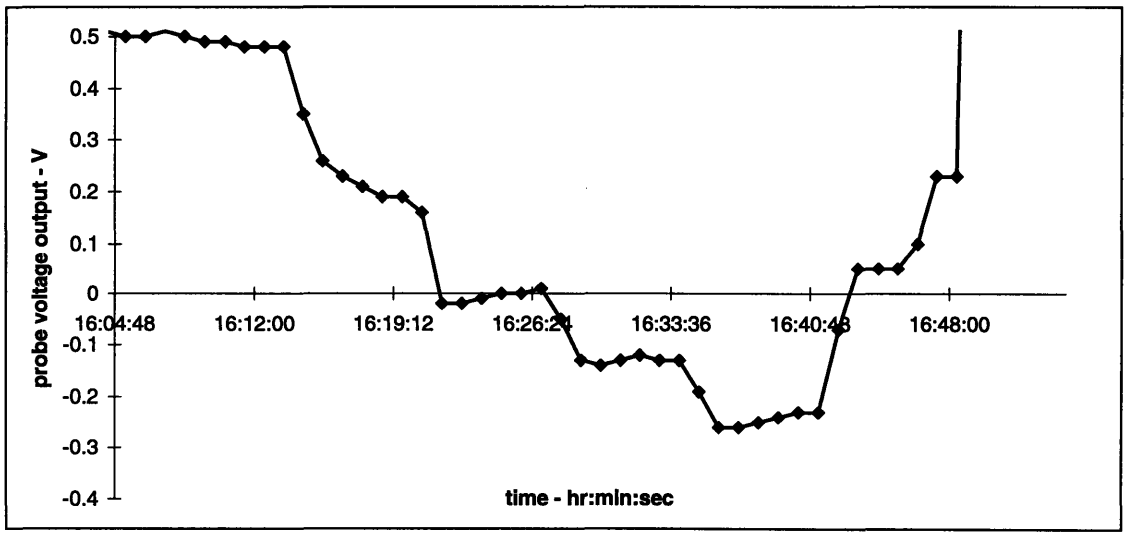

Figure 2.9: Probe Output Voltage with Empty Bushing-Well and Power Reduced Incrementally

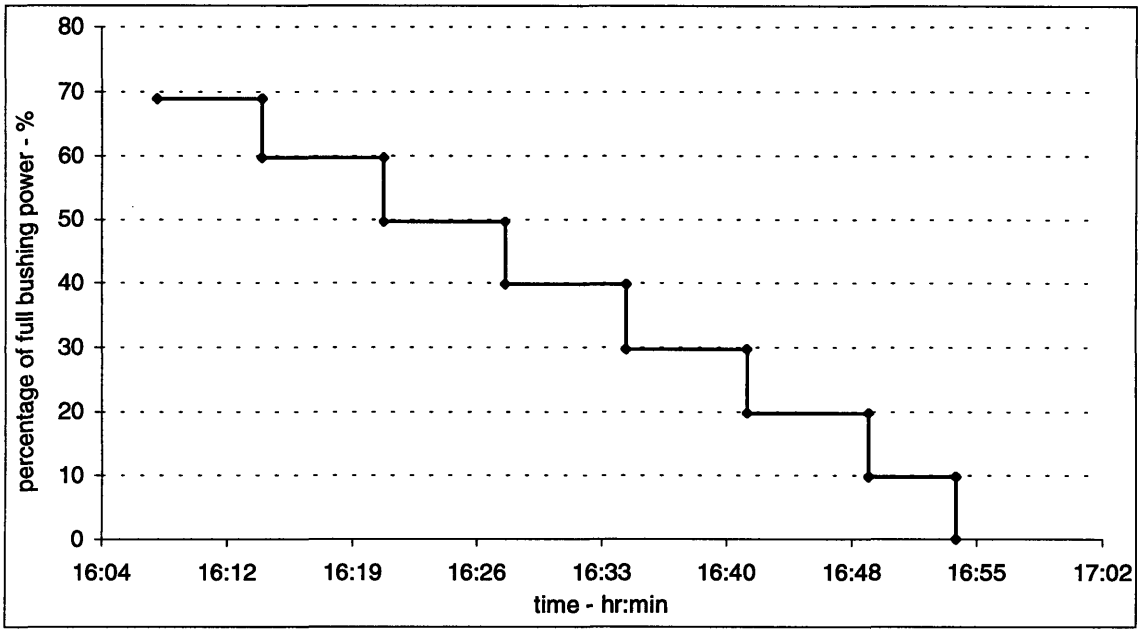

Figure 2.10: Power Settings For Bushing Power Response Test

Since the electronics for the probe run on an AC signal the system is phase sensitive, the sign of output from the rectifier is determined based on whether the signal coming out of the Wheatstone bridge leads or lags the input signal. Power to the bushing is also AC and flows through the bushing well from one side to the other. The system was tested with the probe bent so that it was no longer centered in the well, thus it should be more responsive to the bushing power on the side it was bent towards. Probe voltage output readings were then taken as the probe was rotated within the bushing well at approximately 15-minute intervals. This was intended to be a qualitative rather than a quantitative test, as it is unknown how far off the probe was actually skewed from the center. It was initially offset by about 6.4 mm (0.25 inches) or 9.5 mm (0.375 inches) but since the probe deforms easily at high temperature it was uncertain how closely the probe retained this positioning. Another source of uncertainty in this test is what magnitude of an effect the probe being at different locations within the bushing well would cause. The precise level of bushing power at different locations is not known.

After rotating the probe at 45° intervals twice around the bushing well it was found that the probe had been rotationally deflected by about 15° from the external reference. This added another measure of uncertainty. Despite all of these uncertainties some effect from moving the probe was found. When the

probe was facing to the right side of the bushing (where the ground of the probe electronics is attached and where one of the two ears that feeds power to the bushing is attached) the output voltage was much lower than in all other positions. Figure 2.11 shows the results of this test for several different glass levels. Since the precise glass levels are not known, the trials are marked only by what date they were taken on.

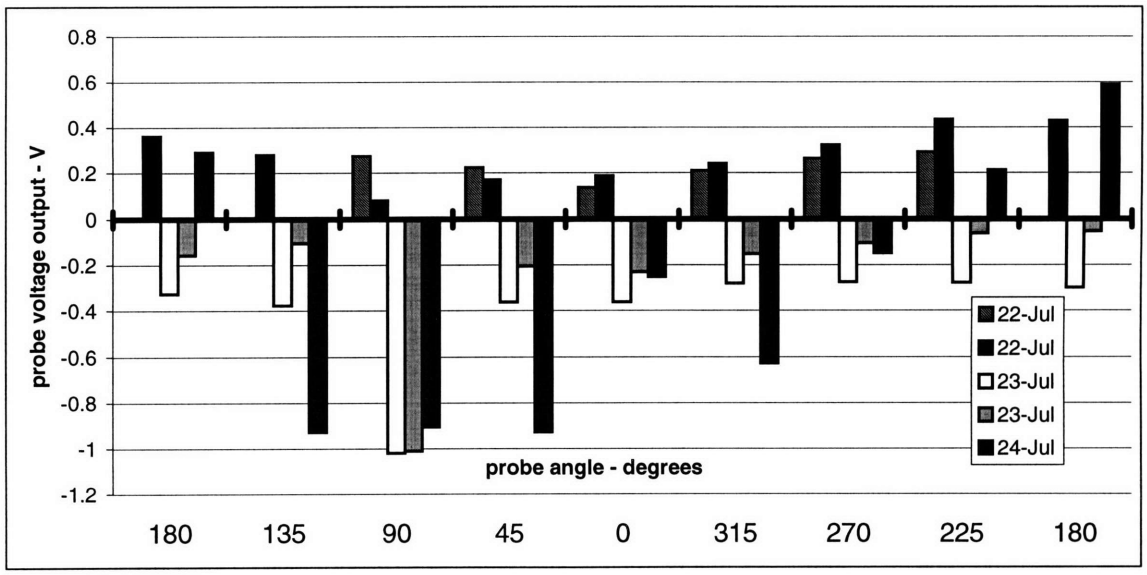

Figure 2.11: Probe Voltage Output for Skewed Probe With Various Glass Levels

During these trials the glass level was frozen off with an air hose so that very little glass dripped over the course of the day (on the order of 1 gram per cycle around the bushing well). The zero reference for angle was the back of the bushing well, the side facing the power transformer. At each point the probe was held for at least 15 minutes, not counting the time to reposition the probe. Each above point is an average of 10 minutes during this interval; the first three minutes were not counted as it was assumed that this time would allow the system to equalize to the new conditions. No attempt was made to correlate output to glass depth, as the above data is qualitative rather than quantitative due to numerous uncertainties; the correlation would not be very meaningful. However, some of the above variation was thought to have been caused by variation in the depth of the probe after each adjustment. The probe was moved by loosening the nut that holds it in place, rotating it to the new angle, and resetting the depth before tightening the nut. Error in setting depth would not have exceeded ±1.6 mm (±0.0625 inches).

Data shown in Figure 2.12 was taken with the probe set at 180°, to determine how much of an effect changing the probe height has on the voltage output. This indicates that error would be in the range of 0.1 V and could not account for the magnitude of the variations seen in the above graph. Bushing power effects must be the answer.

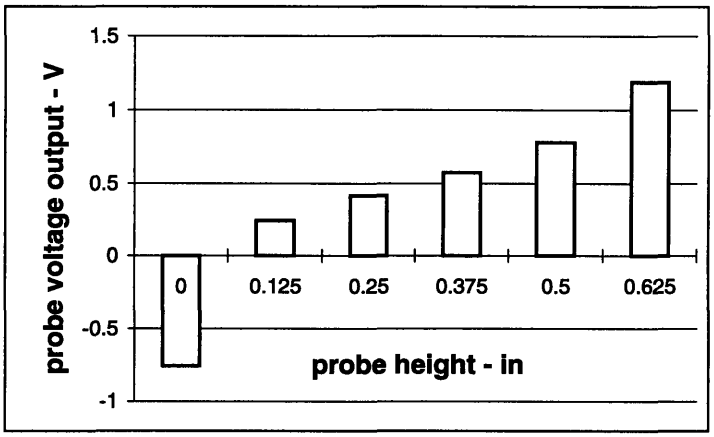

Figure 2.12: Probe Voltage Output vs. Probe Height Above Bushing

Once it was determined that bushing power was causing problems, an attempt to remove the effects was made. The probe electronics were grounded to the bushing frame (metal support structure), in addition to the ground connection to the bushing well, which was already in place. After doing this probe output voltages were observed in the appropriate range and with great reduction in high frequency fluctuations. It is not entirely clear why this was effective.

Another problem encountered were pressure losses due to leakage of the gasket seal between the platinum and brass sections of the melting well. This caused air head pressure settings of significantly higher than 5.5 kPa (0.8 psi) to be necessary in order for glass to flow rapidly enough for fibers to form. Resealing this gasket eliminated the problem and the system was able to run with the pressure again in the 1psi range. It was then decided that a new pressure control valve should account for this increased range, in case the problem was encountered again.

Finally, problems were encountered hooking up the pressure adjust valve to power. The first power supply was damaged in the process. New copies of both were purchased and the new power supply was fused to prevent over-current conditions.

2.6 Probe Calibration Results

Data in this section is presented first as raw data of voltage vs. time, the way it was collected from the data acquisition system. Data are labeled with conditions relevant to the run as well as the date on which the data was taken, for the purpose of distinguishing the various curves. Graphs of glass depth as calculated using Equation 2.3 vs. time are presented next, as well as curve-fits to this data and their polynomial equations. The polynomial fits and accompanying R^2 values are presented, where t is the time in days (because the graphing program formats time that way). The R^2 value indicates the accuracy of the curvefit and is calculated by the following formula:

Equation 2.5
$$R^2 = 1 - \frac{\sum\left(Y_j - \tilde{Y}_j\right)^2}{\left(\sum Y_j^2\right) - \frac{\left(\sum Y_j\right)^2}{n}}$$

Where Y_j are the data points and $\tilde{Y}_j$ are the values calculated using the curve-fit. The data are then combined and graphs of voltage vs. depth are presented. Finally curve-fits of the voltage vs. depth data representation are presented along with the data they represent, with each curve being formed from a combination of all data taken at a given temperature setting. These graphs are included separately from the graphs of voltage vs. depth data because them large number of data sets obscure the curve-fit. All such graphs are sorted by the bushing temperature at which the data was taken. For the purpose of comparison curve-fits for all temperatures are presented together.

2.6.1 Single Tip Results

Run conditions in this section are standard, as defined in section 2.4, unless otherwise indicated. Because of time constraints, each temperature is represented by only two data sets. The bushing temperature 1505 K (2250° F) has a greater number of data sets because it was used as the standard condition. It is the temperature at which the final system will most often be run. The polynomial curve-fit for the data at 1505 K (2250° F) includes the data at altered pressure and winder conditions, as it was concluded that the probe output is not affected by changing these conditions. The lowest of the five data sets was, however, removed from the curve-fit, because it differed significantly from the other four and it was therefore thought that it was not representative of actual probe behavior. The lower data set is still represented in the graph of original data sets and the graph of voltage vs. depth data.

	Bushing Temperature			
	1490 K (2225°F)	1505 K (2250°F)	1520 K (2275°F)	1535 K (2300°F)
Raw Data, V vs. Time	Fig. 2.13	Fig. 2.17	Fig. 2.21	Fig. 2.25
Depth vs. Time	Fig. 2.14 Equ. 2.6-7	Fig. 2.18 Equ. 2.9-13	Fig. 2.22 Equ. 2.15-16	Fig. 2.26 Equ. 2.18-19
Voltage vs. Depth	Fig. 2.15	Fig. 2.19	Fig. 2.23	Fig. 2.27
Curve-fit of V vs. Depth	Fig. 2.16 Equ. 2.8	Fig. 2.20 Equ. 2.14	Fig. 2.24 Equ. 2.17	Fig. 2.28 Equ. 2.20

Table 2.1: Single-Tip Data Representation by Figure Number and Equation Numbers

Data at 1490 K

Equation 2.6: ***Depth vs. Time curve fit for data Aug 6***

$$depth = -25326t^6 + 87737t^5 - 125311t^4 + 94399t^3 - 39539t^2 + 8715.6t - 783.63$$

$R^2 = 0.9999$

Equation 2.7: ***Depth vs. Time curve fit for data Aug 12***

$$depth = 11.709t^2 - 28.7t + 13.422$$

$R^2 = 1$

Equation 2.8: ***Depth vs. Voltage curve fit for data at 1490 K***

$$depth = 0.0095V^4 - 0.2053V^3 + 1.69V^2 - 6.7548V + 12.994$$

$R^2 = 0.9946$

Data at 1505 K

Equation 2.9: ***Depth vs. Time curve fit for data July 29***

$$depth = 1.5938t^2 - 17.051t + 11.411$$

$R^2 = 1$

Equation 2.10: ***Depth vs. Time curve fit for data July 30***

$$depth = 9.184t^2 - 25.843t + 13.85$$

$R^2 = 1$:

Equation 2.11: ***Depth vs. Time curve fit for data July 31***

$$depth = 4.2924t^2 - 18.636t + 10.992$$

$R^2 = 0.9999$

Equation 2.12: ***Depth vs. Time curve fit for data Aug 3***

$$depth = 7.5677t^2 - 22.899t + 12.385$$

$R^2 = 1$

Equation 2.13: ***Depth vs. Time curve fit for data Aug 4***

$$depth = 14.547t^2 - 37.291t + 17.325$$

$R^2 = 1$

Equation 2.14: ***Depth vs. Voltage curve fit for data at 1505 K***

$$depth = 0.0058t^4 - 0.1295t^3 + 1.1304t^2 - 4.8548t + 10.108$$

$R^2 = 0.9673$

Data at 1520 K:

Equation 2.15: ***Depth vs. Time curve fit for data Aug 5***

$$depth = 10.884t^2 - 29.116t + 14.485$$

$R^2 = 1$

Equation 2.16: ***Depth vs. Time curve fit for data Aug. 13***

$$depth = 10.784t^2 - 26.296t + 12.905$$

$R^2 = 1$

Equation 2.17: ***Depth vs. Voltage curve fit for data at 1520 K***

$$depth = 0.0116t^4 - 0.2356t^3 + 1.813t^2 - 6.6158t + 11.312$$

$R^2 = 0.9984$

Data at 1535 K

Equation 2.18: ***Depth vs. Time curve fit for data Aug 7***

$$depth = 52551t^5 - 134501t^4 + 137039t^3 - 69468t^2 + 17499t - 1745.5$$

$R^2 = 0.9999$

Equation 2.19: ***Depth vs. Time curve fit for data Aug 11***

$$depth = 12.827t^2 - 31.839t + 14.983$$

$R^2 = 1$

Equation 2.20: ***Polynomial equation for curve fit of 1535 K data***

$$depth = -0.0014V^5 + 0.0395V^4 - 0.4469V^3 + 2.5691V^2 - 7.8642V + 11.783$$

$R2 = 0.995$

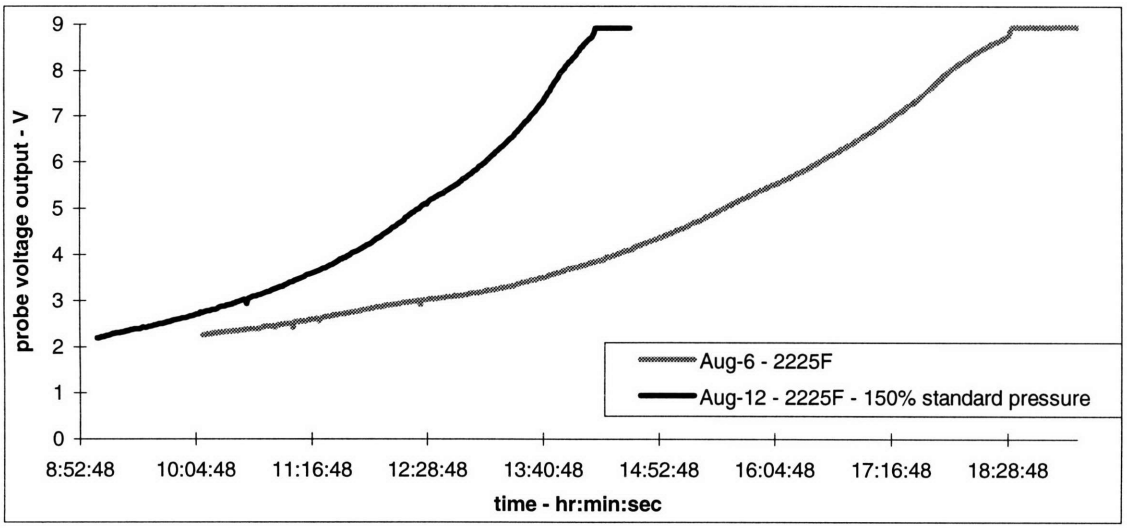

Figure 2.13: Raw Data for Calibration Curves at 1490 K (2225°F) Bushing Temperature on Single-Tip Bushing

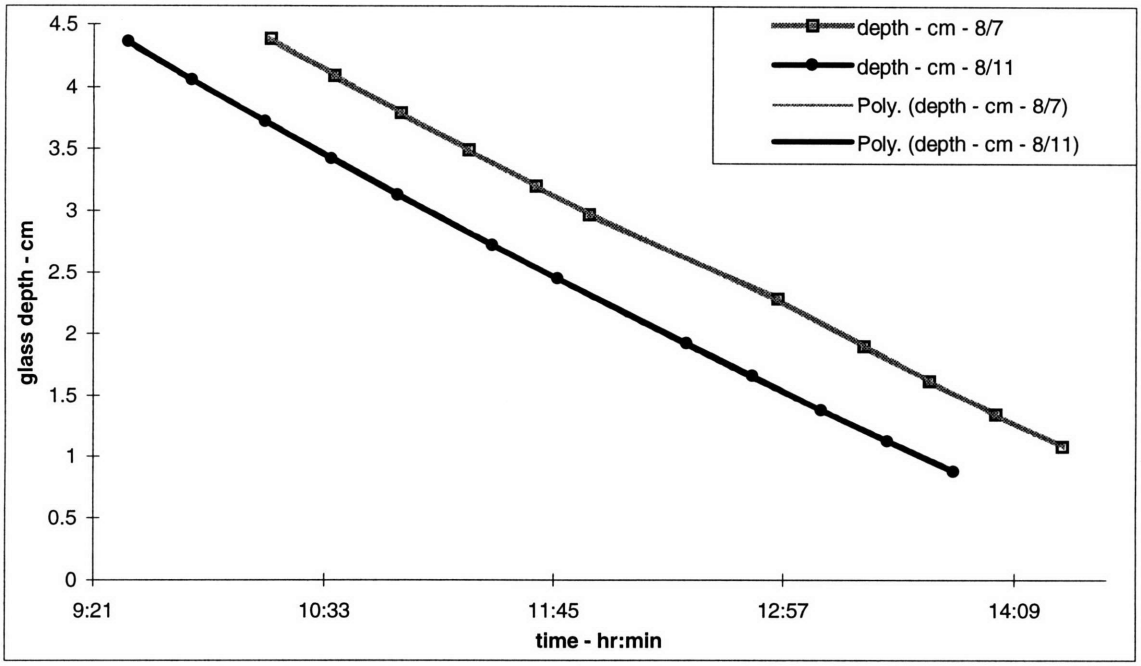

Figure 2.14: Depth vs Time Data and Curvefits for 1490 K (2225°F) Calibration Curves on Single-Tip Bushing

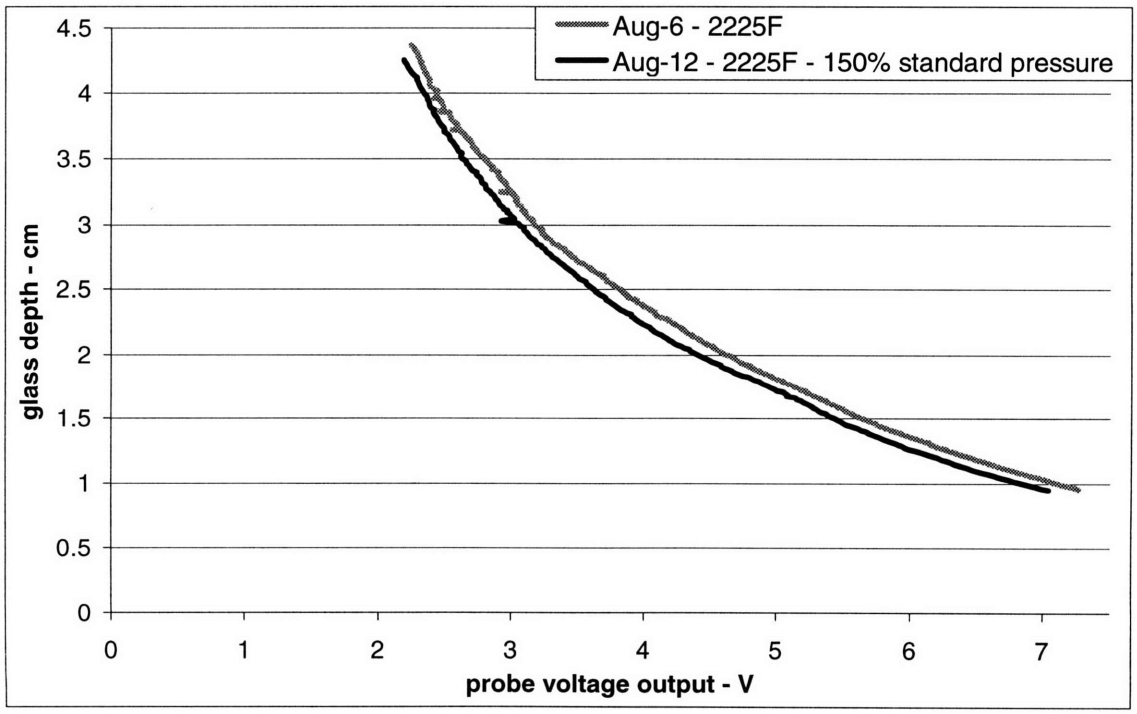

Figure 2.15: Voltage Output vs. Probe Depth at 1490 K (2225°F) on Single-Tip Bushing

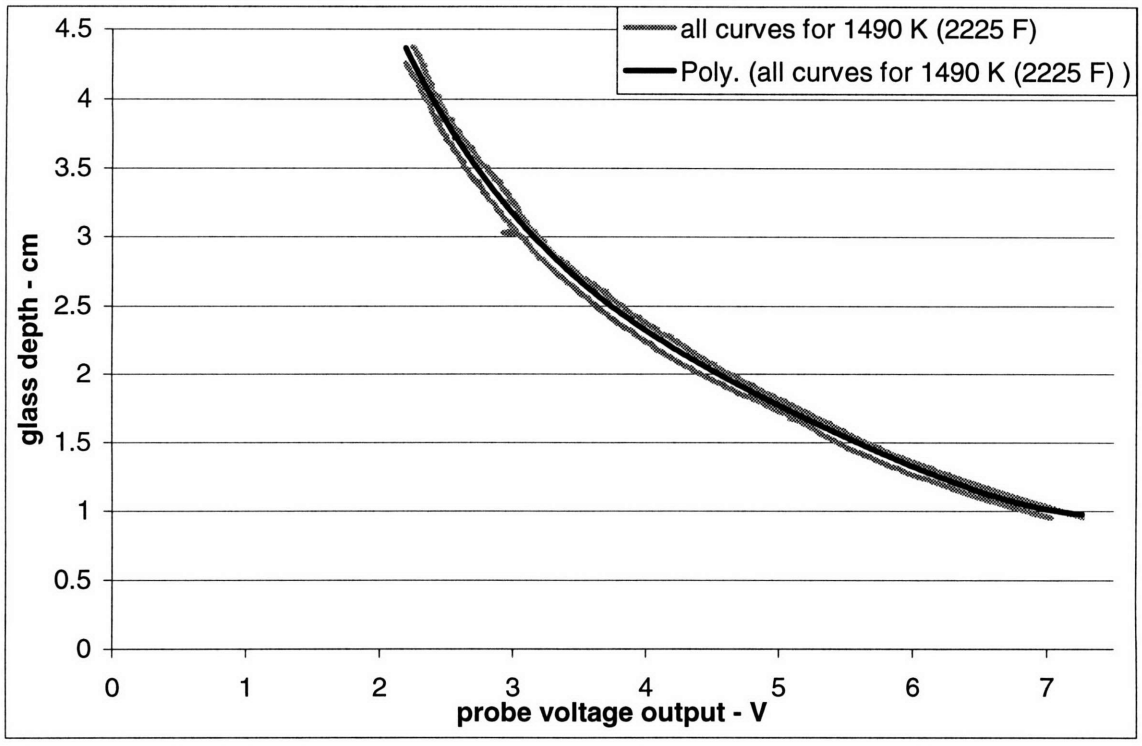

Figure 2.16: Polynomial Curve-Fit for All Data Sets at 1490 K (2225°F) on Single-Tip Bushing

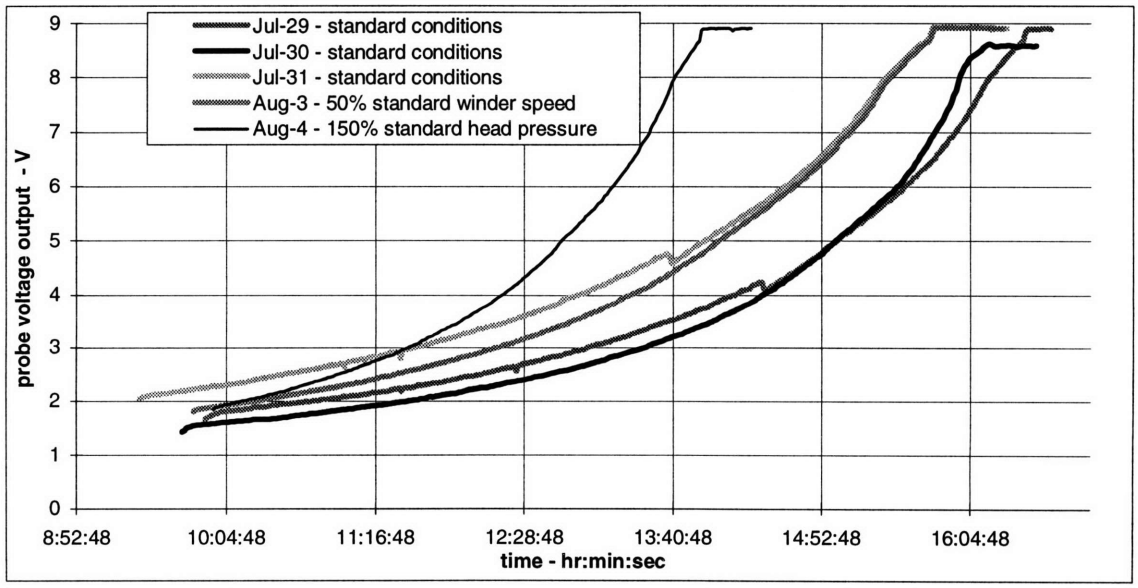

Figure 2.17: Raw Data for Calibration Curves at 1505 K (2250°F) Bushing Temperature on Single-Tip Bushing

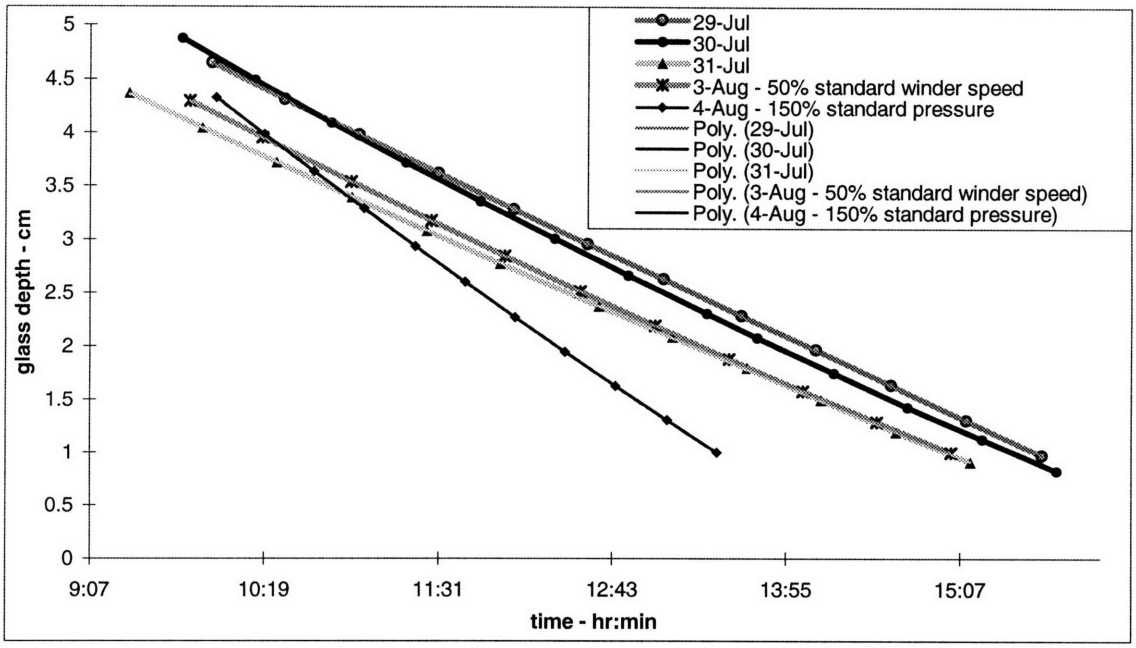

Figure 2.18: Depth vs Time Data and Curvefits for 1505 K (2250°F) Calibration Curves on Single-Tip Bushing

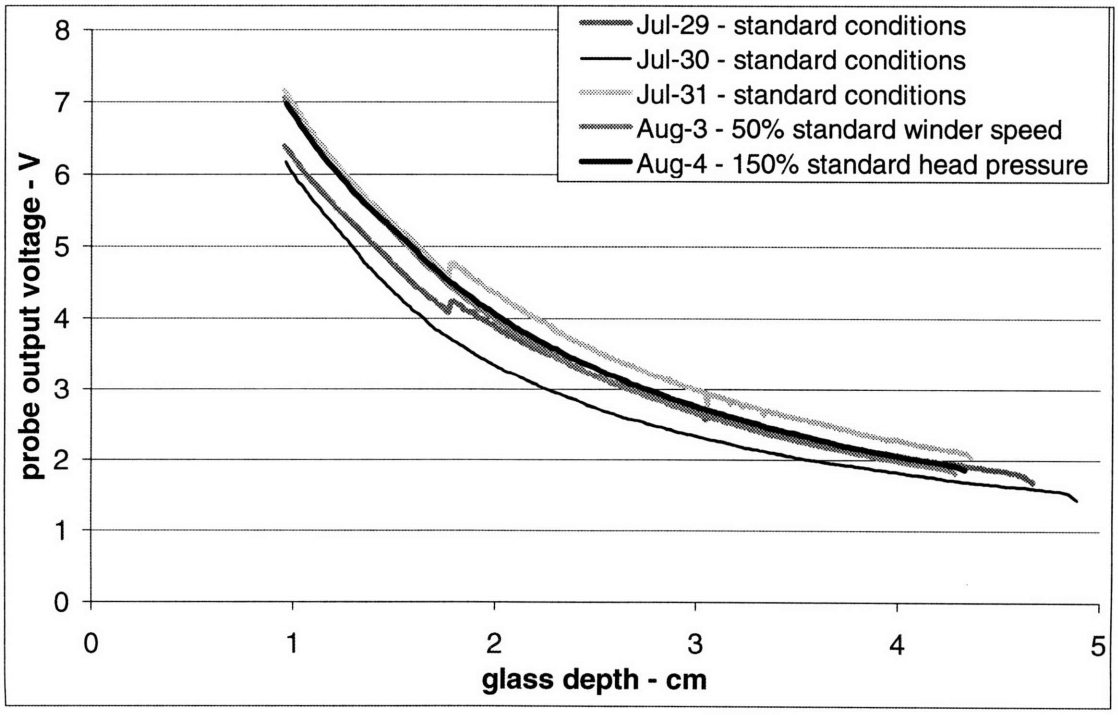

Figure 2.19: Voltage Output vs. Probe Depth at 1505 K (2250°F) on Single-Tip Bushing

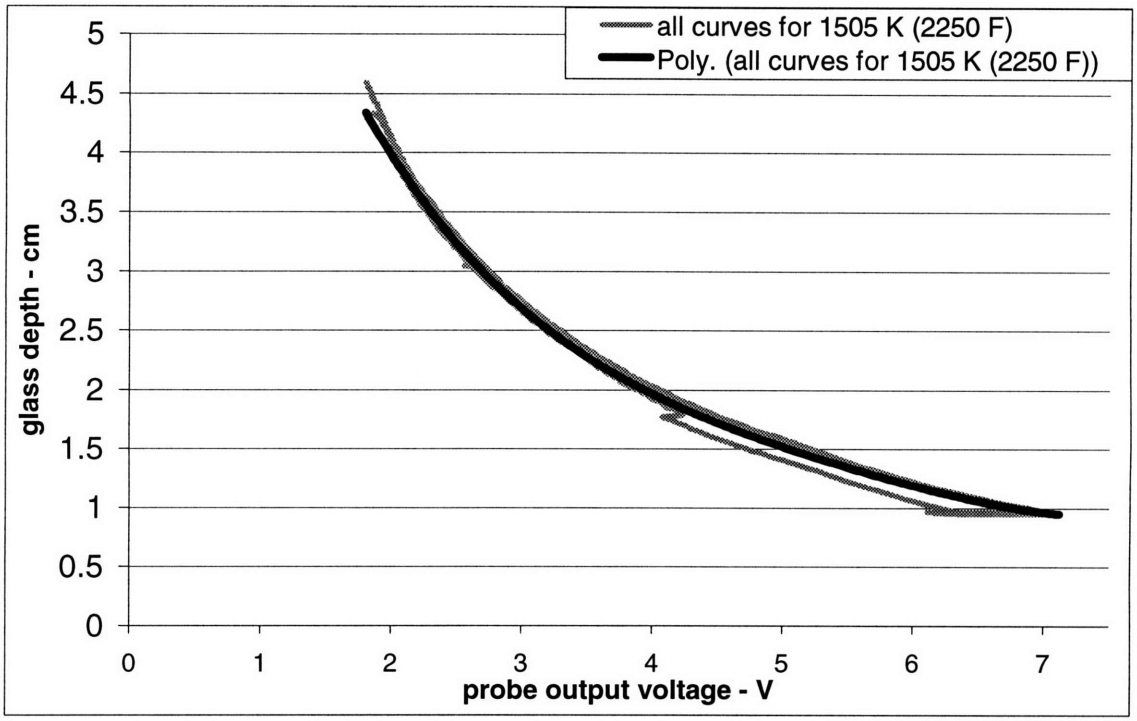

Figure 2.20: Polynomial Curve-Fit for Data Sets at 1505 K (2250°F) on Single-Tip Bushing

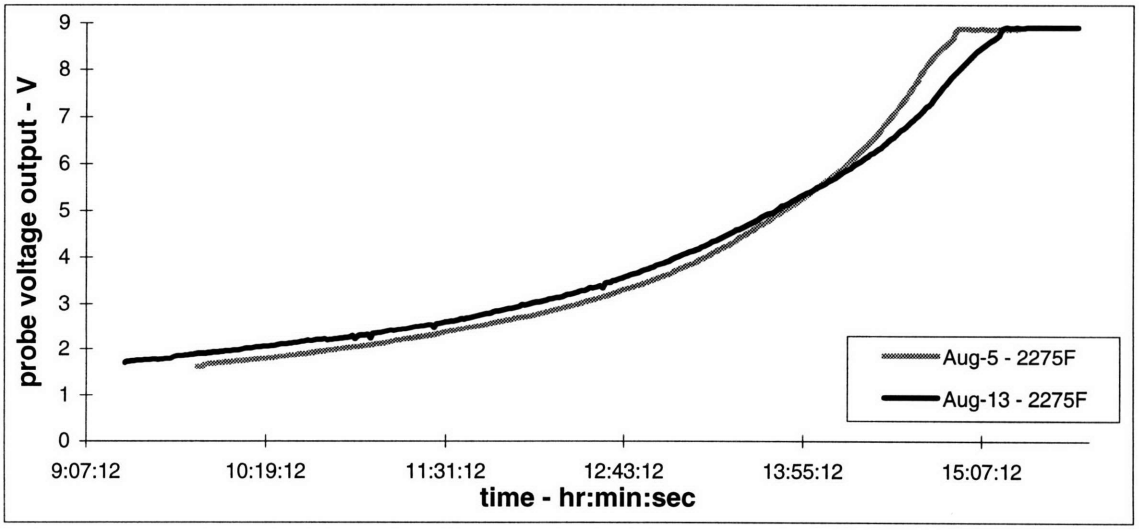

Figure 2.21: Raw Data for Calibration Curves at 1520 K (2275°F) Bushing Temperature on Single-Tip Bushing

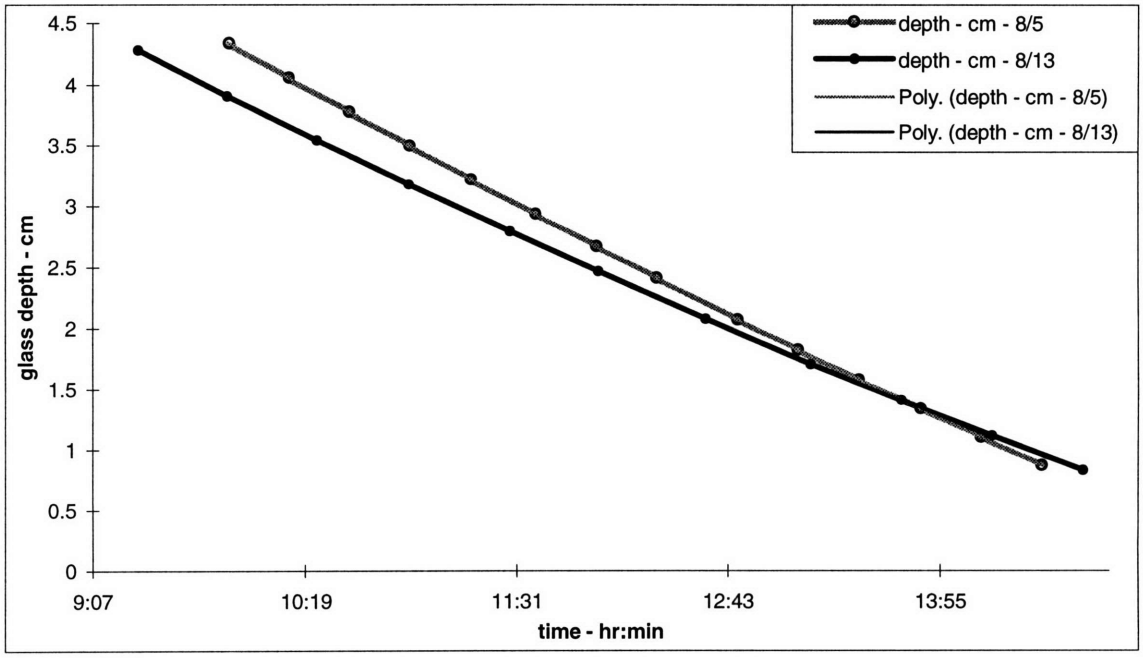

Figure 2.22: Depth vs Time Data and Curvefits for 1520 K (2275°F) Calibration Curves on Single-Tip Bushing

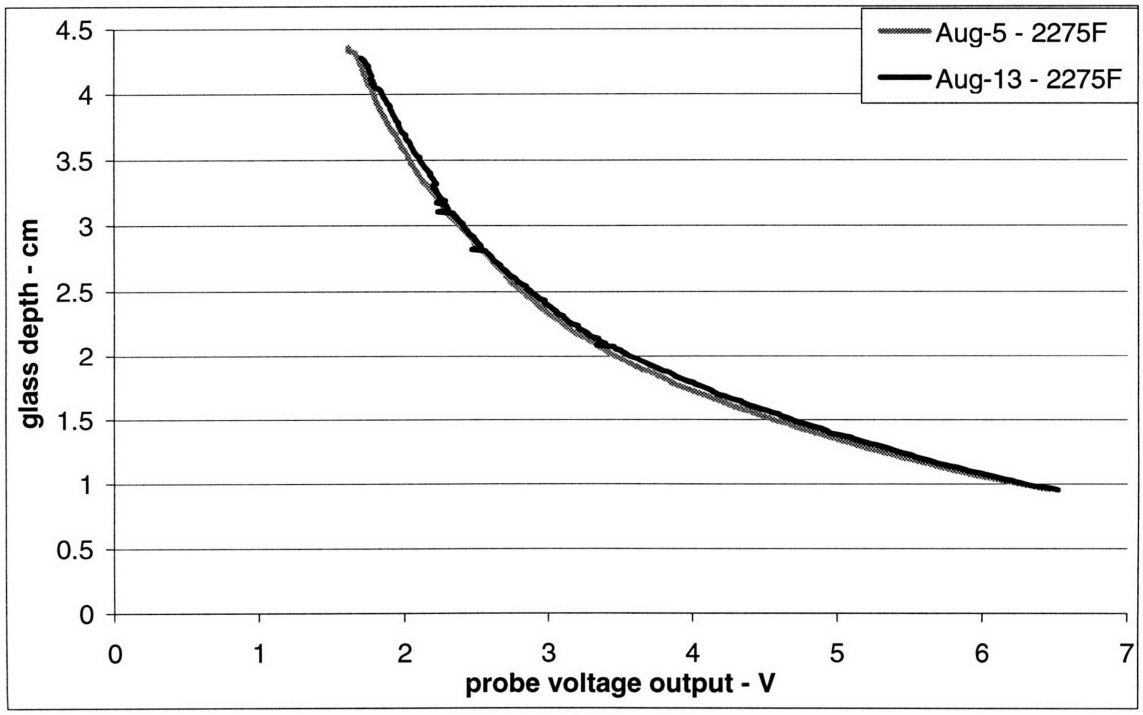

Figure 2.23: Voltage Output vs. Probe Depth at 1520 K (2275°F) on Single-Tip Bushing

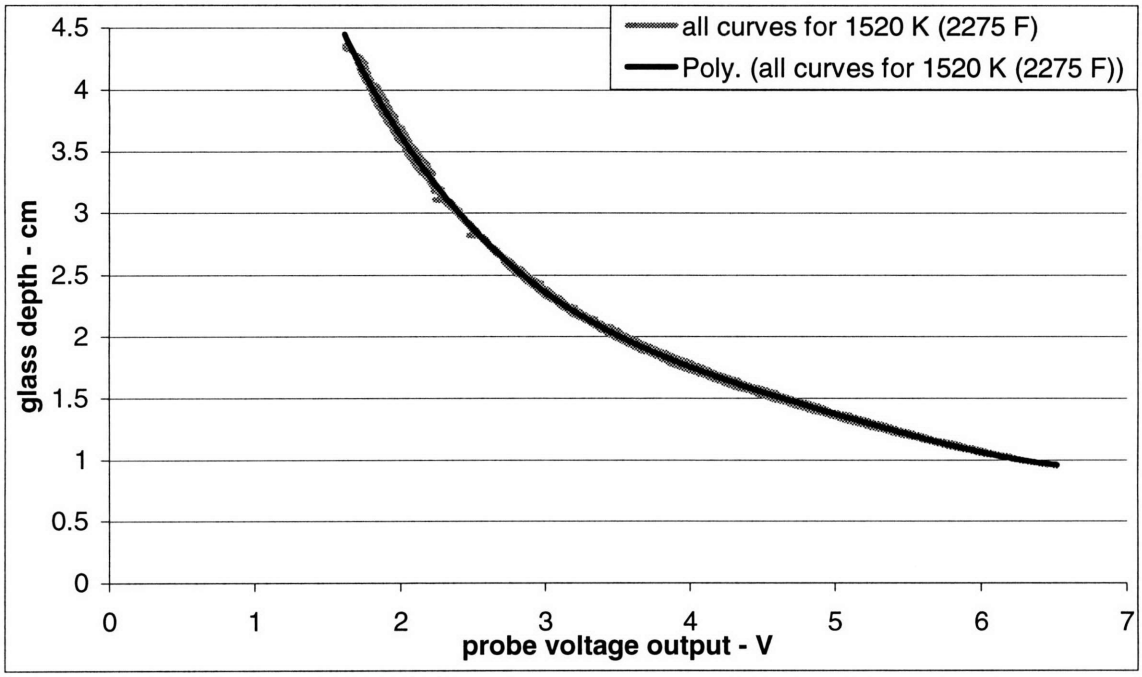

Figure 2.24: Polynomial Curve-Fit for All Data Sets at 1520 K (2275°F) on Single-Tip Bushing

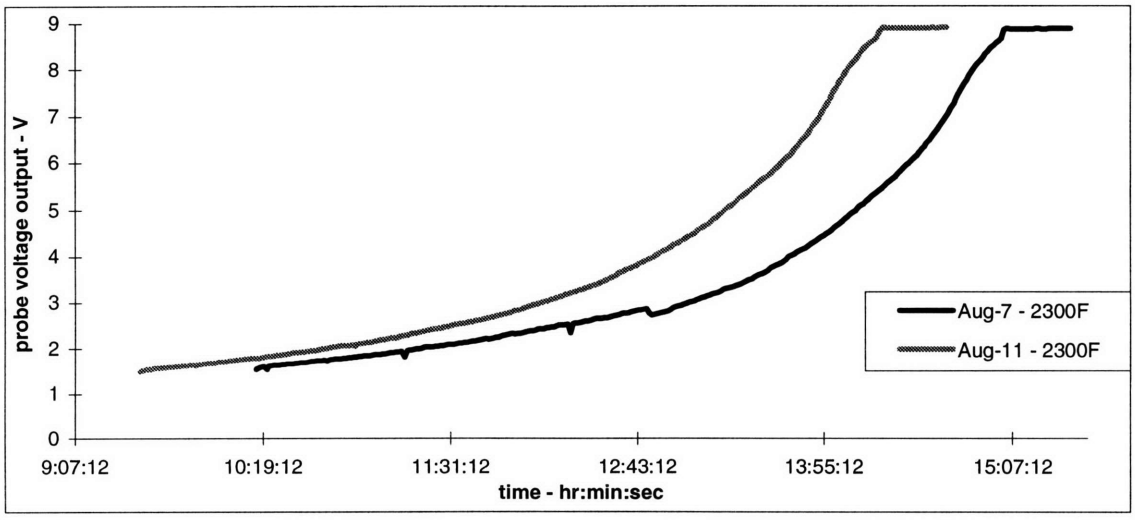

Figure 2.25: Raw Data for Calibration Curves at 1535 K (2300°F) Bushing Temperature on Single-Tip Bushing

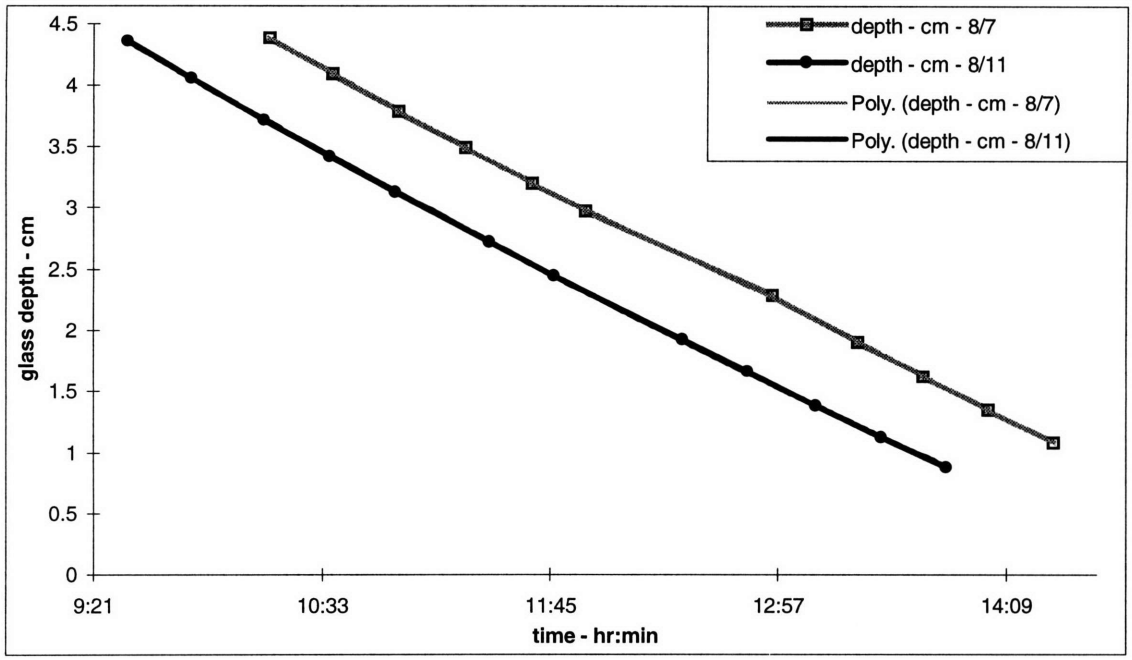

Figure 2.26: Depth vs Time Data and Curvefits for 1535 K (2300°F) Calibration Curves on Single-Tip Bushing

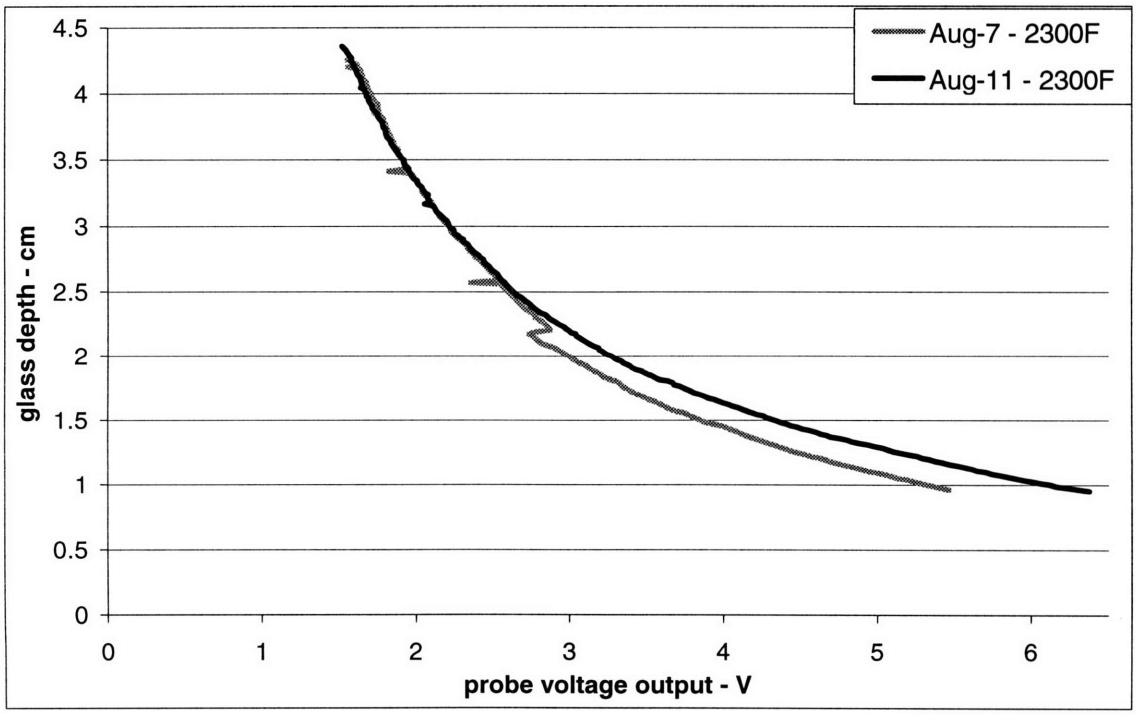

Figure 2.27: Voltage Output vs. Probe Depth at 1535 K (2300°F) on Single-Tip Bushing

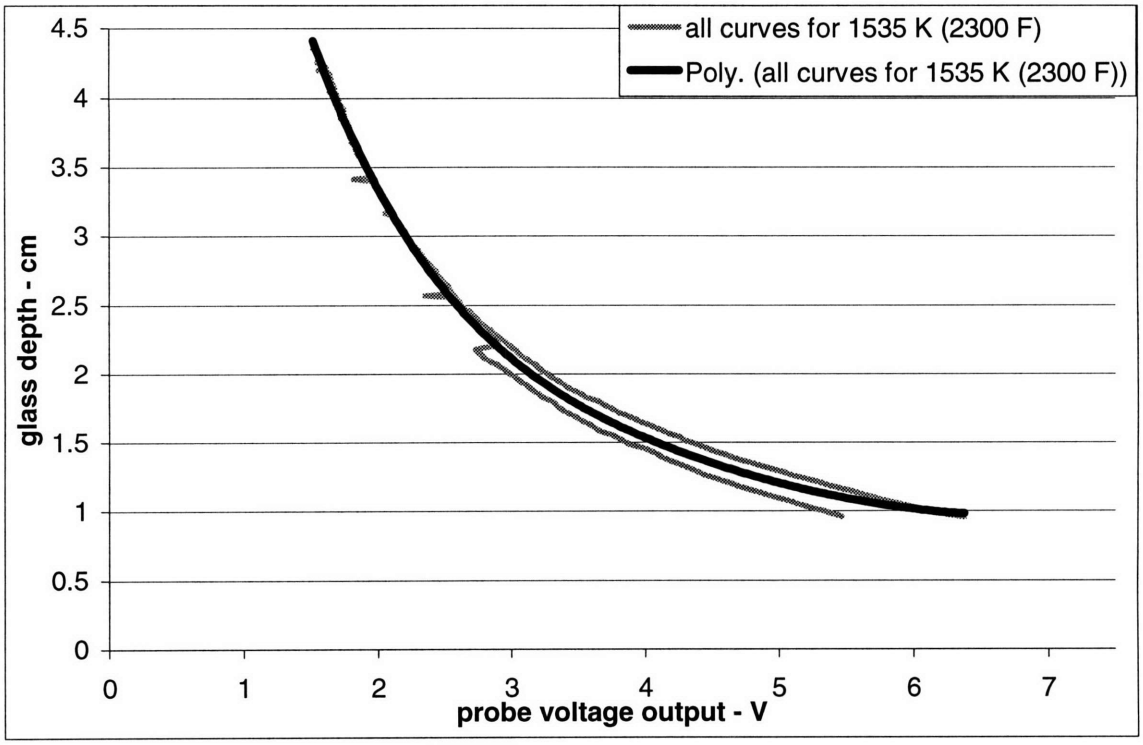

Figure 2.28: Polynomial Curve-Fit for All Data Sets at 1535 K (2300°F) on Single-Tip Bushing

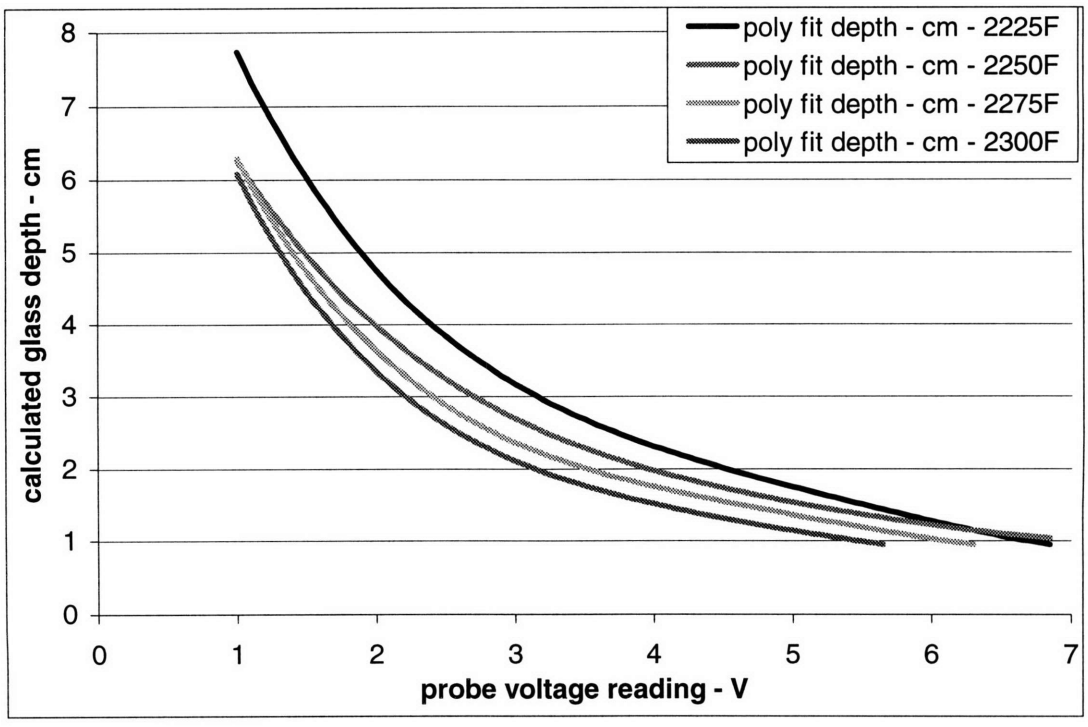

Figure 2.29: Comparison of Polynomial Curve-Fits for 1490 K, 1505 K, 1520 K and 1535 K on Single-Tip Bushing

2.6.2 Nine-Tip Results

Run conditions in this section are not kept to any standard of winder speed and head pressure, as work on the single tip position indicated that changing these only affects mass flow, which is being recorded. Thus head pressure and winder speed settings are not reported. Because of time constraints, 1520 K (2225° F) and 1535 K (2300° F) are represented by only two data sets and 1490 K (2225° F) by only one. The temperature 1505 K (2250°F) has a greater number of data sets because it was used as the standard condition. It is the temperature at which the final system will most often be run. In the curve-fit for these sets of data the lowest of the four was eliminated because it differed significantly from the other three and it was therefore thought that it was not representative of actual probe behavior. The lower data set is still represented in the graph of original data sets and the graph of voltage vs. depth data.

Data sets below all indicate data collected at 25 scans per second and averaged over 15 seconds. Some of the data sets below show a large amount of noise at high glass depths. This noise is thought to be due to uneven wetting of the level-sensing probe. The noise is believed to have occurred on days when the probe was inserted into the glass well later in the warm-up cycle, compared to days when the data is smooth. The solution to this problem is, first of all, to insure that the probe is inserted early during actual operation, and secondly to average the data over a longer period of time. In the formation of curve-fits on the noisy data sets some averaging was done and some of the points which were obviously noise were removed. Averaging was performed on data from two days: Mar. 22 and Mar. 25. Altered data points represent the average of three minutes of data in the range where noise was high and one minute in the regions where noise was low. The unaltered data is represented in the graphs of voltage output vs. probe depth and the smoothed data is represented in the graphs of the curve-fits.

	Bushing Temperature			
	1490 K (2225°F)	1505 K (2250°F)	1520 K (2275°F)	1535 K (2300°F)
Raw Data, V vs. Time	Fig. 2.30	Fig. 2.34	Fig. 2.38	Fig. 2.42
Depth vs. Time	Fig. 2.31 Equ. 2.21	Fig. 2.35 Equ. 2.23-26	Fig. 2.39 Equ. 2.28-31	Fig. 2.43 Equ. 2.33-34
Voltage vs. Depth	Fig. 2.32	Fig. 2.36	Fig. 2.40	Fig. 2.44
Curve-fit of V vs. Depth	Fig. 2.33 Equ. 2.22	Fig. 2.37 Equ. 2. 27	Fig. 2.41 Equ. 2.32	Fig. 2.45 Equ. 2.35

Table 2.2: Nine-Tip Data Representation by Figure Number and Equation Numbers

Data at 1490 K

Equation 2.21: ***Depth vs. Time curve fit for data Mar 25***

$$depth = 111.99t^2 - 198.97t + 84.038$$

$R^2 = 0.9999$

Equation 2.22: ***Depth vs. Voltage curve fit for data at 1490 K***

$$depth = -0.00222V^4 + 0.00566V^3 + 0.52718V^2 - 5.50123V + 17.48262$$

$R^2 = 0.99650$

Data at 1505 K

Equation 2.23: ***Depth vs. Time curve fit for data Mar 4***

$$depth = 492.89t^4 - 986.02t^2 + 601.93t - 103.63$$

$R^2 = 1$

Equation 2.24: ***Depth vs. Time curve fit for data Mar 16***

$$depth = 464.68t^3 - 798t^2 + 410.07t - 155285$$

$R^2 = 9994$

Equation 2.25: ***Depth vs. Time curve fit for data Mar 18, run 1***

$$depth = 6887.9t^3 - 9681.3t^2 + 4412.6t - 645.52$$

$R^2 = 0.9998$

Equation 2.26: ***Depth vs. Time curve fit for data Mar 18, run 2***

$$depth = 28799t^3 - 53614t^2 + 33146t - 6801.6$$

$R^2 = 0.9994$

Equation 2.27: ***Depth vs. Voltage curve fit for data at 1505 K***

$$depth = 0.00208V^6 - 0.07631V^5 + 1.1431V^4 - 8.9576V^3 + 38.851V^2 - 89.558V + 89.673$$

$R^2 = 0.98523$

Data at 1520 K

Depth vs. Time curve fit for data Mar. 2, in 3 parts

Equation 2.28: ***From start to 11:39***

$$depth = -2242t^3 + 3244.9t^2 - 1619t + 282.45$$

$R^2 = 0.9998$

Equation 2.29: ***From 11:39 to 13:39***

$$depth = -2.8142t + 5.3296$$

$R^2 = 1$

Equation 2.30: ***From 13:39 to end***

$$depth = 155.56t^2 - 233.93t + 86.482$$

$R^2 = 0.9991$

Equation 2.31: ***Depth vs. Time curve fit for data Mar. 23***

$$depth = 702.26t^3 - 1280.5t^2 + 723.51t - 119.21$$

$R^2 = 0.9999$

Equation 2.32: ***Depth vs. Voltage curve fit for data at 1520 K***

$$depth = 0.00073V^6 - 0.02659V^5 + 0.39862V^4 - 3.1776V^3 + 14.397V^2 - 36.091V + 42.192$$

$R^2 = 0.94672$

Data at 1535 K

Equation 2.33: ***Depth vs. Time curve fit for data Mar. 14***

$$depth = 697.08t^3 - 1136.5t^2 + 554.68t - 71.577$$

$R^2 = 1$

Equation 2.34: ***Depth vs. Time curve fit for data Mar. 30***

$$depth = 44205t^3 - 57181t^2 + 24519t - 3482.3$$

$R^2 = 0.9966$

Equation 2.35: ***Depth vs. Voltage curve fit for curve fit of 1535 K data***

$$depth = -0.00174V^5 + 0.05528V^4 - 0.69900V^3 + 4.405641V^2 - 14.20519V + 20.88949$$

$R^2 = 0.97440$

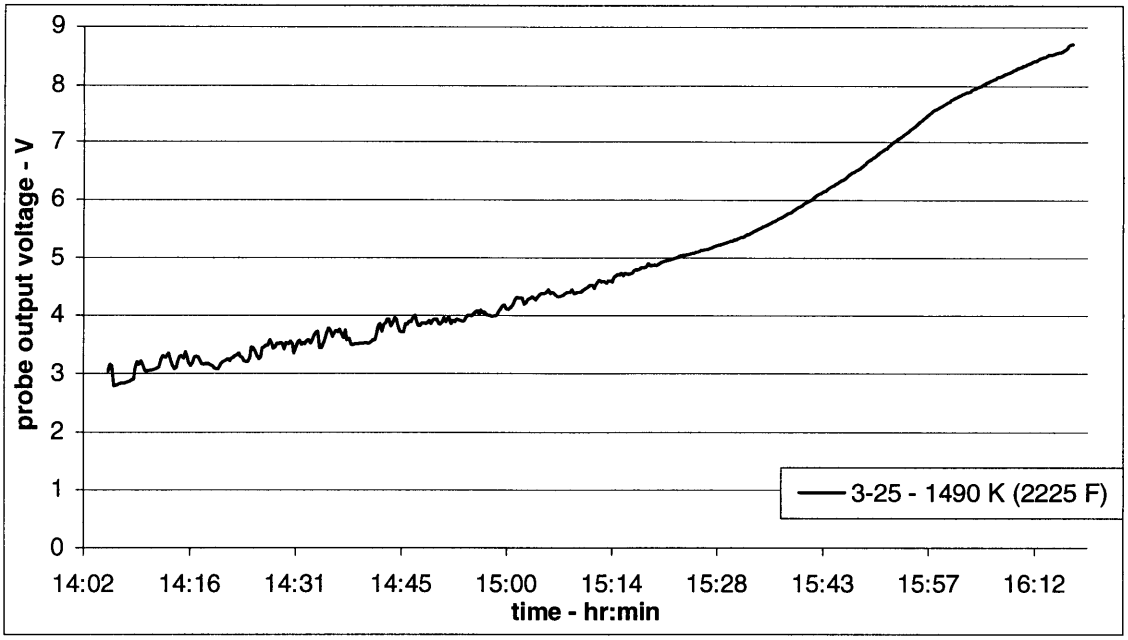

Figure 2.30: Raw Data for Calibration Curves at 1490 K (2225°F) Bushing Temperature on Nine-Tip Bushing

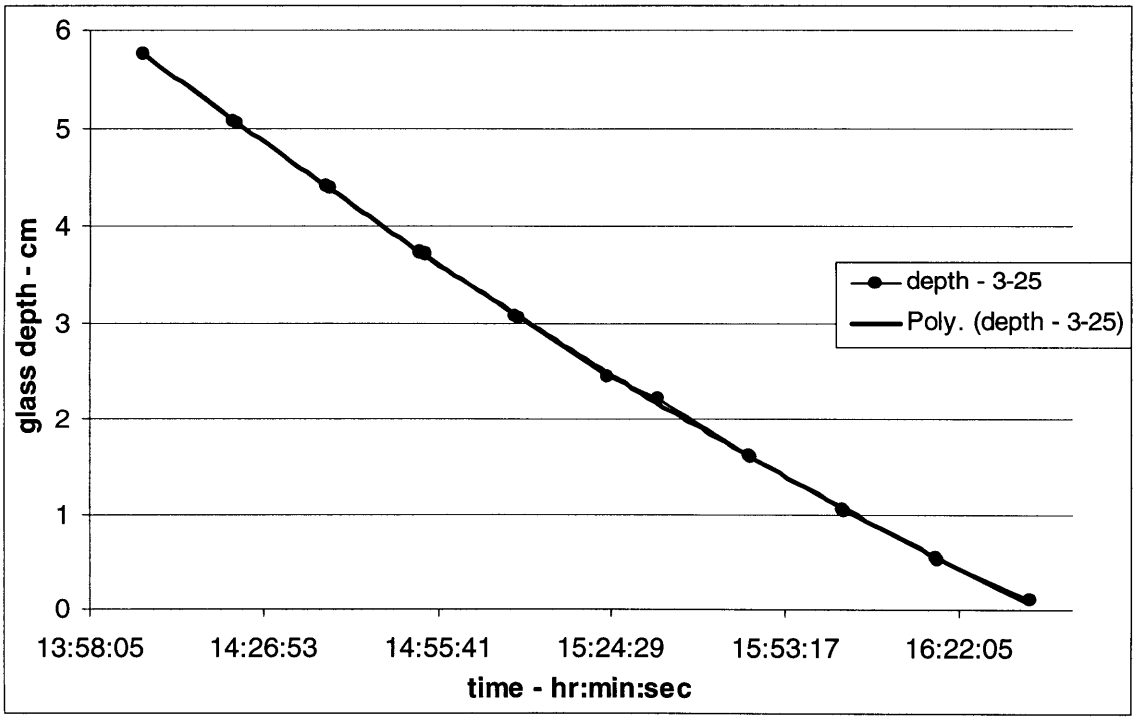

Figure 2.31: Depth vs Time Data and Curvefits for 1490 K (2225°F) Calibration Curves on Nine-Tip Bushing

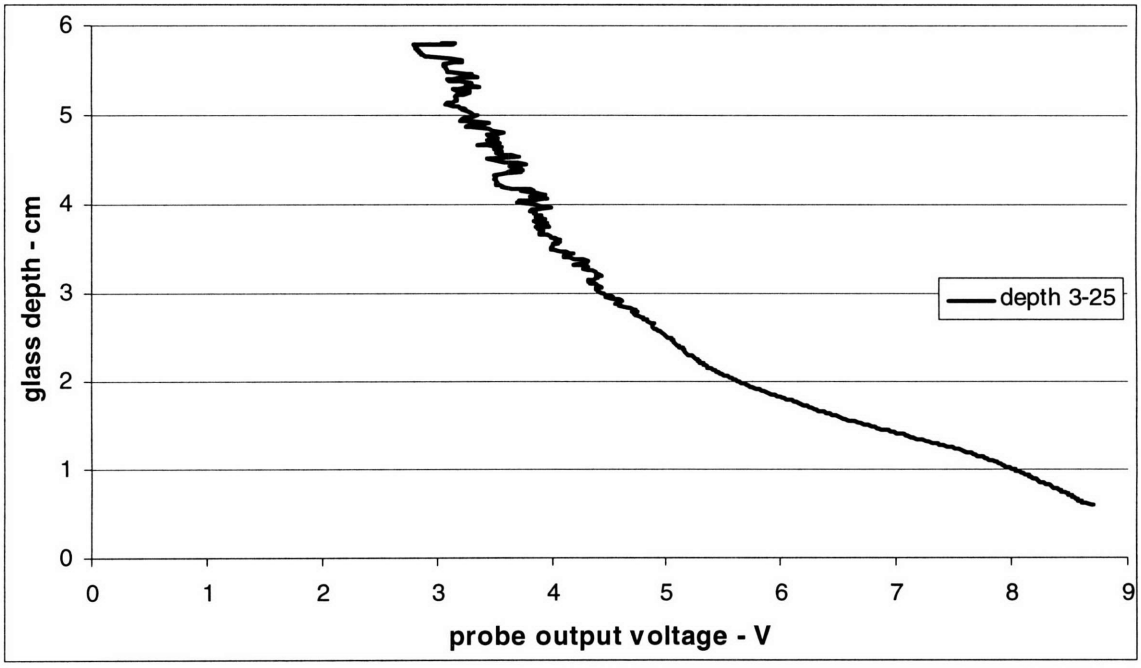

Figure 2.32: Voltage Output vs. Probe Depth on Nine-Tip Bushing at 1490 K (2225°F)

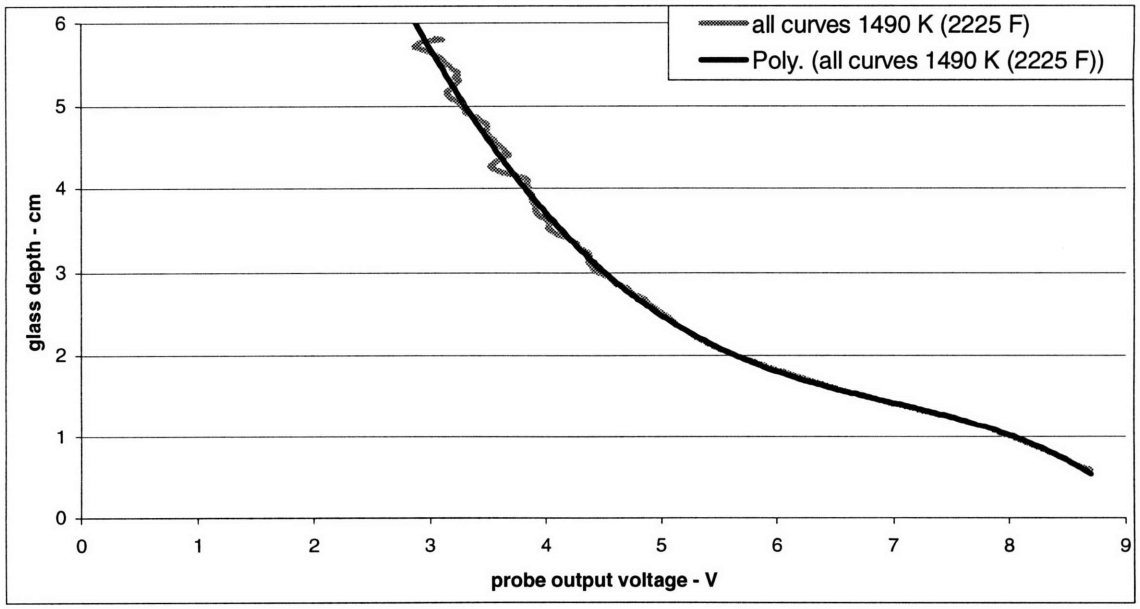

Figure 2.33: Polynomial Curve-Fit for All Data Sets at 1490 K (2225°F) on Nine-Tip Bushing

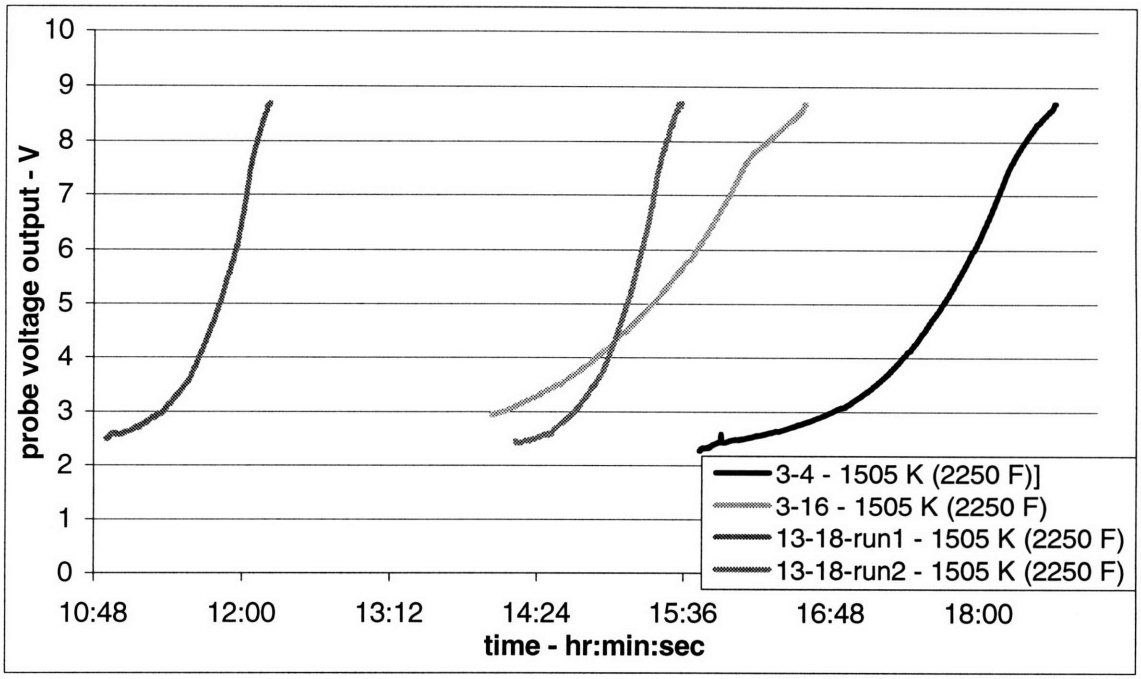

Figure 2.34: Raw Data for Calibration Curves at 1505 K (2250°F) Bushing Temperature on Nine-Tip Bushing

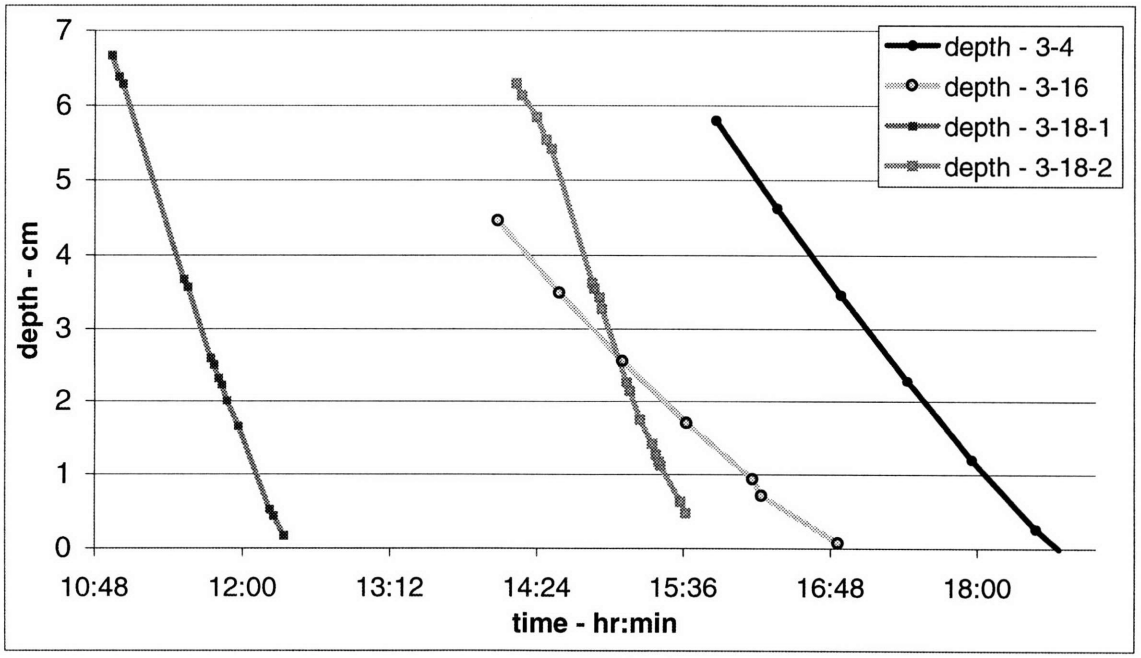

Figure 2.35: Depth vs Time Data and Curvefits for 1505 K (2250°F) Calibration Curves on Nine-Tip Bushing

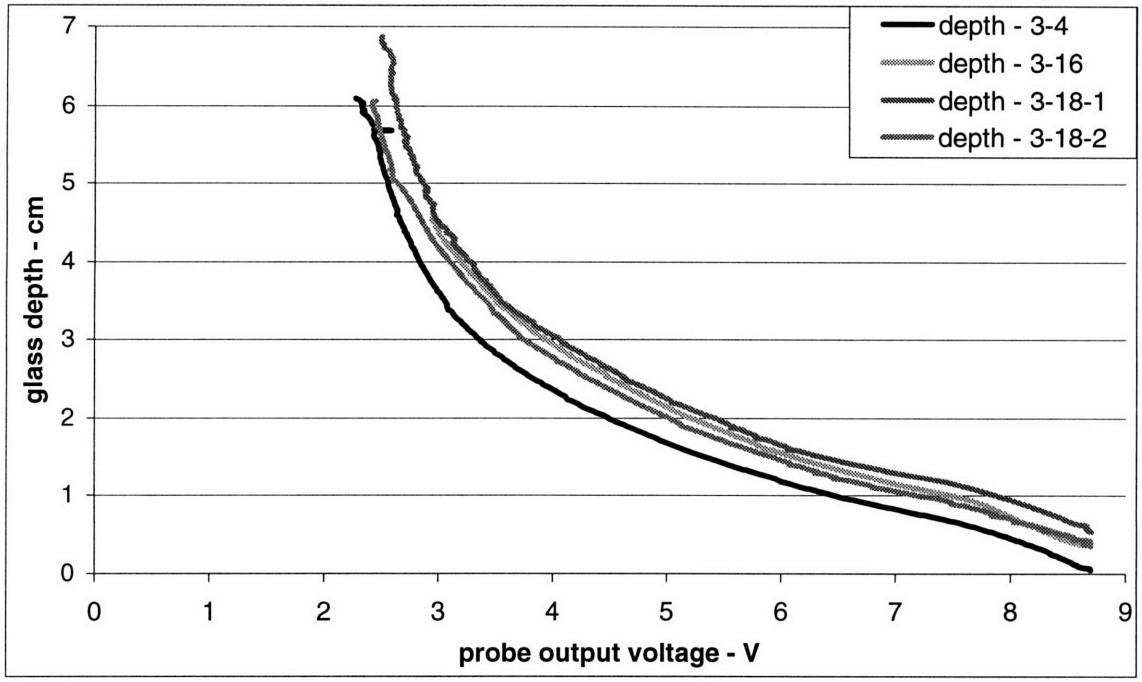

Figure 2.36: Voltage Output vs. Probe Depth on Nine-Tip Bushing at 1505 K (2250°F)

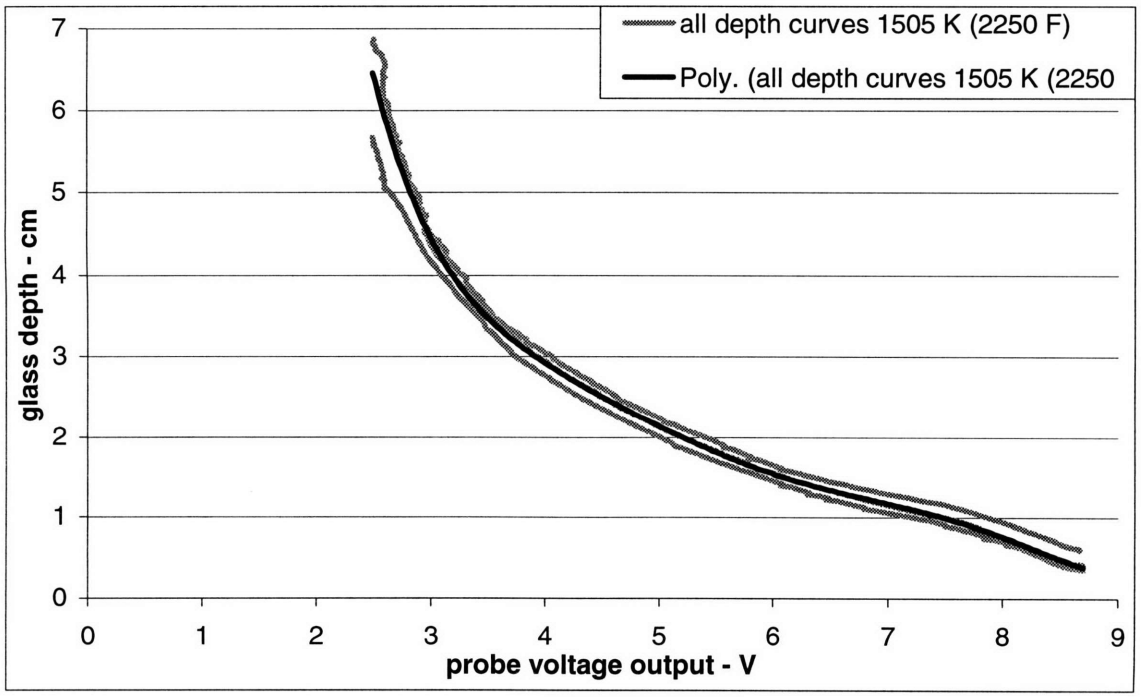

Figure 2.37: Polynomial Curve-Fit for All Data Sets at 1505 K (2250°F) on Nine-Tip Bushing

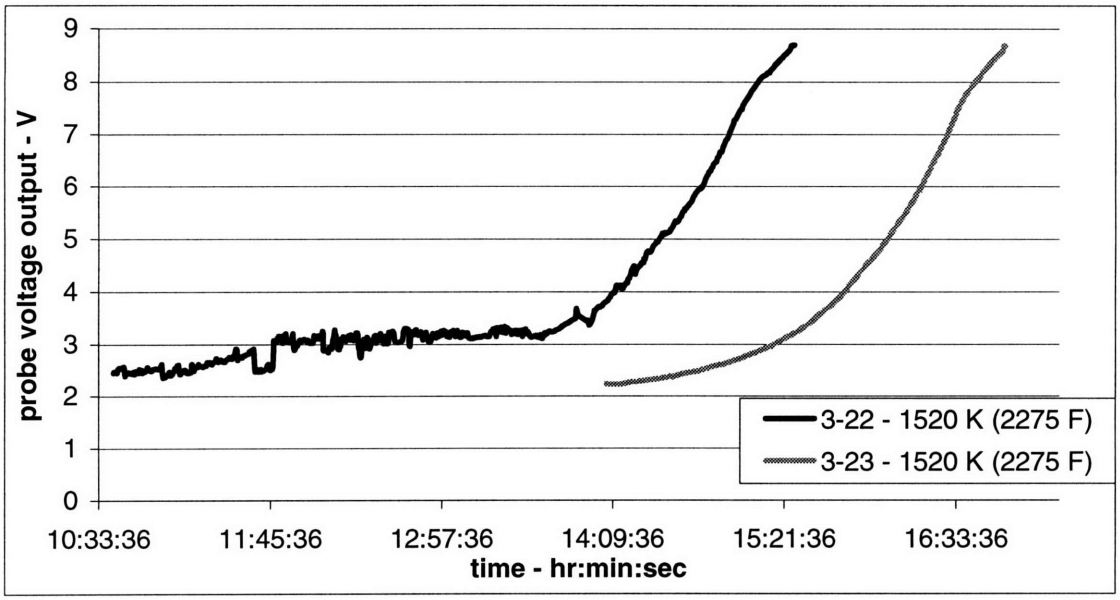

Figure 2.38: Raw Data for Calibration Curves at 1520 K (2275°F) Bushing Temperature on Nine-Tip Bushing

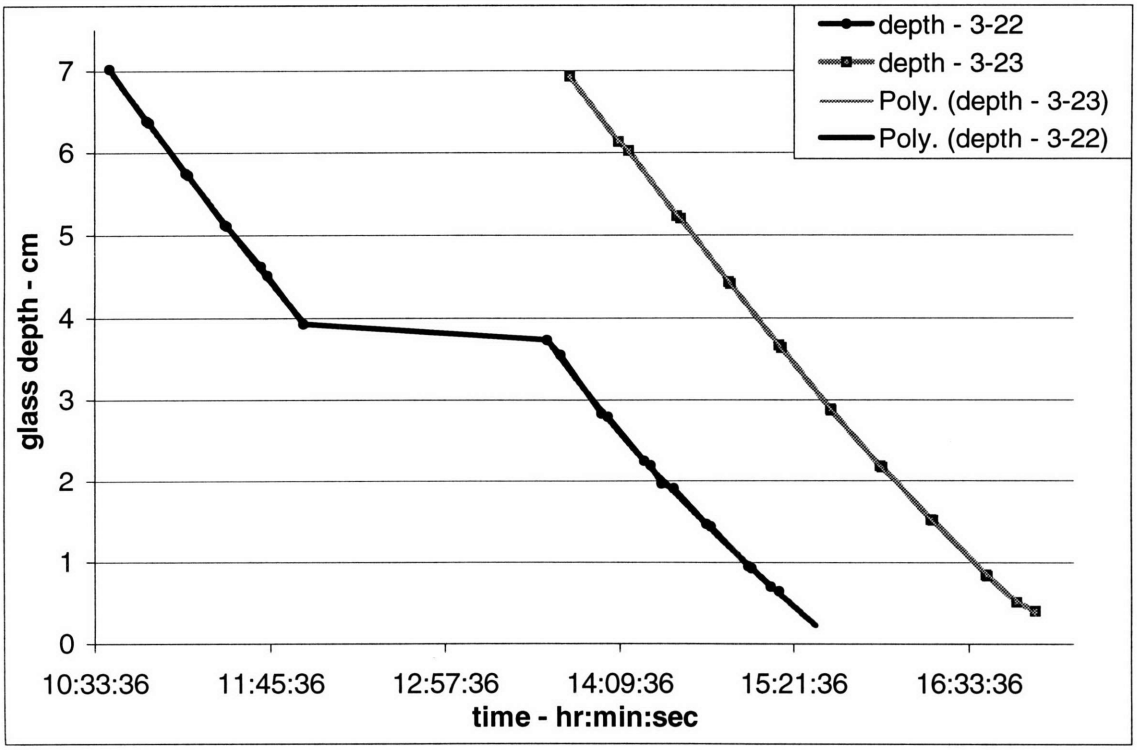

Figure 2.39: Depth vs. Time Data and Curve-fits for 1520 K (2275°F) Calibration Curves on Nine-Tip Bushing

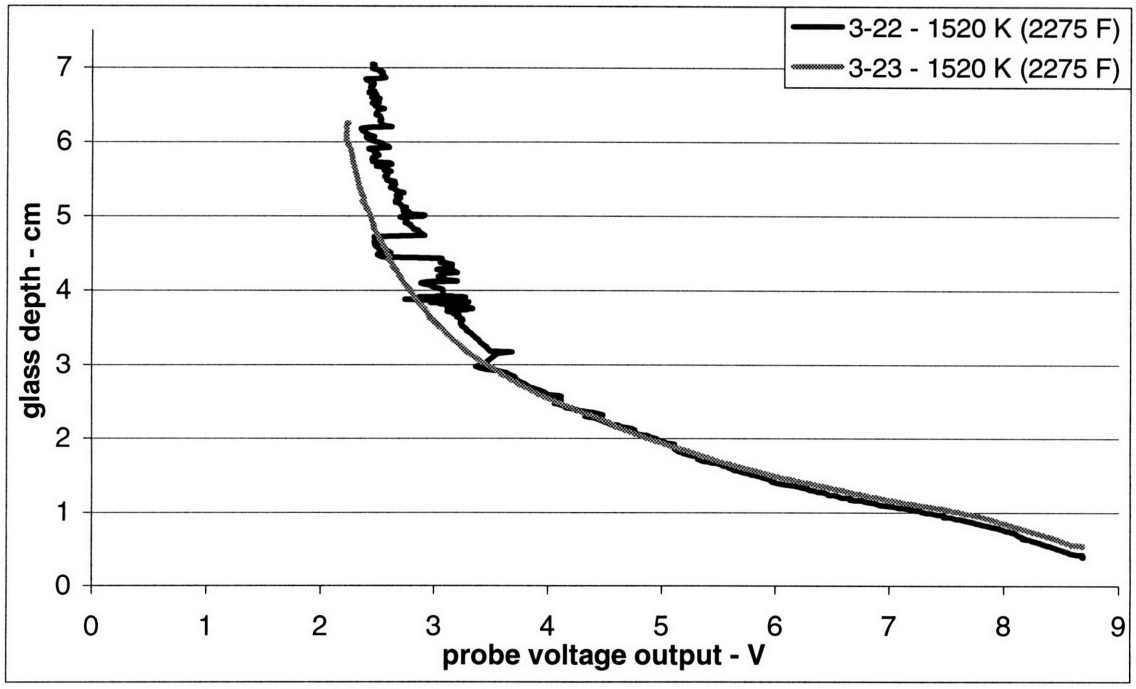

Figure 2.40: Voltage Output vs. Probe Depth on Nine-Tip Bushing at 1520 K (2275°F)

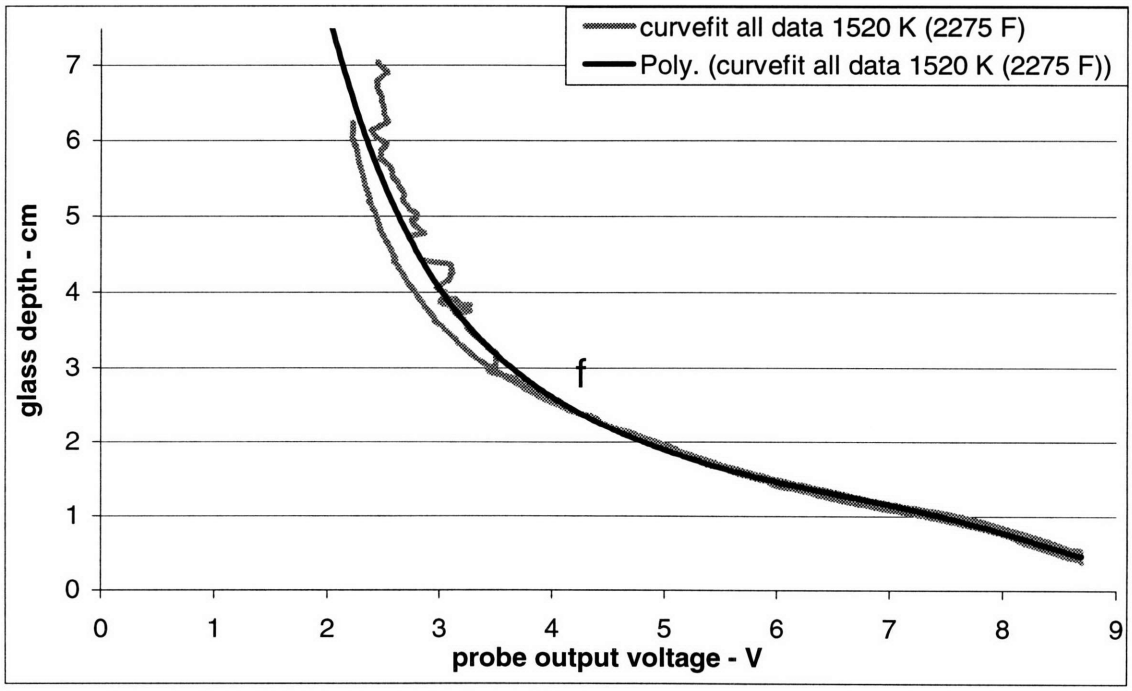

Figure 2.41: Polynomial Curve-Fit for Data Sets at 1520 K (2275°F) on Nine-Tip Bushing

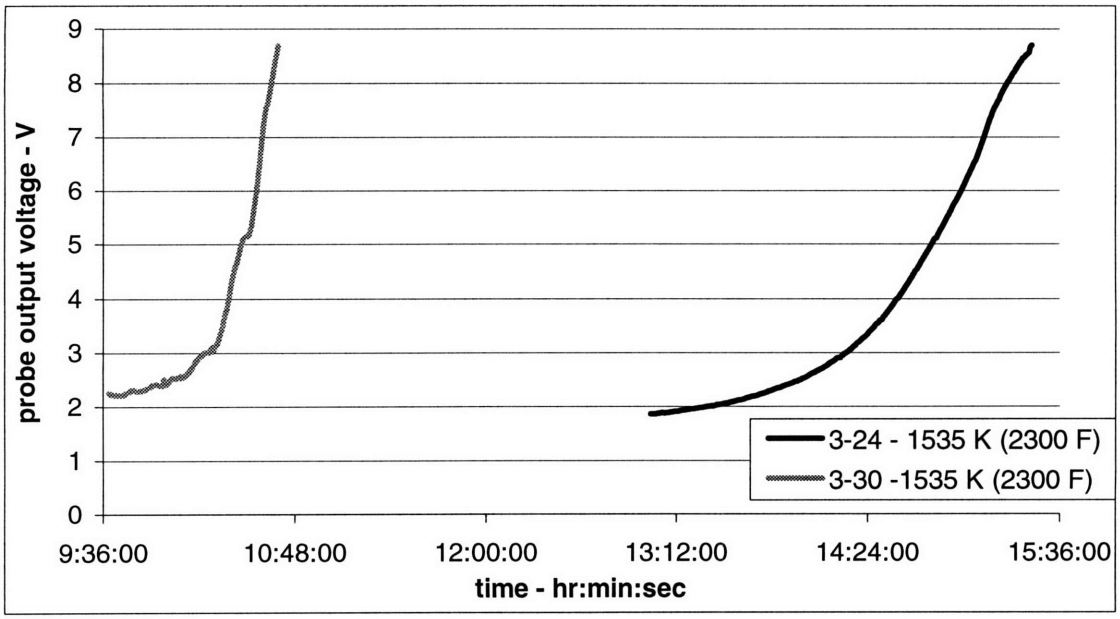

Figure 2.42: Raw Data for Calibration Curves at 1535 K (2300°F) Bushing Temperature on Nine-Tip Bushing

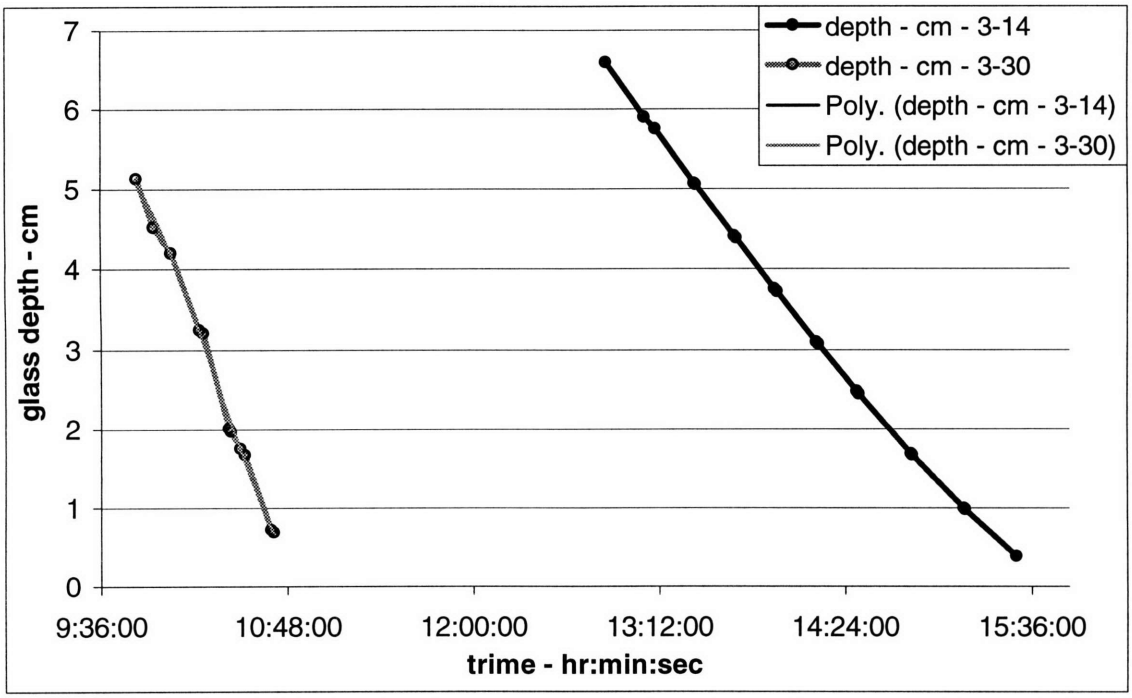

Figure 2.43: Depth vs. Time Data and Curve-fits for 1535 K (2300°F) Calibration Curves on Nine-Tip Bushing

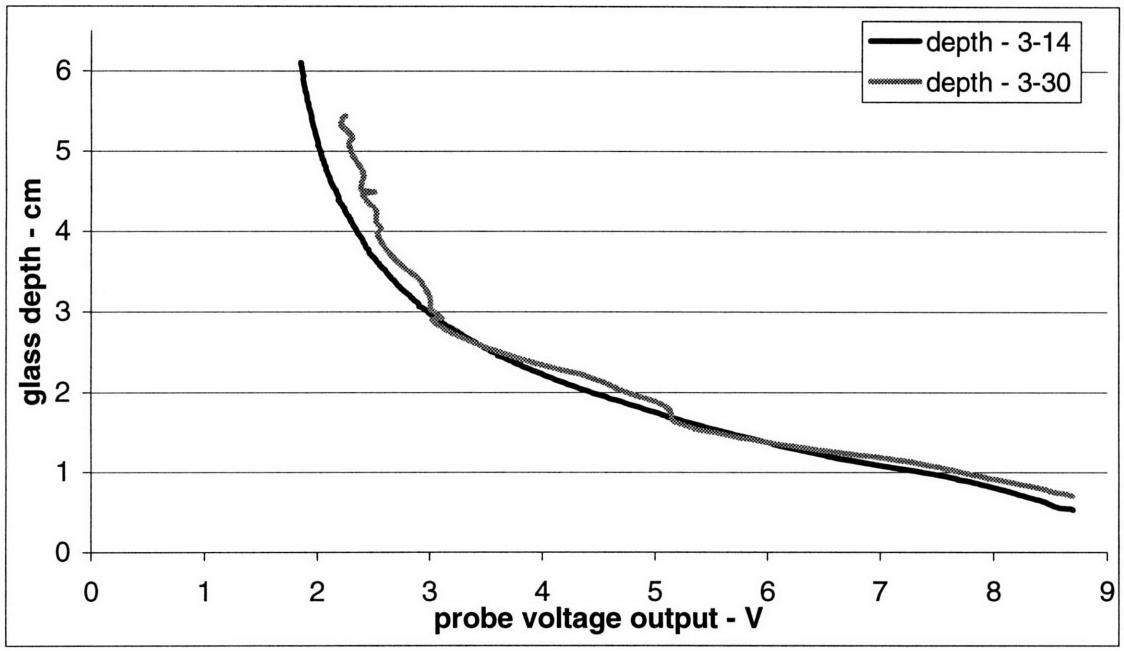

Figure 2.44: Voltage Output vs. Probe Depth on Nine-Tip Bushing at 1535 K (2300°F)

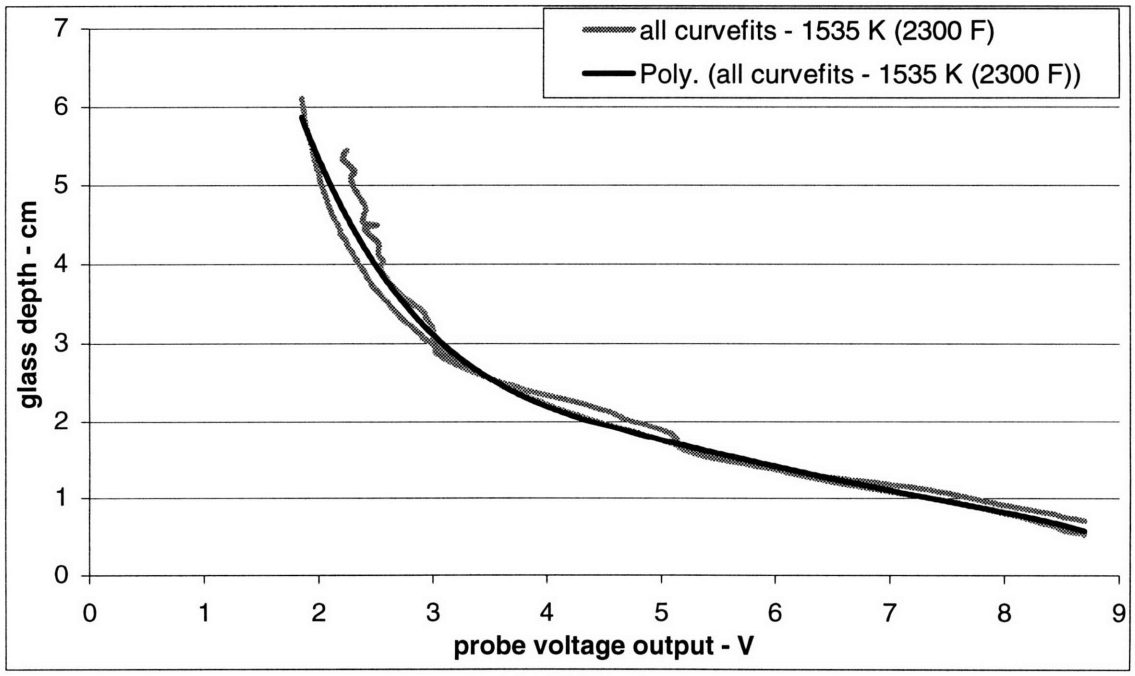

Figure 2.45: Polynomial Curve-Fit for Data Sets at 1535 K (2300°F) on Nine-Tip Bushing

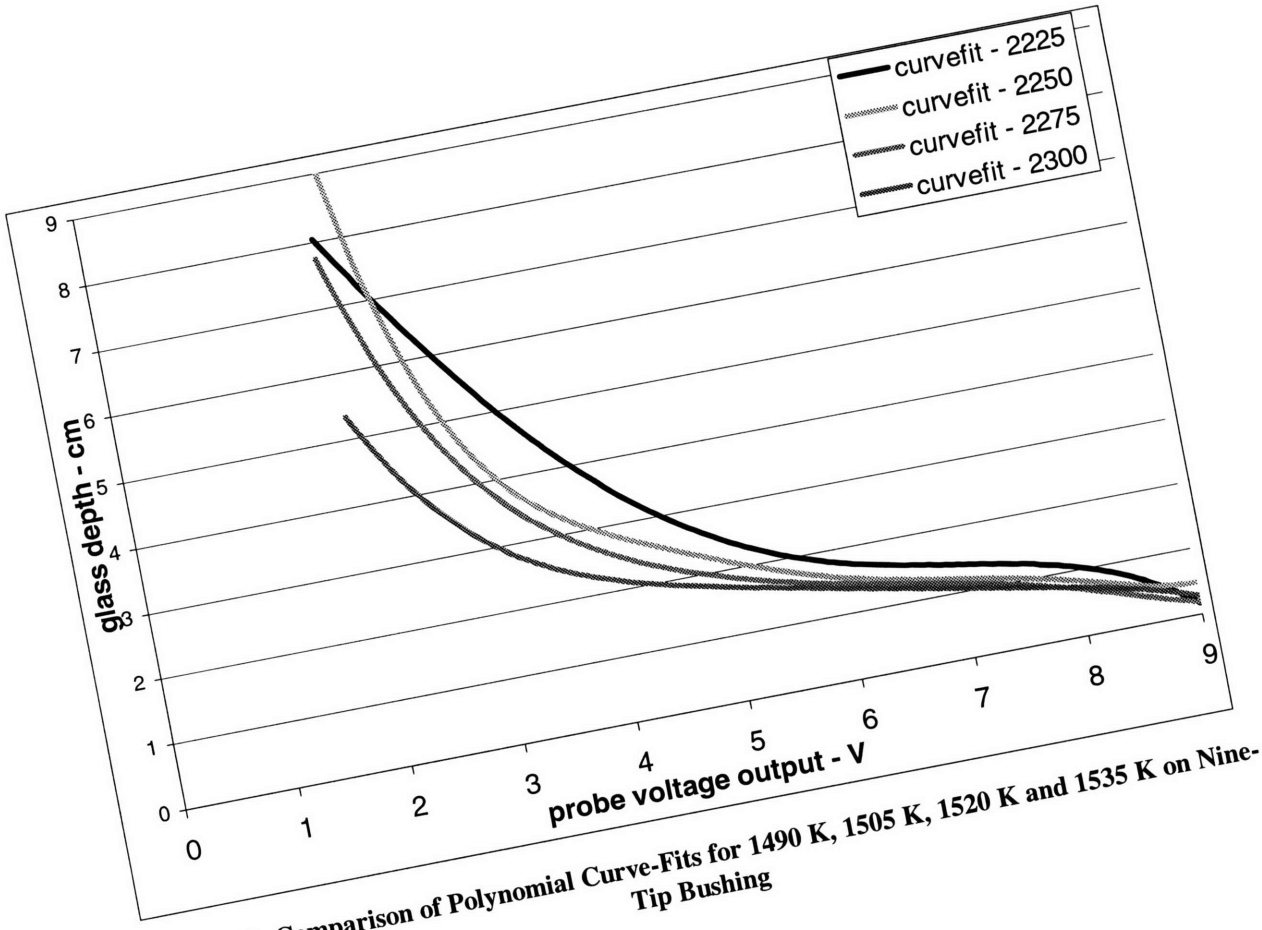

Figure 2.46: Comparison of Polynomial Curve-Fits for 1490 K, 1505 K, 1520 K and 1535 K on Nine-Tip Bushing

Chapter 3

3 Winder Control

3.1 Requirements

The fiber winding system on the fiber forming production line consists of a large 30 cm (12 inch) diameter drum mounted to a high speed motor. A computer controls the angular speed of the motor, causing it to slow as fibers building up on the drum change the effective diameter. The entire drum is moved back and forth along its axis in order to distribute fibers along its entire length. Fibers travel from a bundling point at a graphite disk to an attachment called a spiral before being wound onto the drum. The spiral consists of rotating brass rods that push the fiber back and forth. The spin rate of the spiral is slower than that of the winder and causes the fibers to be wound onto the drum in a crisscrossing pattern that facilitates later unwinding of the fibers and eliminates the edge effects caused by the axially moving drum changing direction.

The fiber winding system currently in use on the single tip position is inadequate for the purposes of research being done at MIT. Rather than replicate the single-tip system on the nine-tip position set up at MIT, this project has undertaken to identify components for and build a new fiber winding system. The winding system, as defined by this project, consists of a variable speed motor, a large drum on which fibers accumulate, and a means of moving the fiber along the drum axially so that fibers do not build up in one place on the drum. The motor and the drum that it drives are referred to collectively as a winder and the means of axial fiber motion is referred to as a reciprocator. The current fiber winding system on the single tip does not have very fine speed control, changes winding speed without warning and does not

have controlled speed degeneration capabilities. It also has an inefficient system for reciprocation and package build, and it may be inducing vibrations in the fibers.

Variations in winder speed lead to variations in fiber diameter, due mainly to conservation of mass. As discussed in Chapter 2, mass flow through the fiber-forming tips is controlled mainly by the head pressure above the pool of molten glass. In other words, it is largely an extrusion process. If a given mass of glass is drawn more rapidly downward its length increases and its diameter must decrease, since the density of the solidified glass is constant. There is also some effect of forces from below on the rate glass flows out of the bushing tips. Changes in winder speed may lead to temperature variations in the fiber-forming environment and at the tip plate due to changes in the thermal and fluid boundary layer that forms around the fiber. Changes in temperature directly at the exit of the tip will not necessarily be detected by the bushing thermocouple and thus will not be corrected for. The change in temperature will lead to a change in glass viscosity and this may actually change the mass flow rate. More viscous glass will tend to pull more glass with it, but it may also cause restriction of mass flow due to the increased force of pulling a more viscous substance through a small orifice. This project has not undertaken to quantify such effects. The main motivation is to eliminate winder speed variation such that the effects described above are no longer a concern.

The fiber winding system needs to have easy to use and reliable RPM control, limited vibration, and reciprocation ability to keep fibers from accumulating in a small region on the winder drum. Due to the small volume of accumulated fibers (relative to the production line), degeneration of winder speed will not be necessary for single-tip or small-number-tip positions. This is discussed in more detail below. The addition of a spiral will also not be necessary, as the fiber packages formed are not intended to be unwound and used and because the edge effects are small enough to be ignored. The speed range necessary for the winder has been determined by the range of the LDV (Laser Doppler Velocimetry) equipment that will be used for further research on the nine-tip fiber forming position at MIT. This equipment operates optimally at 10 m/sec (30 ft/sec) and has a full range of 1-40 m/sec (3-130 ft/sec). A reliability of a few percent of the fiber speed setting is desired. A winder drum 30 cm (12 inches) in

diameter and a motor with a 100-2500 RPM speed range would provide a fiber speed range of 1.6-40 m/s (5-130 ft/sec).

In determining the necessity of winder speed degeneration, some simple calculations reveal how much fiber pull speed would be effected by glass buildup over the course of a day. Assuming an initial volume of 60cc (the equivalent of 15 marbles, the capacity of the nine-tip bushing well), the cross-sectional area of the package for different winder drum diameters was calculated. The worst-case assumption is that the fibers are square-packed (see Figure 3.1), which leads to an area increase of a factor of 1.273, which can be seen in the following equation:

Equation 3.1
$$\frac{A_{total}}{A_{fiber}} = \frac{4r^2}{\pi r^2} = \frac{4}{\pi}$$

where r is the fiber radius, A_{fiber} is the area of the fiber cross section and A_{total} is the cross sectional area of fibers plus the are of the enclosed air space.

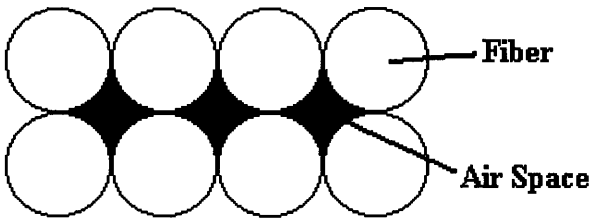

Figure 3.1: Cross Section of Square-Packed Fibers

If the 60 cm^3 of glass fibers were spread over a reciprocation range of 5 cm (2 inches) on a 30.48 cm (12 inches) diameter drum the equivalent drum diameter, after all 60 cm^3 of fibers had been deposited, would be 30.82 cm (12.13 inches), an increase of 1.105%.

Equation 3.2
$$D_{equivalent} = D_{original} + 2\left(\frac{V_{glass}}{C_{drum}L_{reciprocation-range}} \times \frac{4}{\pi}\right) = 30.48 + 2 \times 0.16 = 30.82cm$$

In the above equation $D_{original}$ is the actual winder drum diameter, $D_{equivalent}$ is the winder drum diameter with accumulated fibers, V_{glass} is the total volume of deposited glass, C_{drum} is the winder drum

circumfrence and $L_{reciprocation\text{-}range}$ is the length over which the reciprocator travels. Thus a fiber set speed of 40 m/sec would become 40.44 m/sec. To maintain a constant surface speed the winder speed would have to be decreased from 2500 RPM (at the beginning of the day) to 2472 RPM at the end. Considering that glass on the nine-tip bushing would run out faster than on the single tip, it is not unreasonable to assume that a scenario where all the glass was dispensed onto the winder. It was decided that this was a small enough change that winder speed degeneration is not necessary.

3.2 Equipment

After research was done into various possibilities, the following motor and speed control system was selected. The motor is a Bodine 3/8 HP, 2500 rpm brushless DC motor. The controller is a Filtered SRC BLDC Control which takes 115 V AC in and can control the motor from 100 RPM to 2500 RPM. It gives a tachometer output of 12 pulses per second. The controller can be adjusted by a hand controlled dial or by an input voltage of 0-10 V. An Analog Interface and Isolation Module is required in order that the voltage can be set as an output from the DAQ card. This way the speed is simple to set and the entire single-tip system can be integrated in the same program. The DAQ card being used by this project is an AT-MIO-16E-10 from National Instruments, with has two output channels, which is sufficient to control the pressure adjust valve and the motor speed controller. The winder drum for this system will have to be approximately 30 cm (12 inches) in diameter. This will give a speed range of 1.6-40 m/s (5-130 ft/sec). The error of the controller is 1%. As discussed in section 3.1, with a 30 cm (12 inch) winder and a 5 cm (2 inch) reciprocation range the increase in speed due to package buildup will be 1.105%, on the same order as the error of the motor speed controller. Therefore winder speed degeneration will not be necessary (although it would be possible with the computer control that is being used).

An event counter VI (Virtual Instrument) in Lab View was modified to count tachometer pulses and calculate the actual motor speed. This VI was incorporated as a sub-VI in the overall VI that will monitor and control both the pressure-control system and the winder speed-control system. Before the tachometer could be used some signal conditioning had to be done. The rising edge of the tachometer output pulse

was not steep enough for the DAQ counter input to detect, even after a pull-up resistor was put in place. A Schmitt-trigger had to be used to ensure a clean rising edge. An inverting Schmitt-trigger was installed on a small breadboard inside the terminal block of the DAQ card. The signal was run through two inversions so that the final signal had the same polarity at the tachometer output.

The winder drum was initially built with the body consisting of a 15 cm (6 inch) length of 33 cm (13 inch) diameter PVC pipe connector. Larger diameter simply means the winder will run at a slightly slower RPM. Since the controller seems to function adequately in the range below 100 RPM (as discussed in section 3.3), no functionality is lost. The flat sides were two pieces of 30 x 30 cm (12x12 inch) aluminum, 4.8 mm (0.1875 inch) in thickness, screwed to the edges of the PVC pipe. The central shaft was 2.54 cm (1 inch) diameter Delrin plastic rod and was mounted to the drum with shaft supports, which are aluminum with 4 screw holes on a flange and a screw-adjustable shaft hole of 2.54 cm (1 inch) nominal diameter.

This winder drum was determined to be inadequate. PVC was originally selected for its lightweight and easy availability, but the PVC pipe is susceptible to being burned by hot glass beads and is easily deformed. The flexibility of the PVC lead to the drum being assembled with some eccentricity and thus not being balanced. It vibrates somewhat excessively at high speeds.

A new drum was built of aluminum pipe that is 31.75 cm (12.5 inches) in outer diameter and aluminum plate for the faces of 4.6 cm (0.18 inches) in thickness. The shaft and shaft supports from the former winder were retained. The screw holes had to be drilled out slightly larger than the original so that there would be flexibility in placement of the flange. Illustration of drum assembly is shown in Figure 3.2.

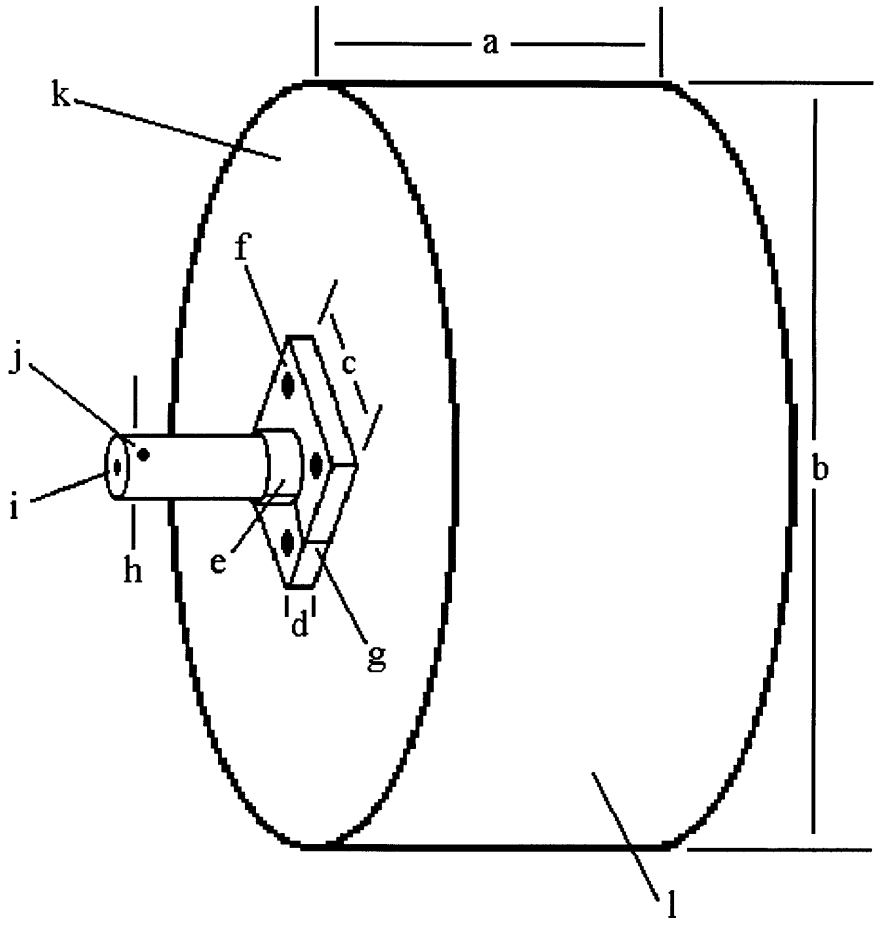

Figure 3.2: Winder Drum

a: 15 cm (6 inches)
b: 31.75 cm (12.5 inches)
c: 7 cm (2.75 inches)
d: 1.59 cm (0.625 inches)
e: flange extension: 3.8 cm (1.5 inches) outer diameter, 1.59 cm (0.625 inches) length
f: screw holes through flange: 6.75 mm (0.266 inches) diameter, plate tapped for ¼-20 screws
g: slit for tightening flange around shaft
h: 2.54 cm (1 inch)
i: hole for motor shaft 1.27 cm (0.5 inches) diameter
j: set screw for attachment to motor shaft
k: Aluminum plate, 4.8 mm (0.190 inches) thickness
l: Aluminum pipe, 9.5 mm (0.375 inches) thickness

The motor is mounted to a 30 x 15 cm (12 x 6 inches), 6.35mm (0.25 inches) thick aluminum plate. The plate is attached to two angle pieces of aluminum, 6.35 mm (0.25 inches) thick and 3.34 cm (1.25 inches) on a side. The channel steel is mounted by means of couplings that can be slid up and down to adjust the height. Holes drilled in the aluminum plate line up with threaded holes in the front of the motor.

Vibration damping plate mounts connect the angle aluminum to two crosspieces of Uni-Strut channel steel. The motor was initially mounted using 4 small damping coupling plate mounts. Each damping coupling supports 17.8 N (4 lbs.) in compression. It was found that this configuration was too compliant and it was remounted using 8 larger, 40 N (9 lbs.) support, plate mounts such that it was more constrained. Illustration of the configurations, along with size measurements for the vibration damping plate mounts, is shown in Figures 3.3 and 3.4.

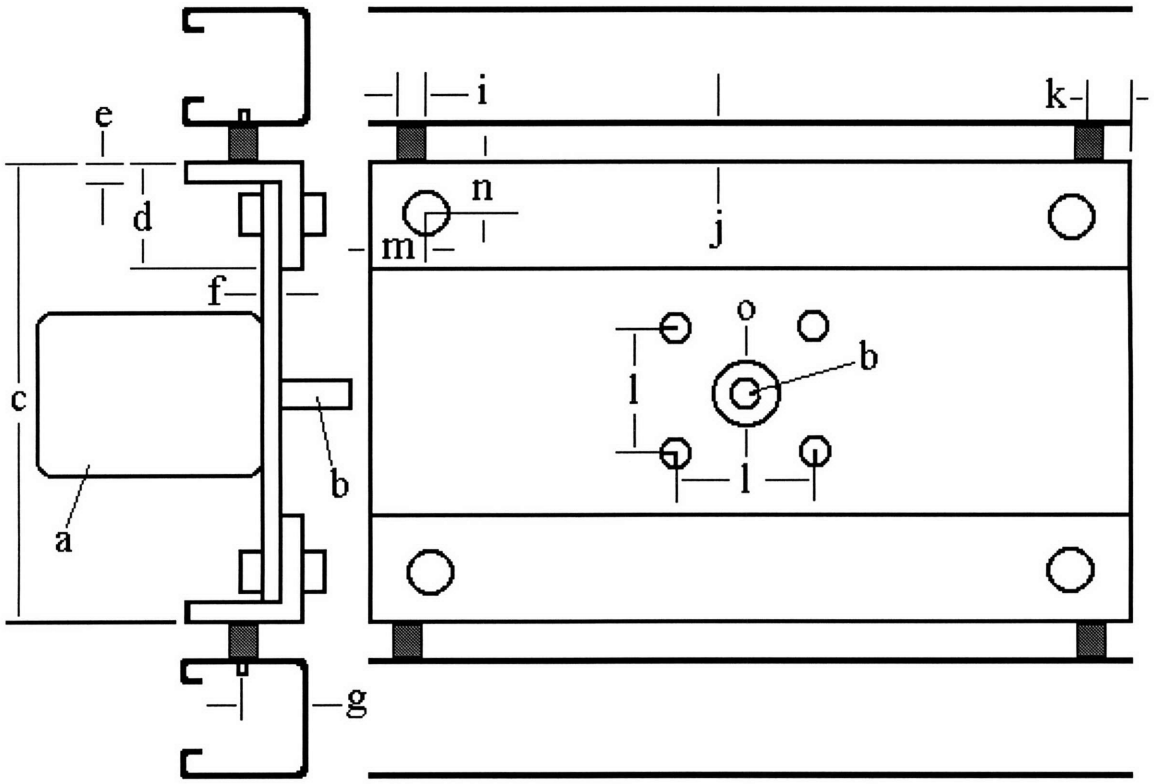

Figure 3.3: Motor Mount Assembly with Initial Damping Coupling Configuration

a: motor - 100-2500 RPM variable speed
b: 1.27cm (0.5 inches) diameter motor shaft - attached to winder drum (see figure 3.2)
c: 16.5cm (6.5 inches)
d: 3.81cm (1.5 inches)
e: 6.35mm (0.25 inches)
f: 6.35mm (0.25 inches)
g: 1.59cm (0.625 inches)
h: not applicable to this configuration
i: 1.42 cm (0.56 inches)
j: 1.27 cm (0.5 inches)
k: 2.54 cm (1 inch)
l: 6.35 cm (2.5 inches)
m: 1.9 cm (0.75 inches)
n: 1.9 cm (0.75 inches)
o: 2.54 cm (1 inch) diameter hole for motor shaft to pass through

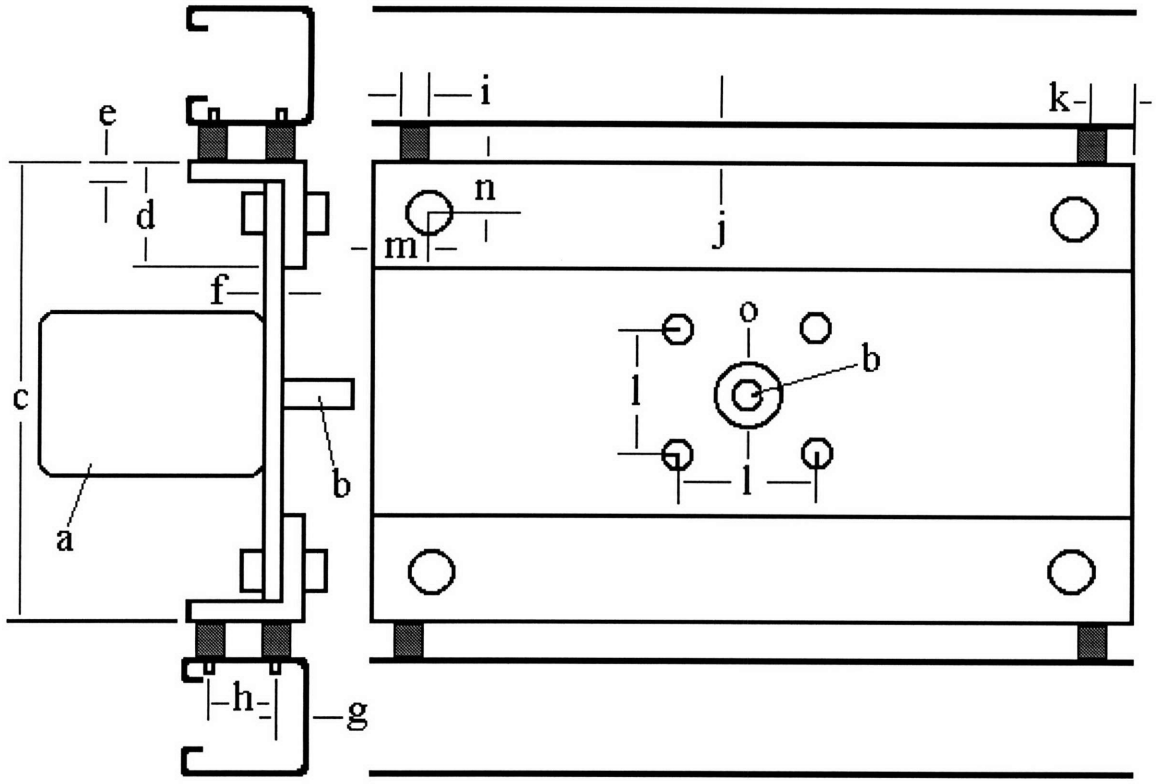

Figure 3.4: Motor Mount Assembly with Final Damping Coupling Configuration

a: motor - 100-2500 RPM variable speed
b: 1.27cm (0.5 inches) diameter motor shaft - attached to winder drum (see figure 3.2)
c: 16.5cm (6.5 inches)
d: 3.81cm (1.5 inches)
e: 6.35mm (0.25 inches)
f: 6.35mm (0.25 inches)
g: 1.6mm (0.0625 inches)
h: 2.39 cm (0.94 inches)
i: 1.42 cm (0.56 inches)
j: 1.27 cm (0.5 inches)
k: 2.54 cm (1 inch)
l: 6.35 cm (2.5 inches)
m: 1.9 cm (0.75 inches)
n: 1.9 cm (0.75 inches)
o: 2.54 cm (1 inch) diameter hole for motor shaft to pass through

It was initially thought that the reciprocator could be made with ceramic linear bearings sliding on two parallel 6.35 mm (0.25 inches) aluminum shafts. Aluminum pillow blocks would support the shafts at either end. The idea to use ceramic bearings and aluminum shafts and assemble a slide did not work. The bearings could not take the amount of rotational force on them without binding. Instead a linear slide was purchased. It has a slide range of 22 cm (8.5 inches) and can withstand a rotational load of 13.6 N-m (10 ft.-lbs.) The arm that pushes the shaft is about 7.6 cm (3 inches) long and the combined weight on the sliding block is on the order of several ounces so this is more than adequate. It can also take a load of 2650 N (595 lbs.) vertically or horizontally, and has 2 sliding blocks, though only one is being used. The

holes on the sliding blocks did not line up with the holes on the pillow block shaft supports, so an aluminum block with appropriate drilled holes was placed between the shaft supports and the linear slide.

A 20 RPM AC gear-motor drives the reciprocator. An aluminum disk is mounted to the motor shaft and a shaft will extend from one edge of it to the bearings on the shafts. Both ends of the extended shaft are mounted to rotary bearings that are made of nylon and glass such that no rusting will occur when the water sprays are in operation. The other end of the shaft will connect to another 6.35 mm (0.25 inch) aluminum shaft, on which the graphite shoe is mounted. The bearings are mounted inside a hole in the disk with epoxy and to a slot in the end of an aluminum shaft, also with epoxy.

The shoes that guide the fiber have been mounted to 6.35 mm (0.25 inch) aluminum shafts, supported by pillow blocks. One shoe is mounted to the slide. The other is stationary. The stationary shaft actually has 3 shoes on it such that the fibers may be separated into 3 separate bundles, if required. This may be necessary to take some measurements of air speed and temperature between the fibers. When originally assembled the reciprocating shoe was placed level with the stationary shoe, about 91 cm (3 ft.) below the bushing and 91 cm (3 ft.) above the winder drum. It was found that the system was too unstable in this configuration and the reciprocating shoe was moved lower, until it was about 5 cm (2 inches) above the winder. This configuration causes fewer breakouts. Illustration of the reciprocation system is shown in Figure 3.5. Photographs of both the reciprocator and the motor and drum assembly follow, in figures 3.6, 3.7 and 3.8.

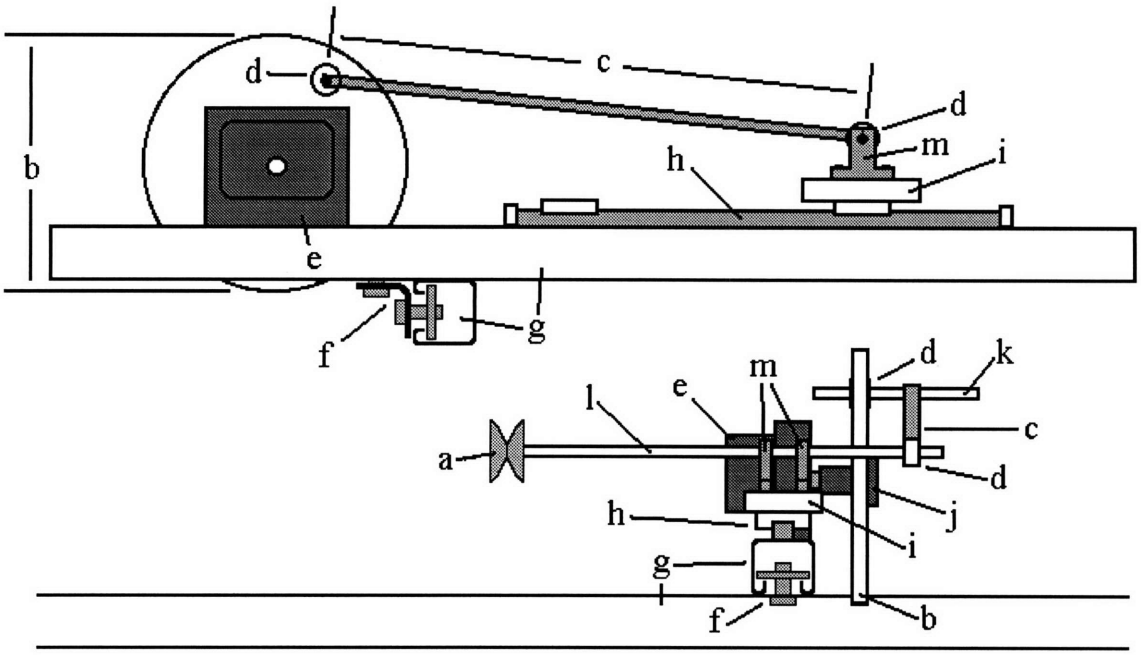

Figure 3.5: Reciprocator, Side View and Front View

a: graphite shoe for fiber control
b: 15 cm (6 inch) diameter, 6.35 mm (0.25 inch) thickness aluminum disk. Bearing mounted 6.35 cm (2.5 inches) from center of disk
c: 9.53 mm (0.375 inch) diameter aluminum shaft
d: nylon and glass rotary bearings, 2.54 cm (1 inch) outer diameter, 6.35 mm (0.25 inch) inner diameter
e: 1/20 RPM AC Gear Motor
f: UniStrut Channel Steel coupling
g: UniStrut channel steel, 4 cm (1.625 inches) square
h: linear slide
i: aluminum block to mount pillow blocks to slide and account for different screw arrangement and sizes
j: aluminum flange to mount disk to motor shaft.
k: 6.35 mm (0.25 inch) diameter aluminum shaft
l: 6.35 mm (0.25 inch) diameter aluminum shaft
m: aluminum pillow block shaft supports

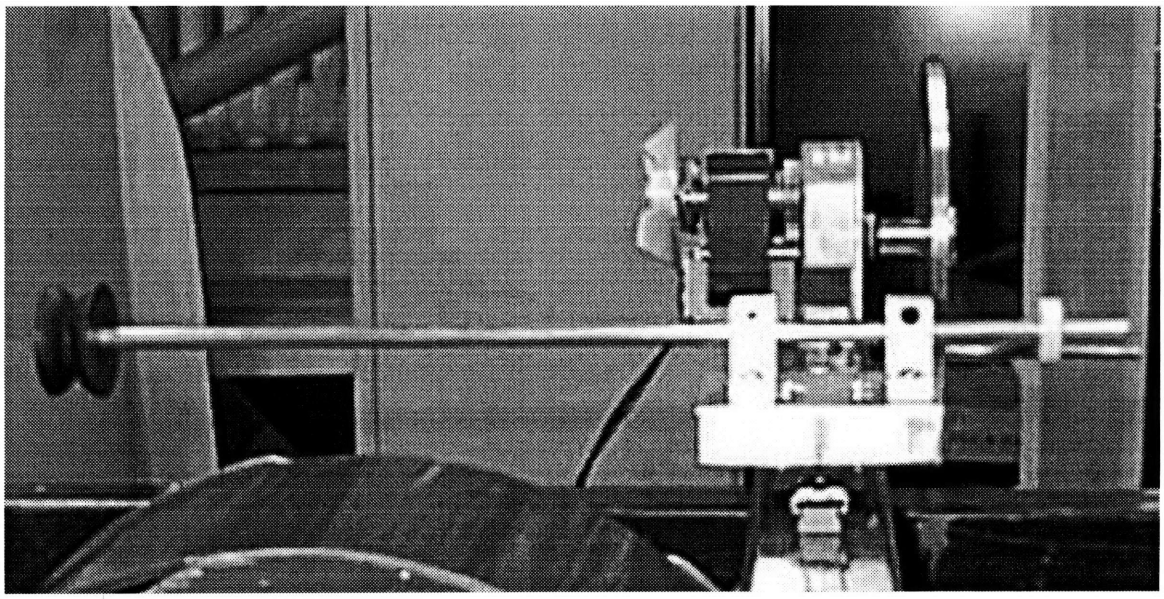

Figure 3.6: Front View of Fiber Reciprocation Assembly

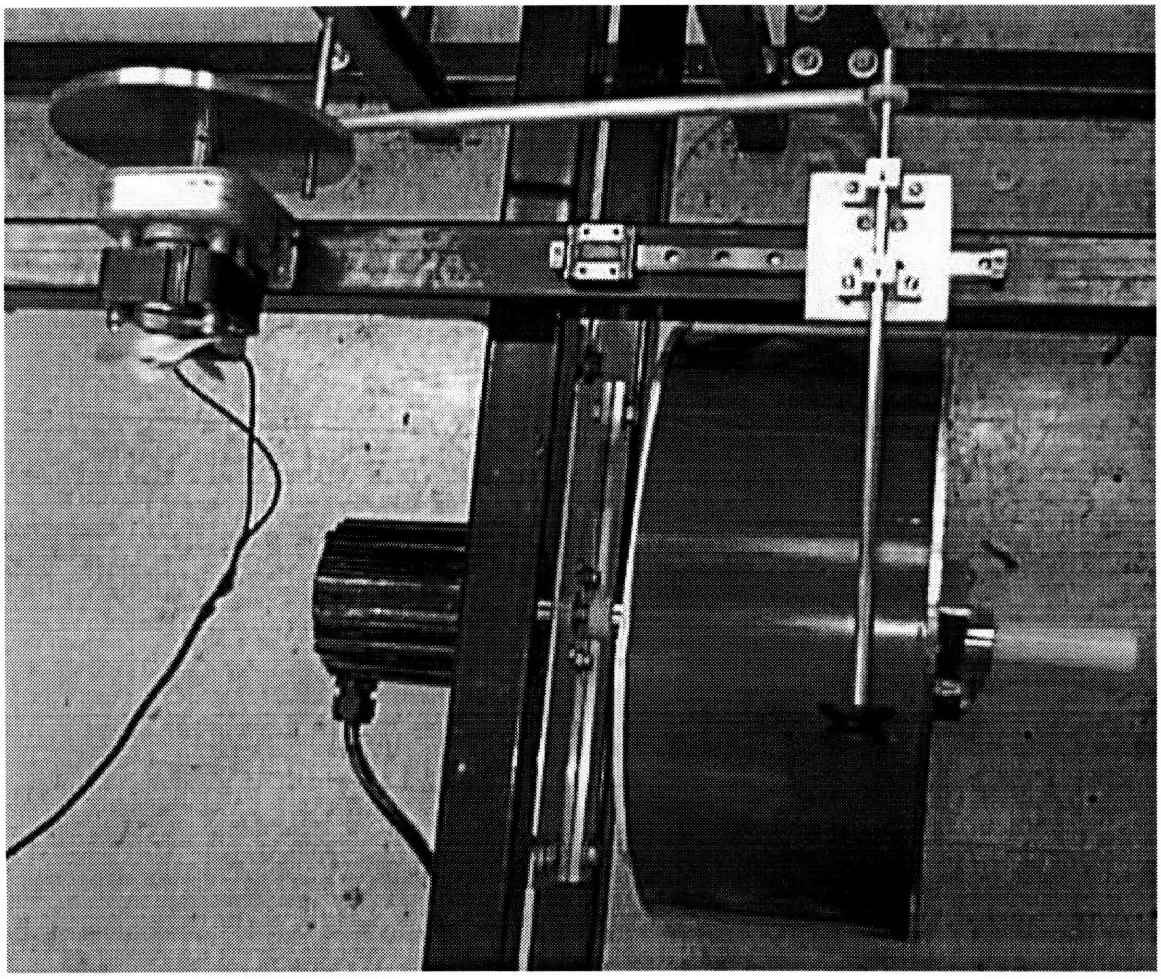

Figure 3.7: Side View of Fiber Reciprocation Assembly and Winding Assembly

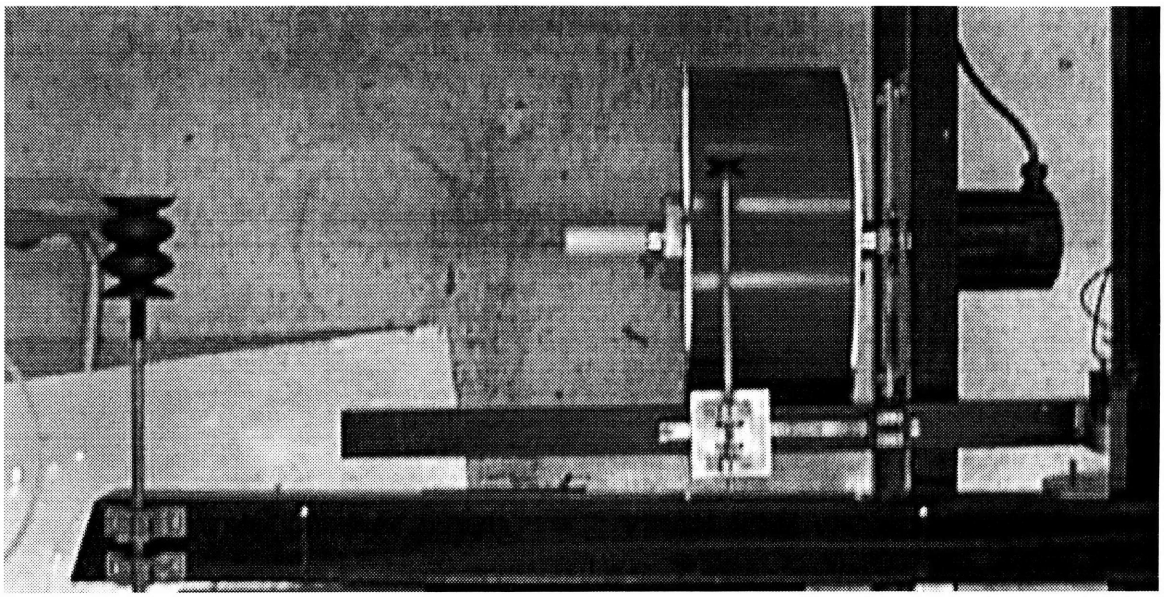

Figure 3.8: Top View of Fiber Winding Assembly, Reciprocation Assembly and Fiber Guidance System

After it was assembled and run one problem was encountered with the fiber guidance, winding and reciprocation systems. The friction of the fibers running along the graphite shoes lead to a build up of static charge. The similar charged fibers tended to repel each other and wind unevenly onto the winder, causing many breakouts. They also caused an accumulation of static charge on the winder drum, which caused the winder controller to shut down. Turning power to the winder controller off and on would reset this, but it would simply happen all over again. To solve this problem the fibers were wetted at the first graphite fiber guidance shoe to neutralize the static charge. A simple absorbent paper wick was inserted into an adjacent water vessel and draped over the graphite shoes to provide a constant moisture supply.

3.3 Calibration

Calibration curves were first recorded for the motor with no load on it. In the first experiment the winder was run at voltage increments of 0.1 V from 0-10 V and the corresponding winder speeds were recorded. The winder ran for 30 seconds taking 50 points per second and the average of this was recorded. Several points were taken per voltage and the number was not uniform. Points were taken in ascending order. This was done for the same points

twice in a row (slowing the winder back to zero in between runs) and the data from the two was curve-fit together. The points and corresponding curve-fit are shown in Figure 3.9, with accompanying R^2 accuracy.

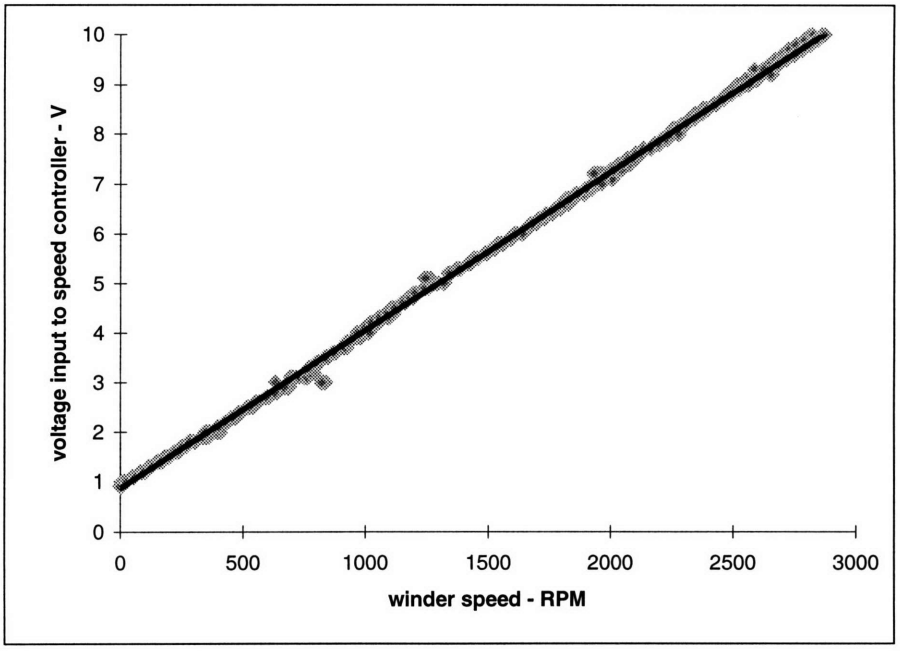

Figure 3.9: Initial Speed Controller Calibration with No Winder Drum

Equation 3.3 $V_{required} = 0.0032 v_{winder} + 0.8604$

$R^2 = 0.99925$

In the above equation (and in all winder calibration equations in this section) v_{winder} is the winder speed in RPM and $V_{required}$ is the voltage necessary to attain that winder speed.

Then the winder control part of the VI was set up to decrement the winder speed by 1 RPM per minute, and to take the average of 50 points per second over each full minute. The voltage output was set based on the above computed curve-fit. Desired winder speed, actual winder speed and output voltage were all recorded. In this case the winder was started at 2850 RPM and run continuously down to 0 RPM. This took a total of about 43 hours but it did not need to be constantly monitored. A graph of the actual vs. desired winder speeds is shown in Figure 3.10 along with a curve-fit to indicate accuracy.

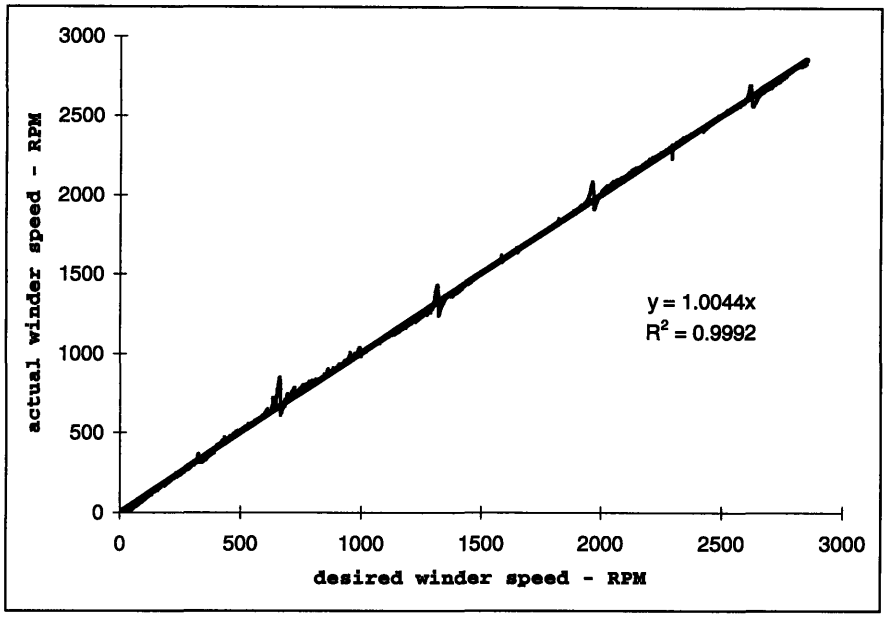

Figure 3.10: Comparison of Initial Speed Calibration to New Measured Speeds

This indicates that the original calibration was very accurate. It was assumed that this new curve was more accurate due to the larger number of data points and the curve-fit equation from this was substituted into the winder control VI. The calibration curve is as follows:

Equation 3.4 $V_{required} = 0.00319 v_{winder} + 0.85920$

$R^2 = 0.99922$

One notable thing about that data in Figure 3.10 is the presence of evenly spaced spikes of larger error. The cause of these is not known. Perhaps there is some resonance and the frequencies with error are harmonics of some natural frequency in the system.

The fact that the controller can run the winder above 2500 RPM at all indicates a problem with the speed controller adjustment. The speed controller has zero and span adjustment potentiometers. They should be adjusted such that the winder speed at an input of 10 V is at the maximum of 2500 RPM. It does not seem that it is possible to have the winder spin at only 2500 RPM for a 10 V signal - the maximum speed always exceeds this. The new calibration curves were not done with the winder attached and thus they still do not adequately reflect the final winder speed. They are not included in this section, as they would be largely redundant.

Finally a calibration curve was made with the winder drum attached, shown in Figure 3.11. Points were taken every 0.05 V from 0-10 V. Each point consisted of 10 scans per second for 10 seconds and 6 points were taken at each voltage setting.

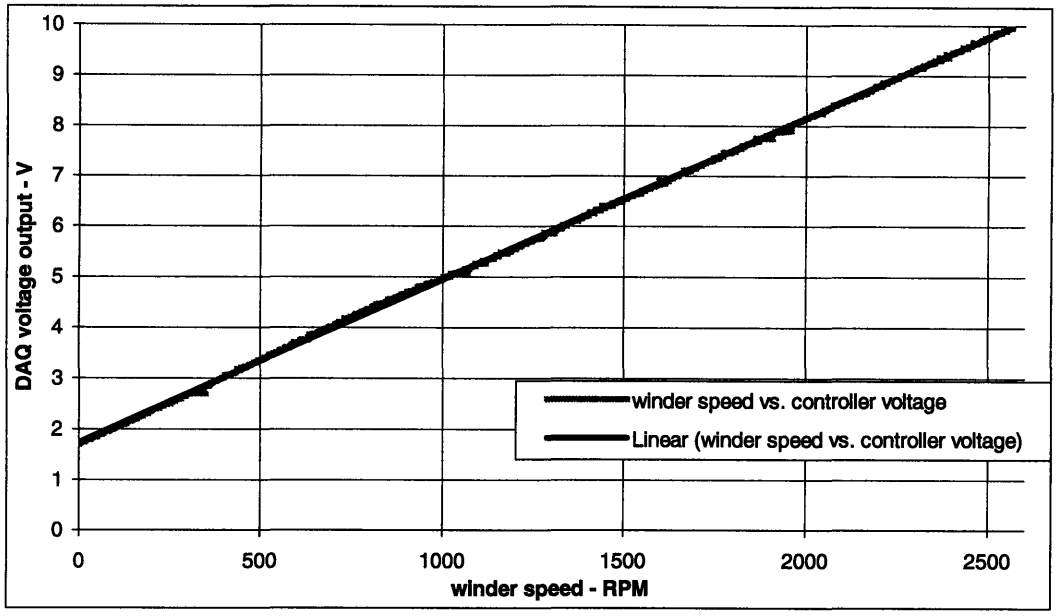

Figure 3.11: Final Winder Calibration With Drum Attached

Equation 3.5 $V_{required} - 0.003209v_{winder} + 1.728055$

$R^2 = 0.99982$

It is noteworthy that the above curve is very straight and smooth. The mass of the winder drum carries momentum and thus eliminates a lot of the tendency for speed to fluctuate. The harmonics observed in Figure 3.8 do not appear.

This calibration was incorporated into the nine-tip control VI in LabView. Multiplication by the drum circumference of 0.9975 m and division by 60 seconds/minute provides the speed in meters/second, which was also put on the display. Multiplication by a circumference of 3.27 ft. and division by 60 seconds/minute provides the speed in feet/sec, which is also added to the display.

Chapter 4

4 User Interface

Although many of the issues relating to the interface of equipment designed in this project have been discussed in previous chapters, it is important enough that it was thought necessary to bring all of that and more together in a separate section.

4.1 Requirements

A primary goal of this project was to make the equipment designed for it automated and easy to use. For this purpose the pressure control valve identified is controllable with a voltage signal from a DAQ card, as is the winder speed controller. The interface to these two systems should allow complete control and monitoring of these systems. It should also warn the user, when possible, of possible problems in the systems being controlled.

4.2 Final Configuration

Figure 4.1 shows the final configuration of the user interface. When the system is started it runs continuously until the stop button is pushed. The pressure and winder speed settings default to zero on startup of the program so that the operator can start the program without having the fiberglass forming setup completely ready for operation.

The user is given the option of whether to save data that the system collects during a run. If they have chosen yes they are prompted for a filename. The data is saved as tab delimited text for easy importation into Matlab or Excel. The user is allowed a comment line to identify the conditions the data was taken under and provide any

other useful information. Data that the system saves include; probe voltage reading, pressure setting, winder voltage setting, winder speed in RPM and the time at which the data was saved. The data saving feature was put in place largely for the purposes of calibrating the system, so it is assumed that most operators will not use the save feature. It is set to default to not saving.

The user is given control over how often input voltages are read (the scan rate) and how many seconds of such data are averaged together. A longer averaging time means more smoothing of noise, but it also means that the operator can control system settings less often. The data gathering loop runs for the full time specified before taking in new settings and running again. A display of the last time data was collected lets the user know what the data onscreen represent. A default of 120 seconds is recommended as long enough to assure smoothing of probe voltage data and short enough to allow reasonably frequent alteration of system settings. A user sets these parameters for the duration of the run and must restart the program to change them.

The user is given control over winder speed in RPM and pressure setting in kPa. The user is also prompted to enter the bushing temperature set point, as the level sensing system uses this value in depth calculations. It is assumed that the user will want to change these settings in the middle of a run and so the settings can be changed every time a new data collection and averaging cycle is begun. The range of the input fields is limited to the range that the system is built to control. Winder speed can only be set between 0 and 2500 RPM, pressure can only be set between 0 and 55 kPa and bushing temperature can only be set between 2210° F and 2315° F. This input is in °F because that unit is used on the bushing controller. Since users may also want to know the system settings in terms of other units, pressure setting is set to display in PSI and cm of glass depth, and winder speed setting it set to display in ft/sec and m/s. A companion VI to make these calculations immediately has also been provided, as the main control VI is not able to update immediately, but must wait to finish a data set first.

Graphs of winder speed and input and output voltages are included in case the user wants to see a history of the system settings. They are given control over the domain and range settings of the graphs by using the settings boxes to the lower left of the graphs. The graphs are also included in order to give the user feedback about possible problems with the system. The voltage graph indicates the voltage setting that is being sent to the pressure valve as well as a feedback voltage from the valve, the latter of which should match the former or lag slightly behind it. If this is not the case the user should begin troubleshooting the system for problems such as having insufficient

supply air pressure or having forgotten to turn on power to the pressure control valve. Warning lights are included to let the user know when glass is about to run out and if the winder speed reading and winder speed setting have a discrepancy of more than 1.5%.

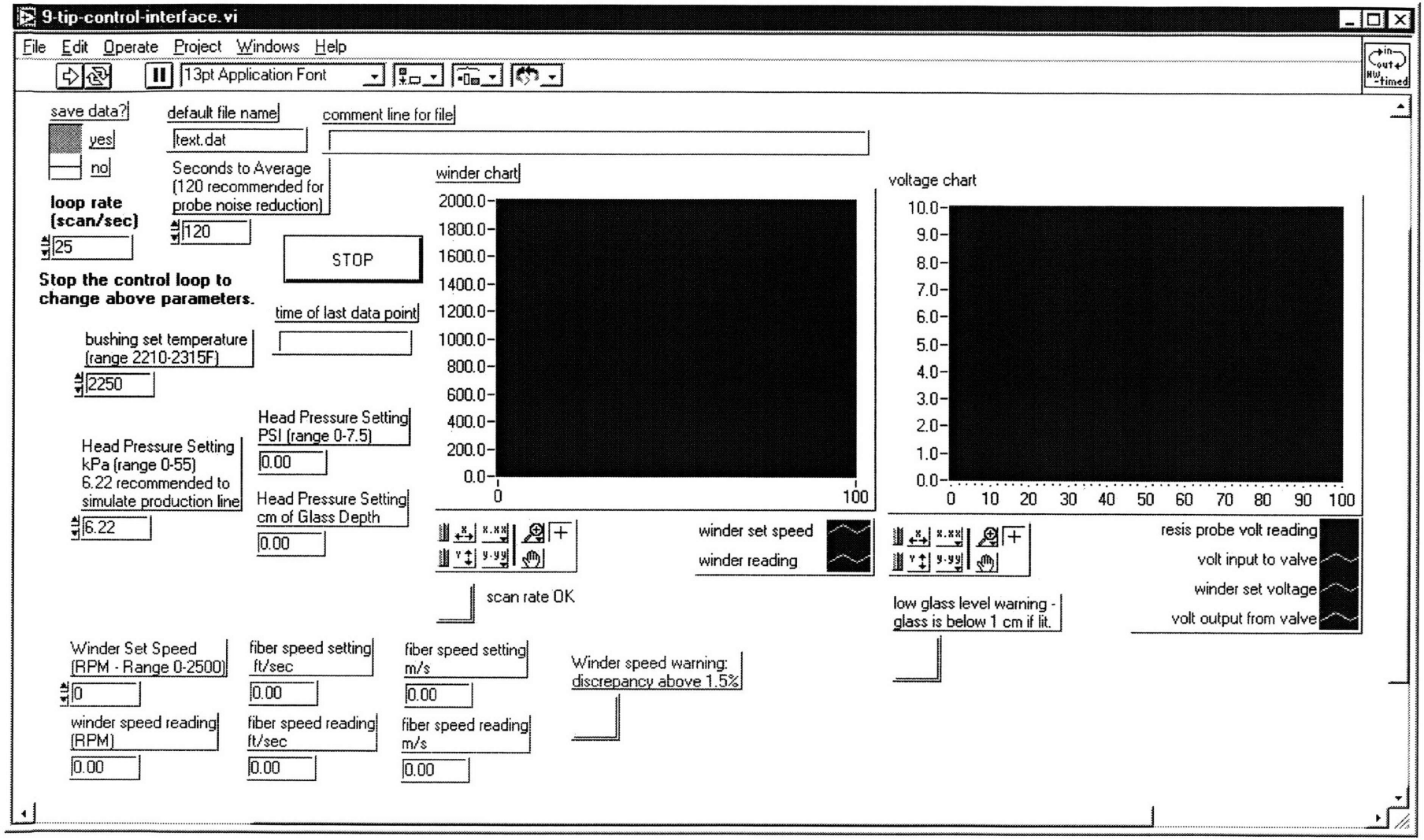

Figure 4.1: Setup of LabView Program User Interface

Appendix A

A User Instructions

A.1 Startup and Glass Cure

1. Disconnect air hose from bushing well cap by pushing in out outer sheath. It is a quick-disconnect and should pop off.
2. Unscrew cap to bushing well and carefully remove cap and platinum probe from well
3. Load marbles into bushing well – not more than 15 marbles (no more should fit)
4. Turn on transformer- and bushing-cooling water – handle should rotate 30-45°
5. Make sure bushing controller is set to manual power control at zero power
6. Turn on bushing power with large wall switch
7. Set bushing temperature set-point to 2400° F
8. Change bushing power to automatic.
9. Wait for temperature to come up to 2400° F. This should take about 45 minutes to 1 hour.
10. Before bushing reaches 2000° F, place a pan or barrel under the glass to catch drips. If the container has water in it this is ideal to cool the glass quickly and prevent hot beads from bouncing out and burning the floor or other nearby burnable objects.
11. By the time the bushing reaches 2400° F glass in the well should have melted enough to make room for the probe. Check well to make sure marbles are at least 3 inches below the top of the well. They do not have to be completely melted – some are expected to still be solid. If they are not down far enough, wait another 10 minutes and check again.
12. Loosen brass fitting on top of bushing well screw cap. Probe and sheath should now be able to slide freely through cap. Slide both up so that only a few inches are sticking out below the cap. Do not allow alumina sheath to slide completely through.
13. Check platinum probe for straightness and straighten if it has been bent
14. Screw cap onto top of bushing well, being careful to insert probe into well without bending.
15. Reattach air hose by pushing. It is a quick-connect and should snap into place.
16. Allow probe to slide down until it rests on top of the still solid glass. If probe is sticking in fitting push it down *very* gently, so as not to bend it.

17. Although you can do it later, this is a good time to start the winder and valve control program. Open the program from the icon on the desktop.
18. Turn on power to probe electronics. This should be on a power strip and labeled as such.
19. Make sure that pressure and winder settings are at zero. If the program was just opened they should default to this. Choose whether you want to save data. Choose a scan rate and a data averaging time. You should probably keep the defaults for these, unless you have a specific reason to do otherwise.
20. Press start – the arrow in the upper left of the window. If you are choosing to save data you will be prompted to choose a file name and directory. If you have changed your mind about this you can hit "cancel." This will not cancel the program running – it will only cancel the data-saving part of the operation. If you do this you should expect an error message when you finally stop the program.
21. Glass should stay at 2400° F for an hour. This assures that all marbles have fully melted, air bubbles have percolated out, and impurities that may have been on the surface have burned away. If available, train an air hose on the tips during this time to freeze off the glass and limit loss from dripping.
22. Check probe during this time to ensure that it is sliding down into the well. Push down gently if it is not. When it contacts melted glass you should be able to feel it slide into the viscous material. Do not push in past the 0.375" stop point.
23. Also monitor probe output voltage on voltage graph in user interface. The voltage should start out around 8.9 V when the probe is not inserted into the glass and fall to between 1 and 2 V when the probe is fully inserted to the 0.375" mark. If it does not, or if signal noise is visible, go to section **A5: Troubleshooting**

A.2 Run

1. Make sure probe is at 0.375" mark and tighten brass fitting to hold it in place. Use a wrench as it will be very hot, but it does not need to be tighter than you would be able to tighten by hand.
2. When an hour of curing is done, change bushing set-point to final run temperature – between 2210° F and 2315° F. Wait for temperature reading to drop to new set-point.
3. Make sure that pressure control near wall is completely unscrewed so that when wall pressure is turned on pressure does not go through to pressure adjust valve.
4. Turn on wall pressure, rotating handle about 30-45°
5. Screw in pressure control near wall until dial reads 15 PSI. Supply pressure to pressure control valve should *never* exceed 30 PSI. The dial is only marked to 15 PSI. Make sure it does not max out.
6. Turn on power to the valve. This should be on a marked power strip.
7. Set bushing temperature within program to match the setting on the bushing controller. If you decide to change bushing temperature during the course of a run make sure the setting on the computer interface reflects this.
8. Fill water applicator and make sure wetting pad contacts upper shoes.
9. Input desired head pressure in kPa and desired winder speed in RPM. The companion calculation VI can be used to determine necessary settings to control pressure to appropriate PSI or cm of glass, as well as to control the winder in m/s or ft/sec. This VI can also be found on the desktop. Once the settings are fed through and the next round of data is being collected, the user interface will update to display the settings in these units as well. The companion VI is provided to allow calculation of values in alternate units without sending the setting to the equipment.

10. Make sure any air that has been trained on the tips to freeze the glass is turned off. Once pressure valve is activated glass will begin to flow.
11. Wait for glass to drip down and collect it into a bundle by grabbing the thin, cooled strands. Watch for thicker lumps, which will still be hot even if they are no longer glowing orange.
12. If the glass does not drip in separate strands but instead pools around the bushing tips use the stainless steel poker to scrape between the tips and separate it into strands. There is no specific method for doing this – it just takes trial and error to learn.
13. Pulling the bundle of glass fibers at a constant rate, pass it under the upper shoe, over the lower shoe and around the winder. Set the winder spinning by hand and then turn on the power strip that powers both the winder drum and the reciprocator. It is possible to wind in the glass while the winder is spinning, so you may start the winder first if you prefer.
14. Again check to make sure the fibers are being wetted. If they are not they will cause static charge to build up on the winder drum and the winder motor will shut down. If this happens simply shut off power to the winder and turn it back on again.
15. System should now be ready for other experiments. Alter winder speed and head pressure as needed for duration of run.
16. Monitor system during run, to assure continued functioning of pressure valve and winder. On the voltage graph pressure feedback signal should match or lag only slightly behind pressure setting. Probe voltage reading should be smooth and rise over the course of the day from about 2 V to 8.9 V. Winder error light should not come on unless the winder has been stopped by turning off power.
17. If fibers break, stop the winder drum and repeat steps 11 through 14. To stop winder simply shut off power, or set the speed to zero from within the user interface. The former is probably simpler, as it will stop the reciprocator as well and it will be effective immediately. You can apply friction to the drum to stop it or let it coast to a stop.
18. If low glass warning light comes on either go to section **A3: Refilling the Melting Well** or proceed to section **A4: System Shutdown**. If you are choosing to refill it is a better idea to do so as soon as the light comes on. If you are planning to shut down it is ok to keep running the system for the small amount of time left before glass runs completely out. Pressure control will be somewhat less accurate during this time, so mass flow may fluctuate slightly.

A.3 Refilling the Well

1. Turn the pressure valve set-point to zero.
2. Remove the air hose and unscrew the bushing well cap using a wrench or an insulating glove.
3. Carefully remove the probe from the well, keeping in mind that it is red-hot. Set it down away from the well.
4. Set the bushing controller to manual.
5. Begin refilling the well with marbles. On dropping in the first marble the temperature of the bushing will drop rapidly. Use no more than 14 marbles. If you stopped to refill just as the low glass warning came on there should already be the equivalent of one marble in the well.
6. Wait until temperature is no longer dropping. Set bushing controller to 2400° F and turn bushing controller back to automatic.
7. Wait for controller to come up to 2400° F and wait for an hour at this temperature.

8. Reinsert probe and reattach the air hose as described in section **A1**, steps 11-16 when the marbles have melted low enough to fit it. This will probably not have happened by the time the bushing reaches 2400° F, as the time to reach this temperature will be much shorter and the glass will have had less time to melt.
9. Monitor the probe voltage and make sure that probe slides in to 0.375" mark, as described in section **A1**, steps 22 and 23.
10. Unload glass from winder before restarting. More than one bushing-full of glass will alter the winder diameter by a significant amount and thus alter fiber speed.
11. Return to section **A2: Run**

A.4 System Shutdown

1. If bushing well is already completely empty skip to step 5.
2. Set bushing temperature to 2400° F
3. If pressure setting for run was lower than 10 kPa, turn pressure setting up to 10 kPa. (this step is not necessary – it is merely for the convenience of draining the glass more rapidly)
4. Wait for glass to drain from bushing.
5. Make sure probe has not slipped lower in well than the 0.375" mark. If it has, loosen the brass fitting and slide it up. If it is left touching the bottom of the well it will freeze to the small amount of glass still left there and the next day it will not be able to be removed from the well without first heating the well.
6. Set bushing set-point to 0° F. and leave on automatic.
7. Set winder speed and valve pressure to zero.
8. Turn off power to valve, probe electronics, winder controller and reciprocator.
9. Turn pressure control dial to zero. Turn off supply pressure.
10. Press stop button on data acquisition program and wait for it to stop at next data cycle.
11. Wait for bushing temperature to drop below 500° F. This process can be accelerated somewhat by turning the bushing controller to manual and lowering power a few percent at a time. It should still be done somewhat slowly and take at least 30 minutes. Cooling the bushing too quickly causes it to break down more rapidly.
12. Turn off bushing power at wall switch.
13. Turn off cooling water.

A.5 Troubleshooting

Problem	Solution
Probe signal is noisy	Turn probe back and forth inside well a few times to increase wetting. Check probe electrical connections for secure attachment. Leave system at cure temperature for longer to assure even melting and better probe wetting
Winder will not run	Turn winder off and on and make sure fiber wetting system is functioning
Pressure valve feedback does not match set-point	Make sure supply pressure is at 15 PSI Make sure pressure control valve is powered Make sure air lines are securely screwed in
Fibers keep breaking out	Check fiber wetting system Pressure setting and winder speed may be too extreme. Increase pressure or lower winder speed.
VI quits with the error "Scan rate too fast"	Shut off other programs running on the machine and press start on the program again. While the program is off it will maintain the previous voltage set-points to the winder and pressure adjust valve. If the problem happens with no other pregrams running (including screensavers and the CD player) lower the scan rate and start the program again.
Steam starts coming out of the water hoses	You forgot to turn on the cooling water! Shut down bushing power NOW with the large wall switch and wait for the system to cool before replacing the damaged hoses.
Probe voltage reads zero volts	Turn on probe electronics
Probe voltage is below one volt and/or remains at a constant low voltage for a long time despite glass flowing	Make sure probe is set to 0.375" height. If it is lower and contacts the bushing this short creates a low voltage output.
Probe voltage is constant at about 8.9 V – warning light is on	System is out of glass and needs to be refilled A wire in the electronics setup has been detached. Check probe connection wires.

Table A.1: Troubleshooting Problems with Nine-Tip Equipment

References

[1] Narottam P. Bansal. *Handbook of Glass Properties.* Academic Press, Orlando, 1986.

[2] Robert H. Doremus. *Glass Science, 2nd edition.* Wiley, New York. 1994.

[3] Joan Irene Duffy. *Glass Technology.* Noyes Data Corp., Park Ridge, N.J., 1981.

[4] Reed Grundy, Hal Stedrack and Dana Coyne. *[PPG Internal Report].* PPG Fiber Glass Research Center, Pittsburgh, PA, 1997. (Proprietary material)

[5] F. R. Hartley. *The Chemistry of Platinum and Palladium, With Particular Reference to Complexes of the Elements.* Applied Science Publishers, London, 1973

[6] Jesse Talbot Littleton. *The Electric Properties of Glass.* Wiley, New York, 1933.

[7] Klaus Leopold Lowenstein. *The Manufacturing Technology of Continuous Glass Fibers, 2nd edition.* Elsevier, Amsterdam, 1993

[8] George W. McLellan and Errol B. Shand. *Glass Engineering Handbook, 3rd edition.* Mc-Graw-Hill, New York, 1984.

[9] Evgenii Mikhailovich Savitsky. *The Physical Metallurgy of Platinum Metals.* Mir Publishers, Moscow, 1978.

[10] Jaroslav Stanek. *Electric Melting of Glass.* Elsevier Scientific Pub. Co., Amsterdam, 1977.

[11] Norman M. Tallan. *Electrical Conductivity in Ceramics and Glass.* M. Dekker, New York, 1974.

[12] Fay VaNistle Tooley. *The Handbook of Glass Manufacture: A Book of Reference for The Plant Executive, Technologist, and Engineer, 3rd edition.* Books for the Glass Industry Division, Ashlee Pub. Co., New York, NY, 1984.